The Involvement of Trace Amine-Associated Receptor 1 and Thyroid Hormone Transporters in Non-Classical Pathways of the Thyroid Gland Auto-Regulation

by

Maria Qatato

a Thesis submitted in partial fulfillment
of the requirements for the degree of

Doctor of Philosophy

in Cell Biology

Approved Dissertation Committee

Prof. Dr. Klaudia Brix
Jacobs University Bremen

Prof. Sebastian Springer, DPhil
Jacobs University Bremen

Dr. Georg Homuth
Ernst-Moritz-Arndt-Universität Greifswald

Date of Defence: 16 January 2018

Department of Life Sciences and Chemistry

Statutory Declaration

Family Name, Given/First Name	Qatato, Maria
Matriculation number	20330110
What kind of thesis are you submitting:	PhD Thesis

English: Declaration of Authorship

I hereby declare that the thesis submitted was created and written solely by myself without any external support. Any sources, direct or indirect, are marked as such. I am aware of the fact that the contents of the thesis in digital form may be revised with regard to usage of unauthorized aid as well as whether the whole or parts of it may be identified as plagiarism. I do agree my work to be entered into a database for it to be compared with existing sources, where it will remain in order to enable further comparisons with future theses. This does not grant any rights of reproduction and usage, however.

This document was neither presented to any other examination board nor has it been published.

German: Erklärung der Autorenschaft (Urheberschaft)

Ich erkläre hiermit, dass die vorliegende Arbeit ohne fremde Hilfe ausschließlich von mir erstellt und geschrieben worden ist. Jedwede verwendeten Quellen, direkter oder indirekter Art, sind als solche kenntlich gemacht worden. Mir ist die Tatsache bewusst, dass der Inhalt der Thesis in digitaler Form geprüft werden kann im Hinblick darauf, ob es sich ganz oder in Teilen um ein Plagiat handelt. Ich bin damit einverstanden, dass meine Arbeit in einer Datenbank eingegeben werden kann, um mit bereits bestehenden Quellen verglichen zu werden und dort auch verbleibt, um mit zukünftigen Arbeiten verglichen werden zu können. Dies berechtigt jedoch nicht zur Verwendung oder Vervielfältigung.

Diese Arbeit wurde noch keiner anderen Prüfungsbehörde vorgelegt noch wurde sie bisher veröffentlicht.

……….

Date, Signature

Table of Contents

List of Abbreviation

%	Percent
°C	Degrees Celcius
3-T$_1$AM	3-iodothyronamine
β-PEA	β-phenylalamine
μg	Microgram
μl	Microliter
μm	Micrometre
AADC	Aromatic amino acid decarboxylase
Asn	Asparagine
ATP	Adenosine triphosphate
BLAST	Basic Local Alignment Search Tool
BRET	Bioluminescence resonance energy transfer
BSA	Bovine serum albumin
cAMP	Cyclic adenosine monophosphate
cDNA	Complementary deoxyribonucleic acid
ConA	Concanavalin A
CMF-PBS	Calcium and magnesium free phosphate buffered saline
CNS	Central nervous system
Ctsb$^{-/-}$	Cathepsin B-deficient mouse
Ctsk$^{-/-}$	Cathepsin K-deficient mouse
Ctsl$^{-/-}$	Cathepsin L-deficient mouse
Dio (1, 2 or 3)	Iodothyronine deiodinase (type I, II or III)
DNA	Deoxyribonucleic acid
dNTP	Deoxyribonucleotide
DTT	Dithiotreitol

EDTA	Ethylenediaminetetraacetic acid
EGFP	Enhanced green fluorescent protein
EGTA	Ethylene glycol tetraacetic acid
ELISA	Enzyme-linked immunosorbent assay
EPPTB	N-(3-Ethoxy-phenyl)-4-pyrrolidin-1-yl-3-trifluoromethyl-benzamide
ER	Endoplasmic reticulum
ERGIC	ER-Golgi intermediate complex
FACS	Fluorescence activated cell sorting
FRT	Fisher rat thyroid cells
FBS	Foetal bovine serum
g	acceleration of gravity (9.81 m/sec)
g	gram
G_α	Guanine nucleotide-binding protein, alpha subunit
GM130	Golgi matrix protein 130
GPCR	G protein-coupled receptor
HA	Haemagglutinin tag
HEK 293	Human embryonic kidney 293 cells
HEK 293T	Human embryonic kidney 293 transformed with large T antigen
HEPES	4-(2-hydroxyethyl)-1-piperazineethanesulfonic acid
hr	Hour
HRP	Horseradish peroxidise
kDa	Kilo Dalton
KTC-1	Human thyroid papillary carcinoma cells
KTC-Z	KTC-1 cells stably expressing mTaar1-EGFP
LacZ	Lactose operon
LAMP-2	Lysosomal-associated membrane protein 2

Lat	L-type amino acid transporter
M	Molar
mM	Millimolar
MALDI	Matrix assisted laser desorption ionisation
MAP6	Microtubule associated protein 6
MAPK	Mitogen-activated protein kinase
MAO	Monoamine oxidase
MAO-B	Monoamine oxidase type-B
min	Minutes
ml	Millilitre
MCT8/Mct8	Monocarboxylate transporter 8 (human/rodent)
Mct10	Monocarboxylate transporter 10
$Mct8^{-/y}$	Mct8-deficient (male) mouse
$Mct10^{-/-}$	Mct10-deficient mouse
NIS	Sodium iodide symporter
nM	Nanomolar
Nthy-ori 3-1	Human thyroid follicular epithelial cells
Nthy-Z	Nthy-ori 3-1 cells stably expressing mTaar1-EGFP
OATP1C1	Organic anion-transporting polypeptide 1C1
PAX8	Paired box gene 8
PBS	Phosphate buffered saline
PBS-T	Phosphate buffer saline + 0.3% Tween-20
PCR	Polymerase chain reaction
PFA	Paraformaldehyde
RLuc	*Renilla* luciferase
RXR	Retinoic X receptor

SDS	Sodium dodecyl sulphate
SDS-PAGE	SDS polyacrylamide gel electrophoresis
$t_{1/2}$	Half-life
T_0AM	Thyronamine
T_3	L-3,5,3'-triiodothyronine
T_4	L-3,5,3',5'-tetraiodothyronine (L-thyroxine)
TA	Trace amines
TAAR1/Taar1	Trace amine-associated receptor 1 (human/other)
Taar5	Trace amine-associated receptor 5
Taar8b	Trace amine-associated receptor 8b
Taar1$^{-/-}$	Taar1-deficient mouse
TAM	Thyronamines
Tg	Thyroglobulin
TGN	*Trans*-Golgi network
TH	Thyroid hormones
THT	Thyroid hormone transporter(s)
TRα	Thyroid hormone receptor α
TRβ	Thyroid hormone receptor β
TPO	Thyroid peroxidase
TR	Nuclear thyroid hormone receptors
TRE	Thyroid hormone response elements
TSH	Thyroid-stimulating hormone (thyrotropin)
Tshr	TSH receptor
TTF-1	Thyroid transcription factor-1
TX-100	Triton X-100
WT	Wild type

Publications, and Oral and Poster Presentations

Publications

Szumska J., **Qatato M.**, Rehders M., Führer D., Biebermann H., Grandy D.K., Köhrle J., Brix K. (2015). Trace amine-associated receptor 1 localization at the apical plasma membrane domain of Fisher rat thyroid epithelial cells is confined to cilia. Eur Thyroid J. 4(Suppl 1): 30–41. doi: 10.1159/000434717.

Weber J., McInnes J., Kizilirmak C., Rehders M., **Qatato M.**, Wirth E. K., Schweizer ., Verrey F., Heuer H., Brix K. (2017). Interdependence of thyroglobulin processing and thyroid hormone export in murine thyrocytes. EJCB 96(5): 440-456. doi: 10.1016/j.ejcb.2017.02.002

Brix, K., **M. Qatato**, J. Szumska, V. Venugopalan, and M. Rehders (in press). Thyroglobulin storage and degradation for thyroid hormone liberation. In: The Thyroid and Its Diseases, edited by Markus Luster, Leonidas Duntas, and Leonard Wartofsky, Springer-Verlag Berlin/Heidelberg. REVIEW.

Qatato M.*, Szumska J.*, Skripnik V., Rijntjes E., Köhrle J., Brix K. Canonical TSH regulation of cathepsin-mediated thyroglobulin processing in the thyroid requires Taar1 expression. Frontiers in Pharmacology. [Submitted].
(* equal contribution)

Qatato M., Dallto W., Hein Z., Springer S., Biebermann H., Brix K. Establishing an *in vitro* model to study trafficking of mouse Taar1 in thyroid epithelial cells. [To be submitted].

Presentation (presenting author underlined)

<u>**Qatato M.,**</u> Szumska J., Rehders M., Amoah A., Venugopalan V., Dinter J., Biebermann H., and Brix K., *TAAR over-expression systems in a rat thyroid epithelial cell model.*
Oral presentation at the 29. Arbeitstagung Experimentelle Schilddrüsenforschung (AESF), 12-14 December, 2013, Essen, Germany

<u>**Qatato M.**</u>, Amoah A., Szumska J., Venugopalan V., Babusyte A., Dinter J., Krautwurst D., Biebermann H., Brix K., *TAAR expression in thyroid epithelial cell lines as to establish an in vitro-model for signalling analysis.* Exp Clin Endocrinol Diabetes 2014; 122 - P083, DOI: 10.1055/s-0034-1372100
Poster presentation at the 57. Symposium der Deutsche Gesellschaft für Endokrinologie (DGE), 19-22 March 2014, Dresden, Germany

<u>**Qatato M.,**</u> Venugopalan V., Amoah A., Szumska J., Dinter J., Biebermann H., and Brix K., *Trace Amine-Associated Receptor (Taar) Expression and Trafficking in Rat Thyroid Epithelial Cells.*
Poster presentation at the 1st Thyroid Trans Act (TTA) International Conference, 5-7 December, 2014, Bremen Germany

Szumska J., **Qatato M.,** Venugopalan V., Rehders M., and Brix K., *Sub-cellular localization of trace amine-associated receptor 1 in thyroid epithelial cells treated with cathepsin B, K and L inhibitors.*
Poster presentation at the 1st Thyroid Trans Act (TTA) International Conference, 5-7 December, 2014, Bremen Germany

Qatato M., Venugopalan V., Amoah A., Szumska J., Dinter J., Biebermann H., Brix K., *Visualising Trafficking of Trace Amine-Associated Receptors (Taar) in Polarised Thyroid Epithelial Cells.*
Poster presentation at the 58. Symposium der Deutsche Gesellschaft für Endokrinologie (DGE), 18-21 March, 2015, Lübeck, Germany

Qatato M., Szumska J., Weber J., Dallto U., Rijntjes E., Kohrle J., Grandy DK., Brix K., *Morphometric analysis of the thyroid gland of young Taar1-deficient mice.*
Poster presentation at the Young Researcher in Life Sciences (YRLS), 18-20 May, 2016, Paris, France

1. Abstract

The thyroid gland is an endocrine organ responsible for producing thyroid hormones, which are essential for normal growth and development, and for maintaining functional homeostasis of different organ systems. The thyroid is known to be classically regulated by the hypothalamic-pituitary-thyroid (HPT) axis which, in short, involves hypothalamic release of thyrotropin-releasing hormone (TRH) in response to low levels of thyroid hormones in the circulation. Through positive feedback, the TRH signals to the pituitary to release thyroid stimulating hormone (TSH), which, in turn, binds and activates thyrocytes to release thyroid hormones. Replenishment of thyroid hormones in circulation then serves as a negative feedback to quench TRH and TSH release. Growing evidence, including the non-genomic effect of thyroid hormones (T_3 and T_4), the selective thyroid hormone transporters that regulate cellular thyroid hormone uptake and release (including in the thyrocytes), as well as the discovery of endogenous thyroid hormone derivatives, the thyronamines, and their physiological effects, collectively challenge the classical view on thyroid regulation. The implications of that is that more complex regulatory mechanisms might exist, that are capable modulating thyroid function, also at the level of the thyroid follicle itself – the functional unit of the thyroid gland. Such pathways may be independent of the HPT axis, and are collectively referred to as "thyroid auto-regulation".

The first part of the present study explores the concept of non-classical thyroid auto-regulation in the context of thyroid hormone transporters, namely by investigating the interrelation between the thyroid hormone transporters Mct8 and Mct10 and thyroid hormone liberation by thyroglobulin-processing proteases. This was done by biochemical and morphological assessment of thyroglobulin degradation status in mouse thyroid tissue deficient in Mct8 or/and Mct10, as well as by analysing Mct8 protein levels and localisation in thyroid tissue cryosections from mice deficient in one or more of the thyroglobulin-processing cathepsins B, K or L. The results indicate an upregulation in thyroglobulin-processing cathepsins and thyroid hormone liberation in thyroid tissue lacking either or both Mct8 and Mct10, which correlates to enhanced thyroglobulin proteolysis implying an intrathyroidal thyrotoxic state in the said genotypes, thus, in a counter-intuitive manner. These results further suggest that thyroid hormone transporters are involved in "sensing" intrathyroidal thyroid hormone levels, and thereby, in regulating thyroglobulin-processing cathepsins in a mechanism independent of TSH induction, i.e. in an auto-regulatory fashion.

Abstract

The second and major part of this study focuses on the trace amine-associated receptor 1 (Taar1), as a further candidate to play a role in thyroid auto-regulation. This notion is based on the fact that Taar1, a G protein-coupled receptor, has been suggested as a putative receptor for thyronamines. The latter being endogenous derivatives of the classical thyroid hormone, which were also termed as the non-classical, or "cool thyroid hormones", for potentially eliciting effects antagonistic to those of the classical T_3 and T_4.

Confocal immunofluorescence data showed Taar1 to be expressed in rodent thyroid epithelial cells, and to localise on the apical pole of mouse thyroid epithelial cells *in situ*. This observation prompted establishing an *in vitro*-cell model which stably expresses a chimera of mouse Taar1 with a covalently fused enhanced green fluorescent protein tag on its C-terminus (mTaar1-EGFP), in order to further elucidate Taar1 subcellular localisation and trafficking in thyroid cells, particularly that previous studies in other cell systems showed that Taar1 appears to not reach the surface efficiently. The mTaar1-EGFP was shown to successfully traffic to the cell surface and, notably, to localise on the cilia of structurally-differentiated, polarized thyrocytes. Thus, this model will be used in future studies to investigate thyronamine-induced Taar1 signalling in order to better understand its role in thyroid auto-regulation.

Finally, in order to assess whether Taar1 has a functional role in thyroid morphogenesis and regulation, thyroid tissue from Taar1-deficient male mice was analysed by morphological and biochemical means. Male mice were used to eliminate potential discrepancies due to hormonal fluctuations in females. Immunofluorescence analysis revealed an alteration in the localisation of the TSH receptor, whereby it was predominantly seen to be located in subcellular compartments in Taar1-deficient thyroid tissue sections, as compared to the canonical localisation at the basolateral plasma membrane in thyrocytes of the wild type tissue. Furthermore, the Taar1-deficient mouse features mildly elevated concentrations of serum TSH, despite normal T_3 and T_4 concentrations, as well as a subtle disturbance in proteolytic to anti-proteolytic balance, thus affecting Tg solubilisation and degradation states, in the Taar1-deficient thyroid. All in all, this led to concluding that Taar1 is required to maintain canonical TSH receptor localisation, which also suggests that Taar1 signalling is connected to the hypothalamic-pituitary-thyroid axis.

2. Introduction

2.1 The Thyroid Gland

The thyroid gland is a bilobal endocrine organ positioned ventrally in the neck, overlying the trachea and larynx. The function of the thyroid gland is to produce thyroid hormones (TH), which are crucial regulators of various developmental and differentiation processes, organ function, metabolism and growth (Yen 2001). The function of the thyroid gland is classically regulated by thyrotropic feedback, whereby decreased levels of TH in circulation signals the hypothalamic secretion of the thyrotropin-releasing hormone (TRH; also known as thyroliberin), which in turn triggers the pituitary gland to release thyrotropin, also known (and will be henceforth referred to) as the thyroid-stimulating hormone (TSH), which then modulates TH liberation and release from the thyroid (Dietrich et al. 2012). These components therefore are collectively referred to as the hypothalamic-pituitary-thyroid (HPT) axis, which partly answers for thyroid homeostasis.

2.1.1 Classical thyroid hormones, synthesis and release

The "classical" TH, essentially L-3,5,3'-triiodothyronine (T3), and its precursor L-3,5,3',5'-tetraiodothyronine, also known as thyroxine (T_4). They are released from the thyroid follicles as a result of proteolytic processing of the prohormone thyroglobulin (Tg), stored in covalently cross-linked form in the lumina of thyroid follicles (Dunn et al. 1991, Brix et al. 2001, Friedrichs et al. 2003).

Tg synthesis and processing is regulated by the pituitary-secreted thyroid stimulating hormone TSH, which binds the basolaterally-expressed TSH receptors (TSHR) on thyrocytes, the thyroid functional unit, the follicle (Nussey and Whitehead 2001). Thyrocytes depend on TSH in order to differentiate and form the thyroid follicles (Morgan et al. 2016), in the lumen of which Tg is stored in covalently cross-linked form (Brix et al. 2001). TSHR activation results in the initiation of $G_{\alpha s}$ or the $G_{\alpha q}$ signalling pathways, which results in the activation of adenylate cyclase and phospholipase C, respectively (Nussey and Whitehead 2001). The former raises intracellular levels of cyclic adenosine monophosphate (cAMP), which mediates the long-term effect of TSH stimulation that culminates in the exocytosis of newly synthesised Tg (Chabaud et al. 1988, Chambard et al. 1990). Acute TSH stimulation, however, promotes the short-term effect of TSH stimulation, which signals via the $G_{\alpha q}$ pathway, whereby phospholipase C leads to the initiation of the phosphatidylinositol cascade, leading to an increase in intracellular Ca^{2+} levels,

which mediates Tg proteolysis to release TH, a process marked by an increase in serum T_4 levels (Brix et al. 2001, Nussey and Whitehead 2001). Subsequently, cysteine proteases – namely, cathepsins B, K and L – are relocated to the apical pole of the thyrocyte by retrograde trafficking, where they are secreted into the extracellular lumen to initiate Tg proteolysis extracellularly in order to liberate T_4, the process which accounts for as high as 54% of the total T_4 released (Brix et al. 1996, Tepel et al. 2000, Brix et al. 2001, Linke et al. 2002, Linke et al. 2002, Friedrichs et al. 2003). The partially degraded Tg is then internalised by endocytic uptake into the thyrocytes, where Tg is further degraded inside the endo-lysosomes, resulting in further T_4 as well as T_3 liberation. Tg would then be synthesised *de novo* and stored in the follicular lumen as a long-term TSH-response until another round of TSH activation thyroid follicles.
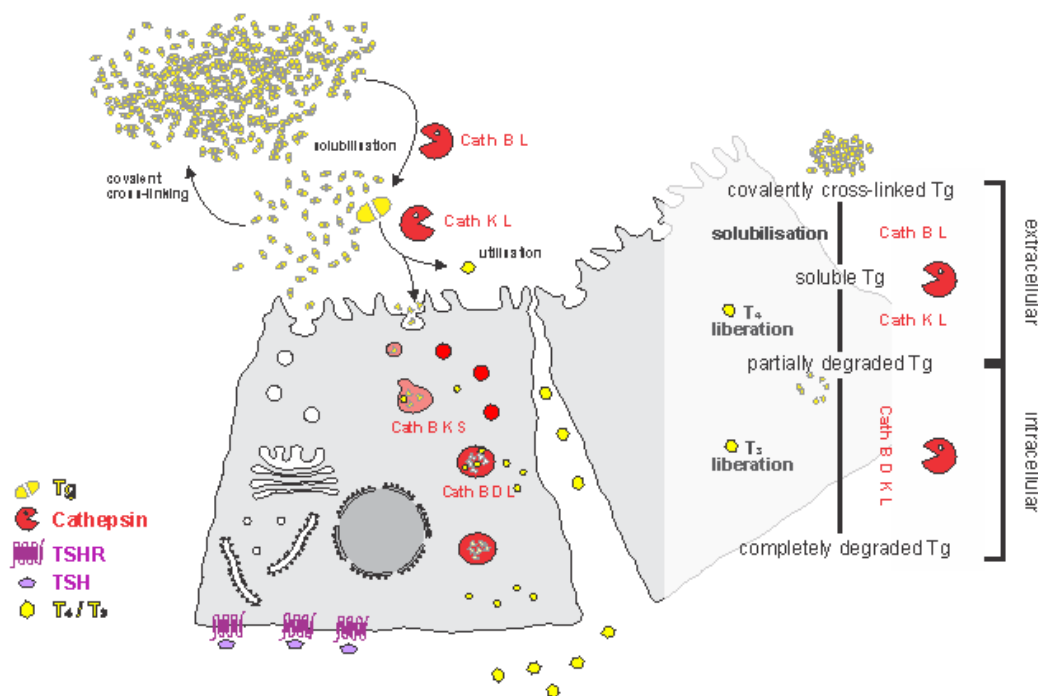
Figure 1: Thyroglobulin (Tg) proteolysis is mediated by cysteine cathepsins that are relocated and secreted into the follicle lumen following TSH stimulation. Tg proteolysis begins in the extracellular lumen, near the apical plasma membrane of thyrocytes. Tg is stored in covalently cross-linked form in the follicular lumen, where it becomes solubilised by action of cathepsins B and L. Soluble Tg is further processed extracellularly by cathepsins K and L, which results in T_4 liberation. The partially degraded Tg is then internalised, where its degradation is completed by cysteine proteases in endo-lysosomal compartments, resulting in T_3 liberation. [Modified from Friedrichs *et al.,* 2003].

The liberated TH is released into the blood stream to be delivered TH target cells, a process facilitated by selective thyroid hormone transporters (THT) (Hennemann et al. 2001, Friesema et al. 2003, Heuer and Visser 2009). In target cells, the T_4:T_3 ratio is adjusted by iodothyronine deiodinases, a sub-family of selenoenzymes, of which type I and type II iodothyronine-5'-deiodinases (Dio1 and Dio2, respectively) are responsible for converting the prohormone T_4 into the active T_3 form, whereas the action of type III deiodinase (Dio3) as well as, to a lesser extent, Dio1, converts TH to mono- or di-iodinated forms, the direct precursors of thyronamines (see section 2.2.3), rendering them incapable of binding to nuclear TH receptors (TR) (Kohrle 2000, St Germain et al. 2009).

2.1.2 Thyroid phenotype of mice deficient in Tg-processing cathepsins

Studies involving mice deficient in one or more Tg-processing cathepsins showed thyrocytes to lose their typical cuboidal morphology to become more flat, which is associated with a reduction in functionality, and is correlated with a decline in serum T_4 concentration and increased serum TSH concentration. Mice deficient in cathepsin K (*Ctsk$^{-/-}$*) have shown that the typical, multilayered arrangement of Tg stored in the extracellular lumen of thyroid follicles is retained in *Ctsk$^{-/-}$* thyroids, with a considerable increase in the size of the thyroid gland when compared to wild type mice, i.e. goitre-like phenotype; however, contrary to predictions, *Ctsk$^{-/-}$* mice do not exhibit the phenotype of hypothyroidism (Friedrichs et al. 2003). On the other hand, mice deficient in either cathepsin B (*Ctsb$^{-/-}$*) or cathepsin L (*Ctsl$^{-/-}$*) show increased amounts of luminally-stored Tg in non-multilayered form, combined with larger follicle areas and lower epithelial extension, with *Ctsl$^{-/-}$* mice additionally exhibiting an accumulation of dead cells in the follicular lumen (Friedrichs et al. 2003). Dead cell remnants were similarly observed in the lumina of *Ctsk$^{-/-}$/Ctsl$^{-/-}$* thyroids follicles, but not in those with a single deficiency in either cathepsin B or K, indicating cathepsin L to be a survival factor for thyroid epithelial cells. Moreover, *Ctsk$^{-/-}$/Ctsl$^{-/-}$* mice featured a significant decrease in serum T_4 levels (Friedrichs et al. 2003). Collectively, this means that any disturbance in proteolysis reflects directly on thyroid function, i.e. Tg-processing cathepsins are essential for thyroid homeostasis and their action and regulation must be taken into consideration when evaluating thyroid function.

It is noteworthy that double deficiencies in both cathepsins B and L proved lethal to mice in early postnatal stages due to brain atrophy (Felbor et al. 2002).

2.1.3 Thyroid hormone transport

Following liberation from Tg, TH were originally proposed to passively diffusing across lipid bilayers (Hillier 1970), a view that was challenged with the discovery of selective thyroid hormone transporters (THT) such as the monocarboxylate transporters 8 and 10 (MCT8 and MCT10), the organic anion transporting polypeptide 1C1 (OATP1C1), and the L-amino acid transporter type 1 and 2 (LAT1 and LAT2) (Hennemann et al. 2001, Friesema et al. 2003, Heuer and Visser 2009, Visser et al. 2011).

Mct8 efficiently transports both T_3 and T_4 (Friesema et al. 2003), and was found to be expressed in different tissue types, including the thyroid gland, in which it is the THT expressed the most, and where it localises to the basolateral membrane domain of thyroid epithelial cells (Di Cosmo et al. 2010). It was additionally found to be expressed in various regions of the mouse central nervous system (CNS), particularly highly in T_3- sensitive neurons (Heuer et al. 2005).

In human, the absence of functional MCT8 results in the X-linked Allan-Herndon-Dudley syndrome (AHDS), characterised by severe psychomotor retardation (Schwartz et al. 2005, Schwartz and Stevenson 2007) due to insufficient T_3 supply in brain neurons during development (Friesema et al. 2006). AHDS patients suffer from disturbances in TH transport, which translates as highly elevated serum T_3 concentrations, which do not correlate with the magnitude of reduction in T_4 nor the normal to slightly increased TSH concentrations (Heuer et al. 2005, Friesema et al. 2006). The Mct8-deficient mouse was developed as an AHDS model (Dumitrescu et al. 2006); however, despite mimicking the serum TH/TSH profiles of the human MCT8-deficient condition (Di Cosmo et al. 2010), the Mct8-deficient mouse does not exhibit signs of motor or neurological impairment like AHDS patients, a phenomenon that was explained by a different THT distribution in the CNS, specifically the blood-brain-barrier, between human and mouse (Visser and Visser 2012, Müller and Heuer 2014). Subsequently, mouse models with a global Mct10-deficiency or double Mct8 and Mct8 deficiencies were generated (Muller et al. 2014). Mct10 is selective for T_3 transport, compared to a much lower affinity to T_4 transport (Friesema et al. 2008), and is the second most expressed THT in the mouse thyroid gland, where its transcript level comprises 14% that of Mct8 (Di Cosmo et al. 2010). However, while a single deficiency in Mct10 only does not result in alterations in mouse serum TH levels, the double Mct8/Mct10-deficient mouse exhibits a partial rescue phenotype in that the serum T_4 concentrations are normalised in comparison to the Mct8-deficient mouse, but retains elevated serum T_3 and TSH levels (Muller et al. 2014). This was accompanied by an increase in TH concentrations in hepatic, renal and thyroid tissue more pronouncedly than in Mct8-only deficient tissues (Muller et al. 2014). Additionally,

upregulation of *Dio1* in the hepatic and renal tissue with both Mct8 and Mct10 deficiencies suggests that the normal serum T_4 content is not the result of reduced T_4 update by the liver and kidney, but rather that thyroidal T_4 release is increased despite the absence of both Mct8 and Mct10 (Muller et al. 2014). This is addressed in this study by analysing the changes in thyroid homeostasis, i.e. the thyroid's capacity to degrade and liberate TH, in Mct8/Mct10-double deficient mice.

2.1.4   Genomic action of thyroid hormone

The classical (i.e. genomic) TH pathway refers to the transcriptional regulatory effect that T_3 exerts on TH target genes through binding and activation of nuclear TH receptors (TR). These are high-affinity, low-capacity T_3-binding proteins that belong to the family of nuclear receptors that act as ligand-inducible transcriptional factors (Bassett et al. 2003). In human, two TR genes, *α* and *β*, located on two different chromosomes, encode variants of TRα and TRβ isoforms, which are variably distributed in a tissue-specific manner (Cheng et al. 2010).

The activation of TR by T_3 induces conformational changes allowing the TR to interact with specific TH responsive elements in the promoter region of TH responsive genes to either activate or repress their transcription (Bassett et al. 2003, Tata 2013, Senese et al. 2014). TR are commonly known to form homodimers or to heterodimerise with other nuclear receptors, such as the retinoic X receptor (RXR), thereby contributing to the diversity of responses they are capable of eliciting upon binding TH responsive elements (Forman et al. 1992).

Importantly, the genomic effect mediated by T_3-TR interaction requires hours and up to days to manifest, and is sensitive to inhibitors of transcription or translation (Yen 2001).

2.1.5   Non-genomic action of thyroid hormones

Conversely, T_3 is also capable of mediating relatively rapid metabolic responses that, contrary to genomically-mediated effects, remain unaffected by inhibitors of transcription or translation (Wrutniak-Cabello et al. 2001, Mullur et al. 2014). Clinical data show low degree of correlation between genetic mutations in transcription factors crucial for thyroid development and function, and the actual prevalence of thyroid pathology and dysgenesis in the population (Kuehnen et al. 2009, Brix et al. 2011). This is in accord with observations that in addition to the T_3-mediated transcriptional effects, TH is involved in various non-genomic, TR-independent signal transduction pathways that are initiated at the plasma membrane, the cytoplasm, or in organelles,

particularly the mitochondria (Wrutniak-Cabello et al. 2001, Cheng et al. 2010, Lanni et al. 2011). Such pathways are mediated *via*, for example, adhesion receptors, such as the alpha(v)beta(3) ($\alpha_v\beta_3$) integrin, which rapidly activates the extracellular-signal-regulated kinase (ERK) pathway (a component of the mitogen-activated protein kinase (MAPK) pathway) (Bergh et al. 2005, Scarlett et al. 2008, Mullur et al. 2014). Moreover, extra-nuclear T_3-TR interaction has been reported to mediate intracellular AKT-mammalian target of rapamycin (mTOR) and p70^{S6K} and phosphatidylinositol 3-kinase-integrin linked kinase-matrix metalloproteinase-2 signalling pathways, to promote growth and metastasis of thyroid cancer in a mouse model expressing mutant TRβ (Furuya et al. 2009). Besides, it has been suggested that T_4 can induce MAPK signalling by activating a GPCR, that is, without requiring transport into the target cell (Lin et al. 1999).

Among the non-genomic, or "non-classical", effects of TH are rapid increases in cardiac contractility and output, vasodilation, and thermogenesis (Lynch et al. 1985, Schmidt et al. 2002, Bassett et al. 2003, Wang et al. 2003). However, many such alternative, non-classical mechanisms of TH signalling, and their physiological significance, remain to be further explored. Some non-genomic effects are induced by non-classical TH molecules, such as the ones discussed below (see section 2.2.3).

2.2 Trace amine-associated receptors

Trace amine-associated receptors (TAARs) are a subclass of rhodopsin-like G-protein coupled receptors (GPCRs) discovered in 2001 (Borowsky et al. 2001, Bunzow et al. 2001), which have been characterised in detail in 2001 as scarcely expressed receptors in various human and rodent tissues, responsive to trace amine (TA) activation. TA, such as p-tyramine, β-phenylalamine (β-PEA), tryptamine and octopamine, which are derived from classical biogenic amines, are found in trace concentrations in the CNS (Boulton 1984, Berry 2004, Hashiguchi and Nishida 2007).

Nine *Taar* genes have been identified in both human and chimpanzee, including 3 and 6 pseudogenes, respectively, as opposed to 16 (including 1 pseudogene) and 19 (including 2 pseudogenes) in mouse and rat, respectively (Lindemann et al. 2005). Sequence analysis of the *Taar* gene sequences led to them being phylogenetically classified into 3 subgroups: *Taar1-4*, *Taar5* and *Taar6-9*, which are also indicative of potential functional differences, judging by the putative ligand binding pockets (Lindemann et al. 2005). In terms of chromosomal localisation, the human *Taar* genes collectively map 109 kb of chromosome 6q23.1, whereas mouse *Taar*

genes are localised on chromosome 10A4 with a total of 192 kb (Lindemann et al. 2005). Coincidentally, the long arm of the sixth human chromosome, on which the cluster of *Taar* genes is localised, has been identified as a susceptibility locus for schizophrenia (Cao et al. 1997). Moreover, human TAAR6 (previously called TAAR4) has been shown to be preferentially expressed in brain regions associated with schizophrenia pathophysiology (Duan et al. 2004). TAAR association with schizophrenia if further commented on in section 2.2.4.

The suggested Taar ligands, TA, are synthesised from their amino acid precursors typically by the enzymatic action of aromatic L-amino acid decarboxylase (AADC), at a rate comparable to the synthesis of classical neurotransmitters (Berry 2004, Lindemann and Hoener 2005). However, they are then rapidly metabolised by monoamine oxidase (mainly type B; MAO-B) (Grimsby et al. 1997), resulting in an estimated half-life for TAs of 30s, therefore ensuring that their concentration in the CNS remains in the nanomolar range, several hundred-fold less than the concentration of classical neurotransmitters (Durden and Philips 1980, Berry 2004). Functionally, TAs have been described as being "sympathomimetics", and are thought to act as neuromodulators by affecting monoamine neurotransmitter synaptic and post-synaptic activity by direct interaction with GPCRs, such as TAAR1 (Berry et al. 1994, Branchek and Blackburn 2003, Burchett and Hicks 2006, Zucchi et al. 2006). This is further supported by the fact that inhibition of MAO-B activity results in elevated levels of β-PEA and enhanced sensitivity to dopamine (Berry et al. 1994, Chen et al. 1999, Holschneider et al. 2001). Moreover, TAs – namely β-PEA, 3-T_1AM and tyrosine – were found to induce concentration-dependent chemosensory migration in subsets of human granulocytes tested positive for both TAAR1 and TAAR2 expression (Babusyte et al. 2013).

With the exception of *Taar1*, all *Taar*'s were found to be selectively expressed in mouse olfactory epithelium and, consequently, were shown to bind volatile amines (Liberles and Buck 2006), suggesting that they perform a chemosensory function in mammals, as well as other vertebrates (Hashiguchi and Nishida 2007, Liberles 2015). *Taar1*, on the other hand, has been found to be distributed in various regions of the human, rhesus monkey and mouse CNS (Borowsky et al. 2001, Lindemann and Hoener 2005, Liberles and Buck 2006, Lindemann et al. 2008). In addition, *Taar1* has been reported to be expressed in low to moderate amounts in human peripheral tissue, including stomach, and kidney (Borowsky et al. 2001), discussed in more detail below.

2.2.1 Trace amine-associated receptor 1

Structurally, TAARs are highly conserved 7-transmembrane domain GPCRs, with an extracellular N-terminal domain and a cytosolic C-terminus (Lindemann et al. 2005). According to the UniProt database, the human TAAR1 (hTAAR1) protein (accession code: Q96RJ0) contains 2 potential N-glycosylation sites at asparagine (Asn) residues number 10 and 17, as well as a disulphide bond linking the second and third extracellular loops – a rather conserved feature of TAAR proteins - making a total of 339 amino acid long protein with a molecular mass of approximately 39.1 kDa. By contrast, the mouse TAAR1 (mTAAR1) protein (Q923Y8) contains a single potential N-glycosylation site at Asn residue 9, in addition to a potential disulphide bond between residues 95 and 181, making up for a predicted molecular mass of 37.6 kDa of the non-glycosylated protein. Inter-species sequence homology for *Taar1* reaches 90% for mouse and rat, but still there is an average of 79% homology between human and rodent *Taar1 (Lindemann et al. 2005, Miller 2011).* Comparison of nucleotide and amino acid sequences of the human *vs.* mouse *Taar1* gene and TAAR1/Taar1 protein, respectively, using the Basic Local Alignment Search Tool (BLAST) provided by the National Center for Biotechnology Information (NCBI, MD, USA)[1] indicate an 80% and 75% gene and protein sequence homology, respectively.

Subsequent studies expanded the spectrum of Taar1 agonists to include other endogenous biogenic amines, including the classical monoamine neurotransmitters, such as dopamine and serotonin, as partial agonists of human and rodent Taar1 (Lindemann and Hoener 2005, Lindemann et al. 2008), in addition to thyronamines (Scanlan et al. 2004) (discussed in section 2.2.3) and exogenous, amphetamine-like psychostimulants, all of which trigger signal cascades eventually resulting in the accumulation of cAMP (Bunzow et al. 2001, Miller et al. 2005, Reese et al. 2007, Wainscott et al. 2007, Barak et al. 2008, Kleinau et al. 2011). This indicated that Taar1 signals via the $G_{\alpha s}$-coupled pathway.

2.2.2 *In vitro* Taar1 expression

The responsiveness of Taar1 to TA, thyronamines and exogenous psychostimulants made it the centre of pharmacological interest as a target for treatment of psychological and neurological disorders (Wolinsky et al. 2007, Lindemann et al. 2008, Xie and Miller 2009, Revel et al. 2011, Pei et al. 2016). This led to many *in vitro* studies whose goal was to pharmacologically analyse the GPCR, therefore human, rhesus monkey or rodent TAAR1/Taar1 were expressed in HEK 293

---

[1] https://blast.ncbi.nlm.nih.gov/Blast.cgi

cells, but also in COS-7 and U2OS cell lines (Borowsky et al. 2001, Bunzow et al. 2001, Miller et al. 2005, Barak et al. 2008). However, this proved a challenge as Taar1 appeared to exhibit poor surface targeting (Grandy 2007, Miller 2011), and Taar1 was consequently suggested to localise to and signal from intracellular compartments (Bunzow et al. 2001). Various approaches have been employed in an attempt to promote Taar1 trafficking to the plasma membrane to enable pharmacological characterisation, including introducing a cleavable 16 amino acid long signal sequence to the N-terminus of rat Taar1 (Bunzow et al. 2001), or modifying the N-terminus, C-terminus and third intracellular loop of the human TAAR1 with those corresponding to the rat Taar1 (Lindemann et al. 2005, Grandy 2007, Reese et al. 2007). The latter chimera, however, was similar to the mouse Taar1 in terms of pharmacological profile (Lindemann et al. 2005, Grandy 2007, Reese et al. 2007). In another experiment, the N-terminus of human TAAR1 was modified to additionally contain the first 9 amino acids of the human β2-adrenergic receptor, which contains an N-linked glycosylation site on the 6th residue (Barak et al. 2008), a post-translational modification that is known to modulate GPCR transport to the cell surface (Dong et al. 2007). Subsequently, the latter construct was used to show that TAAR1 is able to heterodimerise with mouse dopamine D2 receptor when co-expressed in HEK 293 cells, and that the latter modulated the surface expression of TAAR1 (Espinoza et al. 2011).

2.2.3   Thyronamines as Taar1 agonists

Thyronamines (TAM) are metabolic derivatives of classical TH, therefore structurally related to T_3 and T_4 but lacking the carboxyl-group and the alanine side chain (Scanlan et al. 2004, Chiellini et al. 2017).

Although the precise physiological function of TAM remains to yet be determined, they have been described to counter the effects of classical TH. The administration of synthetic 3-iodothyronamine (3-T_1AM) and, though less effectively than the former, thyronamine (T_0AM) to rodents has been shown to decrease metabolic rate, manifesting in a dose-dependent bradycardia, decreased cardiac output, hypothermia, and hyperglycemia (Scanlan et al. 2004, Doyle et al. 2007, Frascarelli et al. 2008, Klieverik et al. 2009, Piehl et al. 2011, Venditti et al. 2011); the latter was also reproduced in the Djungarian hamster, where the carbohydrate metabolism was blocked upon injecting 3-T_1AM, shifting the metabolism towards lipid utilisation

(Braulke et al. 2008, Ghelardoni et al. 2014). TAM have been therefore termed as the "cool thyroid hormones" (Brix, Führer, Biebermann, 2011).
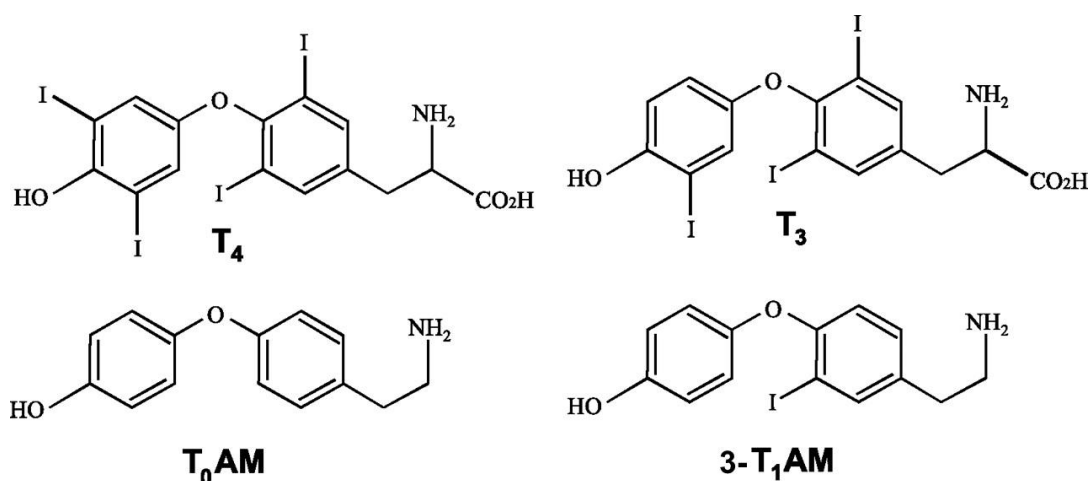
Figure 2: The structure of thyroid hormones (T_4 and T_3) in comparison to thyronamines (3-T_1AM and T_0AM). (Image modified from (Doyle et al. 2007)).

Moreover, 3-T_1AM has been reported to inhibit TH transport by TH transporters, namely the inhibition of OATP1C1, which is believed to be responsible for transporting T_4 across the blood-brain-barrier, as well as inhibiting both T_3 and T_4 transport by the MCT8 receptor (Ianculescu et al. 2010). Contrarily, 3-T_1AM had no effect on OATP1B3 or MCT10. This suggests that 3-T_1AM modulates the delivery of TH to target tissue, including the brain (Ianculescu et al. 2010). Additionally, 3-T_1AM was reported to inhibit monoamine transport into synaptic vesicles in rat brain, and to inhibit dopamine and norepinephrine reuptake, hence suggesting a neuromodulatory role (Snead et al. 2007). TAM, however, have been shown not to interact with nuclear TH receptors (Scanlan et al. 2004, Zucchi et al. 2006), but cellular 3-T_1AM uptake appears to occur independent of sodium chloride, *via* specific transporters, in a pH dependent manner (Ianculescu et al. 2009). Other GPCRs such as the $G_{\alpha s}$-coupled dopamine and β-adrenergic receptors have also been excluded as candidate receptors for TAM as the latter failed to amplify cAMP signalling in HEK 293 cells expressing either of the respective receptors (Scanlan et al. 2004).

On the other hand, 3-T_1AM (and to a lesser extent T_0AM) were found to potently activate mouse and rat Taar1 *via* the $G_{\alpha s}$ pathway, resulting in cAMP accumulation *in vitro* in a dose-dependent manner (Scanlan et al. 2004). However, it remains to be investigated whether this effect is directly induced by 3-T_1AM or is an indirect result of Taar1 stimulation by a metabolite of the said compound. 3-T_1AM was also shown to activate rhesus monkey Taar1 in an *in vitro* system, resulting in cAMP accumulation at levels comparable to those resulting from activation with β-

phenylethylamine, a potent monoamine Taar1 agonist (Panas et al. 2010). However, administration of 3-T_1AM *via* intraperitoneal injection to wild type and Taar1-deficient mice showed no significant difference in the decrease in body temperature between the two treatment groups, concluding that the thermoregulatory effect of 3-T_1AM is not Taar1-mediated (Panas et al. 2010).

Endogenously, 3-T_1AM and T_0AM have been detected in mouse blood serum and peripheral organs, including brain, heart, and liver (Scanlan et al. 2004). 3-T_1AM has also been measured in rat serum, reaching a concentration of 0.3 nM; however, significantly higher concentrations were detected in peripheral tissue (Saba et al. 2010). Scanlan *et al.* estimated the concentration of 3-T_1AM to be in the sub-picomolar range per gram of rat brain, in comparison to 1-6 pmol/g of T_4 in the same tissue (Scanlan et al. 2004). 3-T_1AM has also been detected in human blood (Saba et al. 2010). However, it has also been shown that as high as 90% of 3-T_1AM is present in bound form in human serum, where it binds with high affinity to the lipoprotein apoB100 (Roy et al. 2012). This could, in fact, account for the discrepancies in reported endogenous 3-T_1AM concentration depending on the method of detection (Ackermans et al. 2010, Hoefig et al. 2011, Galli et al. 2012, Hoefig et al. 2016). However, Hoefig *et al.* reported a median serum concentration of 66 ± 26 nM in healthy adults, measured by immunoassay (Hoefig et al. 2011).

There has been much speculation regarding the site of 3-T_1AM synthesis, whether it was a direct metabolite of T_4 and T_3, and whether it originated from the thyroid gland itself, or was of extrathyroidal origin (Ackermans et al. 2010, Hoefig et al. 2011, Hackenmueller et al. 2012, Hoefig et al. 2016). An *in vitro* experiment showed no 3-T_1AM production in primary rat thyrocytes nor FRTL-5 cells following incubation with T_4 (Agretti et al. 2011). Moreover, it was observed that serum 3-T_1AM was comparable to slightly higher in patients receiving T_4-substitute than in healthy, euthyroid individuals, which strongly suggested 3-T_1AM to be an extrathyroidal T_4-derivative (Hoefig et al. 2011).

Conversely, using ^{13}C-labelled T_4, Ackermans *et al.* were able to detect the conversion to T_3, but not to 3-T_1AM, in rat plasma and brain tissue, however, nor were they able to detect any endogenous 3-T_1AM or T_0AM in either rat plasma or human plasma and thyroid tissue (Ackermans et al. 2010). Subsequently, Hackenmueller *et al.* demonstrated that hypothyroid mice that underwent hormone replacement with either T_4 or an isotope-labelled (heavy) T_4 (H-T_4) resulted in elevation in liver T_3 and H-T_3, respectively, but did not affect 3-T_1AM levels. Rather, with the induction of hypothyroidism there was a gradual decrease in liver 3-T_1AM, which could not be recovered by T_4 treatment (Hackenmueller et al. 2012). As such, it is deemed that 3-T_1AM

is produced within the thyroid *via* a process independent but similar to that of T_4 biosynthesis, also requiring a sodium-iodide symporter (NIS, responsible for the active transport of iodide into thyrocytes (Spitzweg and Morris 2002)) and thyroperoxidase (TPO, responsible for the iodination of tyrosine residues in Tg (Ruf and Carayon 2006)), leading the authors to speculate that 3-T_1AM was not of extrathyroidal origin (Hackenmueller et al. 2012). However, Hoefig *et al.* argued that, while hypothyroidism in mice was induced through administering 0.1% methimazole and 0.2% potassium perchlorate, it would cause systemic inhibition of both NIS and TPO, thereby potentially affecting the deiodinating and decarboxylating enzymes needed for 3-T_1AM generation (Hoefig et al. 2015, Hoefig et al. 2016). Contrarily, it is only a lack of thyroidal NIS and TPO in thyroidectomy and/or radiotherapy patients receiving T_4-substitutes orally, as opposed to injected T_4 as in the experimental model (Hoefig et al. 2011). This led the authors to hypothesise and subsequently show *in vitro* that T_4 is metabolised into 3-T_1AM in the intestine (Hoefig et al. 2015). This is done through several deiodination and decarboxylation steps involving ornithine decarboxylase (Hoefig et al. 2015).

2.2.4   Taar1-deficient mouse model

The detection of Taar1 in mouse dopaminergic and serotonergic brain regions led to extensive studies being conducted, focusing on the modulatory role of Taar1 in the monoaminergic system (Lindemann et al. 2008, Xie and Miller 2009, Revel et al. 2011). Accordingly, in rhesus monkey Taar1 has been shown to colocalise with dopamine transporters in brain tissue and to functionally regulate it (Xie and Miller 2007, Xie et al. 2007). Besides, since TA have long been associated with neuropsychiatric disorders, Taar1, being a TA-responsive GPCR expressed in the CNS, elicited much interest for its potential role in depression, attention deficit hyperactivity disorder (ADHD), Parkinson's disease, and schizophrenia (Branchek and Blackburn 2003). Interestingly, the thyroglobulin-processing cysteine protease cathepsin K (section 2.1.1) has also been linked to schizophrenia, since its expression has been found to be up-regulated in the cerebra of chronic schizophrenia patients (Bernstein et al. 2007, Bernstein et al. 2008).

The Taar1-deficient (*Taar1*$^{-/-}$) mouse model has been generated to study the role of Taar1 as a regulator of TA neuromodulatory effects, hailing it as a model "with relevance to schizophrenia" (Wolinsky et al. 2007, Lindemann et al. 2008). The *Taar1*$^{-/-}$ was generated by replacing the entire *Taar1*-coding sequence with a LacZ reporter gene, fused to a nuclear localisation sequence

(NLS), in frame with the original *Taar1* promoter, such that the latter drives the expression of the *LacZ* replacement gene, producing β-galactosidase in tissue where *Taar1* is normally expressed (Lindemann et al. 2008). This enabled tissue screening for *LacZ* expression, through staining *Taar1*^{-/-} tissue with 5-bromo-4-chloro-3-iodoxyl-β-D-galactopyranoside to detect β-galactosidase, resulting in serotonergic and dopaminergic areas of the brain to be identified as Taar1-expressing (Lindemann et al. 2008). No morphological alterations in the *Taar1*^{-/-} mouse brain were observed, nor did the mouse exhibit any developmental or behavioural differences when compared to their wild type (WT) littermates (Lindemann et al. 2008). However, *Taar1*^{-/-} mice demonstrated reduced prepulse inhibition to acoustic stimuli, and elevated sensitivity to amphetamines in comparison to WT littermates, which manifested in enhanced locomotor activity that correlated with higher dopamine and norepinephrine release in the striatum, which is in line with findings that the firing frequency of dopaminergic neurons was increased upon Taar1 inhibition by the selective antagonist N-(3-Ethoxy-phenyl)-4-pyrrolidin-1-yl-3-trifluoromethyl-benzamide (EPPTB) (Bradaia et al. 2009), as well as a significant increase in striatal expression of high-affinity dopamine type 2 receptors, all of which are characteristic symptoms of schizophrenia (Wolinsky et al. 2007, Lindemann et al. 2008, Espinoza et al. 2015, Sukhanov et al. 2016).

Thus, targeting Taar1 as a prospective treatment of psychological disorders has been the centre of numerous studies to date (Revel et al. 2012, Tallman and Grandy 2012, Revel et al. 2013, Alvarsson et al. 2015). However, It is noteworthy that the HPT axis is directly affected in various neuropsychiatric symptoms, with a range of phenotypic deviations from normal thyroid function, including both hypothyroidism and hyperthyroidism, being exhibited in patients with schizophrenia (Othman et al. 1994, Santos et al. 2012), as well as in those suffering from various manifestations of depression (Hage and Azar 2012). The present study is the first to address Taar1 in the context of the thyroid gland, knowing that many psychological disorders are linked to disorders in thyroid function.

3. Aims of the Study

The general aim of this study was to better understand the non-classical pathways by which the thyroid gland can self-regulate its function, i.e. independent of TSH stimulation, and to investigate the potential involvement of THT and Taar1 in such a mechanism.

The thyroid gland is classically regulated by the hypothalamic-pituitary-thyroid axis *via* a series of feedback loops, where the hypothalamus signals to the pituitary to release TSH, which stimulates thyrocytes to liberate TH from the precursor Tg by action of Tg-processing proteases, including cathepsins B, K and L. This ensures an adequate supply of TH in the circulation for target tissues. However, when viewed as simply a TH-releasing gland, many intrinsic regulatory processes that contribute to this overall mechanism and to thyroid gland homeostasis could be overlooked. The concept of thyroid auto-regulation relies first and foremost on approaching the thyroid gland not exclusively as a TH-producing organ, but also as a TH- target itself. Thyrocytes express various THT, thereby have varying capacities for transporting TH molecules. The levels of THT expression are tissue-specific, implying that the process of importing and exporting different TH molecules is a tightly regulated one, also within the thyroid itself. Moreover, despite the notion that all follicles have equal supply of TSH from the circulation, the follicular population within a thyroid gland retains heterogeneity in terms of the degree of activation, i.e. variability in efficiency of Tg production and Tg degradation (TH liberation), at a given time. This further suggests that a mechanism exists that dictates such autonomy of thyroid follicles.

Therefore, a follicle has to have a mechanism by which it senses the levels of intrathyroidal TH, as accordingly regulate Tg-proteolysis in a mechanism additional to the classical, TSH-dependent pathway.

Several THT have been identified that are expressed at different levels in a tissue specific manner. This study is, in part, based on the hypothesis that THT may be involved in a non-classical pathway of thyroid regulation, namely by acting as sensors for intrathyroidal TH concentrations, and by associating with Tg-processing proteases, including cysteine cathepsins, because they are vital for TH liberation from Tg.

Accordingly, a study was designed to investigate the interrelation between the availability of Tg-processing cathepsins, the extent of Tg-degradation and TH liberation, and the expression and localisation of specific THT. To this end, Tg degradation status and Tg-processing cathepsin profiles were assessed in mouse models with single or double deficiencies in Mct8 and/or Mct10, and compared to WT C57BL6/J mice.

An additional potential thyroid regulatory pathway could be mediated by thyronamines, which are the decarboxylated and deiodinated endogenous derivatives of T_3 and T_4. In some tissue types, and under certain physiological states, thyronamines were suggested to mediate the opposite effects of their precursors, therefore, they were referred to as the "cool TH" or non-classical TH. Furthermore, 3-iodothyronamine (3-T_1AM) was suggested to exert a modulatory effect on TH delivery to target tissue by inhibiting TH uptake by THT (Ianculescu et al. 2010). Notably, 3-T_1AM, has been reported to be the putative ligand for Taar1, and whether THT inhibition by 3-T_1AM is Taar1-mediated or not, remains an open question.

Accordingly, the proposed hypothesis is that Taar1 in the thyroid may function as a 3-T_1AM triggered receptor to possibly mediate further regulatory effects on the follicle's capacity for quickly altering Tg storage or Tg utilisation for TH release, which could also be by modulating THT function. Therefore, the present study was designed to characterise Taar1 in the context of the thyroid gland, and its potential involvement in thyroid gland auto-regulation.

In this context, this study questioned whether Taar1 is at all expressed in thyroid epithelial cells and, if so, what is its subcellular localisation. To verify the presence of Taar1 in thyrocytes, thyroid cryosections from WT C57BL6/J male mice were immunolabelled with antibodies specific for mouse Taar1, as testified by its weak reactivity in the Taar1-deficient thyroid tissue cryosections. Following verification of the presence of Taar1 on the apical plasma membrane domain *in situ*, and additionally at ciliary membranes *in vitro*, the next step was to elucidate the trafficking and precise subcellular localisation of Taar1, for which *in vitro* models were established stably expressing mouse Taar1 with a covalently linked C-terminal enhanced green fluorescence protein tag (mTaar1-EGFP). The remaining questions to answer were, if Taar1 has a functional role in the thyroid gland, how does Taar1-deficiency affect the morphological parameters of thyroid epithelia? How does it affect the proteolytic capacity and availability of Tg-processing cathepsins and Tg-degradation status? Morphological parameters, such as follicle and/or lumen size, and epithelial extension, can be representative of a thyroid follicle's functional status since more extended (prismatic) cells are associated with higher cell activation, which could mean more Tg synthesis and/or Tg processing. Synthesised Tg is stored in cross-linked form in the lumina of thyroid follicles, hence an alteration in luminal size can indicate alterations in Tg synthesis, cross-linkage or processing. For the later, Tg-processing and degradation capacity is dependent on the availability and activity of Tg-processing proteases, including cathepsins B, K and L. Therefore, careful assessment of all these parameters can serve as an evaluation method of thyroid function. Additionally, the effect of Taar1-deficiency on the

overall thyroid status is assessed by measuring serum T_3, T_4 and TSH concentration. To this end, the Taar1-deficient model was employed; morphological and biochemical analyses were performed on thyroid epithelial tissue from Taar1-deficient thyroids from both young (5-8 months old) and adult (10-15 months old) male mice, and compared to their WT counterparts.

4. Results

The result of this work is a compilation of five studies, as listed below, each presented in detail as a separate manuscript:

1- Brix, K., **M. Qatato**, J. Szumska, V. Venugopalan, and M. Rehders. Thyroglobulin storage and degradation for thyroid hormone liberation. In: The Thyroid and Its Diseases, edited by Markus Luster, Leonidas Duntas, and Leonard Wartofsky, Springer-Verlag Berlin/Heidelberg. REVIEW. [Submitted on 15/08/2016; in press].

This is a review that explores Tg biosynthesis and storage, and the regulatory processes underlying Tg proteolysis for thyroid hormone liberation, which largely occur through feedback to the hypothalamic-pituitary-thyroid (HPT) axis, but which it also regulated intrafollicularly, in part, by Tg itself. This review therefore also explores the autonomous mechanisms that occur within a particular thyroid follicle, independent of the HPT-axis, leading to several unanswered questions that revolve around the concept of "thyroid auto-regulation", particularly what are the part-takers involved in regulating thyroid follicular homeostasis, and what is the role of Tg-processing cathepsins in this process. The subsequent studies aim at answering some of the open questions in thyroid cell biology.

Contribution: *MQ contributed to topic discussion and manuscript writing.*

2- Weber J., McInnes J., Kizilirmak C., Rehders M., **Qatato M.**, Wirth E. K., Schweizer ., Verrey F., Heuer H., Brix K. (2017). Interdependence of thyroglobulin processing and thyroid hormone export in murine thyrocytes. EJCB 96(5): 440-456. doi: 10.1016/j.ejcb.2017.02.002

This research article focuses on thyroid hormone transporter-deficient mouse models, namely, the Mct8-deficient, Mct10-deficient, and the Mct8/Mct10-double deficient mice, to study the interrelationship between THT and Tg-processing cathepsins, and the effect that THT-deficiency has on Tg-proteolysis. It correlates thyroid hormone transporter deficiency to increased protein levels of Tg-processing cathepsins, and therefore, an increase in intrathyroidal Tg-proteolysis, leading to intra-follicular thyrotoxic states, because the TH liberated in higher amounts cannot be exported from follicles deficient in either Mct8 and/or Mct10. It concludes that THT Mct8 and Mct10 act as sensors of intrathyroidal thyroid hormone

levels, and cross-talk with Tg-processing cathepsins in a counter-intuitive and HPT axis-independent fashion, such that when the sensing mechanism is impaired due to altered THT expression, Tg-proteolysis is enhanced such that intrathyroidal thyrotoxicity results.

Contribution: *MQ contributed to the experiment described in Figure 2 (immunohistochemistry), and was involved in results' discussion and manuscript editing.*

3- Szumska J., **Qatato M.**, Rehders M., Führer D., Biebermann H., Grandy D.K., Köhrle J., Brix K. (2015). Trace amine-associated receptor 1 localization at the apical plasma membrane domain of Fisher rat thyroid epithelial cells is confined to cilia. Eur Thyroid J. 4(Suppl 1): 30–41. doi: 10.1159/000434717.

This research article investigates the subcellular localisation of trace amine-associated receptor (Taar1) in thyroid epithelial cells, Taar1 being a GPCR shown to be responsive to thyronamine stimulation *in vitro.* This study reports Taar1 to localise to primary cilia of FRT cells *in vitro*, as well as to the apical plasma membrane domain of mouse thyroid epithelial cells *in situ*. The latter suggests the primary cilium to constitute the signalling platform for Taar1 and that, being extended into the extracellular luminal space, the Taar1 could be thus exposed to its ligand. Accordingly, if a thyronamine such as 3-T_1AM is the endogenous Taar1 ligand, this may speak in favour of the intrathyroidal origin of 3-T_1AM, or else, of its transport into the luminal space by an unknown pathway. Moreover, since thyronamines are known to antagonise thyromimetic effects, i.e. can act as non-classical TH molecules, Taar1 signalling may contribute to non-classical thyroid regulation.

Contribution: *MQ contributed to preliminary immunocytochemistry experiments, and control experiments (immunoblotting), and was involved in data interpretation and discussion, as well as manuscript writing.*

4- **Qatato M**., Dallto W., Hein Z., Springer S., Biebermann H., Brix K. Establishing an *in vitro* model to study trafficking of mouse Taar1 in thyroid epithelial cells. [To be submitted].

Previous *in vitro* studies suggested that Taar1 may signal from intracellular compartments. However, our study discussed above showed Taar1 to localise apically and on ciliary extensions in rodent thyrocytes, suggesting that at least in the thyroid, Taar1 may signal from the apical plasma domain of thyrocytes *in situ*, where it is exposed to the content of the follicle lumen. This research article represents a study designed to explore mouse Taar1 trafficking, heterologously expressed in rat and human thyroid cell lines in order to establish an *in vitro* system in which Taar1 signalling from the cell surface can be studied. In addition, such a model would be suited answering which effect that signalling may have on thyrocytes' function in terms of Tg-processing cathepsins' activity and/or the expression and function of THT and TSH receptor.

The results show that the chimeric mouse Taar1-EGFP does traffic to the cell surface, and localises particularly to ciliary membranes in polarised thyroid cells featuring a primary cilium. Moreover, mTaar1-EGFP appears to form homodimers and tetramers in stably expressing human thyroid cell lines.

To further address the potential function of Taar1 in the thyroid gland, the thyroid gland of Taar1-deficient male was biochemically and morphometrically assessed in the study below.

Contribution: *MQ contributed to the design of the study, performed experiments described in Figures 2-12, was involved in data discussion and interpretation, and drafted the manuscript.*

5- **Qatato M.***, Szumska J.*, Skripnik V., Rijntjes E., Köhrle J., Grandy D.K., Brix K. Canonical TSH regulation of cathepsin-mediated thyroglobulin processing in the thyroid requires Taar1 expression. Frontiers in Pharmacology. [Submitted on 17/12/2017].
(* contributed equally)

This research article offers insight into the role of Taar1 in thyroid homeostasis through characterising the morphometric parameters of the thyroid gland of Taar1-deficient male mice,

in comparison to their WT counterparts, and by biochemically evaluating and correlating the Tg degradation status to the protein and activity levels of Tg-processing cathepsins, as well as aiming at assessing systemic concentrations of T_3, T_4 and TSH. This study reveals that Taar1-deficiency causes a subtle disbalance in the proteolytic network in the thyroid, but more strikingly, it reveals that Taar1 is required to maintain canonical, basolateral localisation of TSH receptor in mouse thyrocytes, thereby maintaining homeostasis in the HPT axis.

Contribution: *MQ contributed to the design of the study, as well as performed the experiments described in Figures 1, 2A, 3 and 4 (immunolabelling, microscopy, image analysis on CellProfiler, and data analyses), Figures 5F and 6 (SDS-PAGE, silver staining, immunolabelling, microscopy and data analyses), and Figure 10C (TSH ELISA and data analysis), and was involved in data discussion and interpretation, as well as contributed to statistical analysis and manuscript writing.*

This study demonstrates the existence of a functional link between THT and Tg-processing cathepsins, showing that in the thyroid gland, THT not only enable TH transport across thyrocytal membranes, but also involve in regulation of TH liberation in a TSH-independent mode. This study also points out that Taar1 is expressed in the thyroid gland, where it maintains an apical localisation, as well as to localising at cilia in thyrocytes *in vitro*, as demonstrated by studying mTaar1-EGFP trafficking in a cell system stably expressing the chimeric protein. Remarkably, this study suggests a potential functional link between Taar1 and the TSH receptor, where localisation of the latter is altered in mouse thyroid epithelia lacking a functional Taar1. Although the absence of a functional Taar1 does not affect thyroid development to a large extent, and only mildly affects its capacity to liberate TH, the altered TSH receptor localisation presents a novel, interesting finding, and highlights the importance of considering potential side-effects that Taar1-targeting pharmaceuticals might have on thyroid function.

4.1 Thyroglobulin storage and degradation for thyroid hormone liberation

Klaudia Brix*, Maria Qatato, Joanna Szumska, Vaishnavi Venugopalan, Maren Rehders

* Corresponding Author:

Dr. Klaudia Brix, Professor of Cell Biology

Department of Life Sciences and Chemistry

Jacobs University Bremen

Campus Ring 1

D-28757 Bremen

Germany

Phone: +49.421.200.3246

e-mail: k.brix@jacobs-university.de

Abstract

The tasks of the thyroid gland comprise (i) thyroid hormone (TH) generation *via* synthesis of the pro-hormone thyroglobulin (Tg), (ii) import and organification of iodine resulting in the generation of preformed TH bound to Tg, (iii) Tg storage in covalently cross-linked form in the extracellular follicle lumen, (iv) TH demand-driven solubilization of Tg from its storage forms, (v) proteolytic processing of Tg for TH liberation by extra- and intracellular means, (vi) complete degradation of Tg upon its re-internalization, and (vii) TH release into the bloodstream. Therefore, this chapter focuses on thyroid cell biology and describes how classical thyroid hormones are generated, liberated and released from thyroid follicles.

Key-words: cathepsins, covalent cross-linkage, endocytosis, extracellular thyroglobulin processing, intracellular thyroglobulin degradation, lysosomes, proteases, protein processing, thyroglobulin, trafficking

4.2 Interdependence of thyroglobulin processing and thyroid hormone export in the mouse thyroid

Jonas Weber [1], Joseph McInnes [1,†], Cise Kizilirmak [1], Maren Rehders [1], Maria Qatato [1], Eva K. Wirth [2], Ulrich Schweizer [3], Francois Verrey [4], Heike Heuer [5], and Klaudia Brix [1]

[1] Jacobs University Bremen, Department of Life Sciences and Chemistry, Campus Ring 1, D-28759 Bremen, Germany;

[2] Charité-Universitätsmedizin Berlin, Institut für Experimentelle Endokrinologie, Augustenburger Platz 1, D-13353 Berlin, Germany;

[3] Universität Bonn, Institut für Biochemie und Molekularbiologie, Nußallee 11, D-53115 Bonn, Germany;

[4] Universität Zürich, Physiologisches Institut, Winterthurerstrasse 190, CH-8057 Zürich, Switzerland

[5] IUF – Institut für umweltmedizinische Forschung, Auf'm Hennekamp 50, D-40225 Düsseldorf, Germany;

[†] Present address: VIB Center for Brain and Disease Research and KU Leuven Department for Human Genetics, 3000 Leuven, Belgium

Corresponding Author

Dr. Klaudia Brix, Professor of Cell Biology

Jacobs University Bremen, Department of Life Sciences and Chemistry

Campus Ring 1, D-28759 Bremen, Germany

phone: +49.421.200.3246; fax: +49.421.200.3249; e-mail: k.brix@jacobs-university.de

Abstract

Thyroid hormone (TH) target cells need to adopt mechanisms to maintain sufficient levels of TH to ensure regular functions. This includes thyroid epithelial cells, which generate TH in addition to being TH-responsive. However, the cellular and molecular pathways underlying thyroid auto-regulation are insufficiently understood. In order to investigate whether thyroglobulin processing and TH export are sensed by thyrocytes, we inactivated thyroglobulin-processing cathepsins and TH-exporting monocarboxylate transporters (Mct) in the mouse. The states of thyroglobulin storage and its protease-mediated processing and degradation were related to the levels of TH transporter molecules by immunoblotting and immunofluorescence microscopy. Thyroid epithelial cells of cathepsin-deficient mice showed increased Mct8 protein levels at the basolateral plasma membrane domains when compared to wild type controls. While the protein amounts of the thyroglobulin-degrading cathepsin D remained largely unaffected by Mct8 or Mct10 single-deficiencies, a significant increase in the amounts of the thyroglobulin-processing cathepsins B and L was detectable in particular in Mct8/Mct10 double deficiency. In addition, it was observed that larger endo-lysosomes containing cathepsins B, D, and L were typical for Mct8- and/or Mct10-deficient mouse thyroid epithelial cells. These data support the notion of a crosstalk between TH transporters and thyroglobulin-processing proteases in thyroid epithelial cells. We conclude that a defect in exporting thyroxine from thyroid follicles feeds back positively on its cathepsin-mediated proteolytic liberation from the precursor thyroglobulin, thereby adding to the development of auto-thyrotoxic states in Mct8 and/or Mct10 deficiencies. The data suggest TH sensing molecules within thyrocytes that contribute to thyroid auto-regulation.

4.3 Trace amine-associated receptor 1 localization at the apical plasma membrane domain of Fisher rat thyroid epithelial cells is confined to cilia

Joanna Szumska[1], Maria Qatato[1], Maren Rehders[1], Dagmar Führer[2], Heike Biebermann[3], David K. Grandy[5], Josef Köhrle[4], Klaudia Brix[1]

[1] Department of Life Sciences and Chemistry, Jacobs University Bremen, Bremen, Germany
[2] Department of Endocrinology and Metabolism and Division of Laboratory Research, University of Duisburg-Essen, Essen, Germany
[3] Institut fur Experimentelle Padiatrische Endokrinologie, Charite-Universitatsmedizin Berlin, Berlin, Germany
[4] Institut fur Experimentelle Endokrinologie, Charite-Universitatsmedizin Berlin, Berlin, Germany
[5] Department of Physiology and Pharmacology, School of Medicine and the Knight Cardiovascular Institute, Oregon Health & Science University, Portland, Oreg., USA

Corresponding Author:
Dr. Klaudia Brix, Professor of Cell Biology, Jacobs University Bremen, Department of Life Sciences and Chemistry, Campus Ring 1, D-28759 Bremen, Germany.
Phone: +49 (0)421 200 3246
Fax: +49 (0)421 200 3249
E-mail: k.brix@jacobs-university.de

Running Title: Taar1 in cilia of FRT cells (27 characters)

Key-Words: Thyroid gland, Thyroid hormones, Thyronamines, Taar1, Thyroid follicle, G-protein coupled receptors.

Abstract

Background: The trace amine-associated receptor 1 (Taar1) is one member of the Taar family of G-protein-coupled receptors (GPCR) accepting various biogenic amines as ligands. It has been proposed that Taar1 mediates rapid, membrane-initiated effects of thyronamines, the endogenous decarboxylated and deiodinated relatives of the classical thyroid hormones T_4 and T_3.

Objectives: Although the physiological actions of thyronamines in general and 3-iodothyronamine (T_1AM) in particular are incompletely understood, studies published to date suggest that synthetic T_1AM-activated Taar1 signaling antagonizes thyromimetic effects exerted by T_3. However, the location of Taar1 is currently unknown.

Methods: To fill this gap in our knowledge we employed immunofluorescence microscopy and a polyclonal antibody to detect Taar1 protein expression in thyroid tissue from Fisher rats, wild-type and *taar1*-deficient mice, and in the polarized FRT cells.

Results: With this approach we found that Taar1 is expressed in the membranes of subcellular compartments of the secretory pathway and on the apical plasma membrane of FRT cells. Three-dimensional analyses further revealed Taar1 immunoreactivity in cilial extensions of post-confluent FRT cell cultures that had formed follicle-like structures.

Conclusions: The results suggest Taar1 transport along the secretory pathway and its accumulation in the primary cilium of thyrocytes. These findings are of significance considering the increasing interest in the role of cilia in harboring functional GPCR. We hypothesize that thyronamines can reach and activate Taar1 in thyroid follicular epithelia by acting from within the thyroid follicle lumen, their potential site of synthesis, as part of a nonclassical mechanism of thyroid autoregulation.

4.4 Establishing an *in vitro* model to study trafficking of mouse Taar1 in thyroid epithelial cells

Maria Qatato[1], Willred Dallto[1], Zeynep Hein[1], Sebastian Springer[1], Heike Biebermann[2], Klaudia Brix[1]*

[1] Jacobs University Bremen, Department of Life Sciences and Chemistry, Campus Ring 1, D-28759 Bremen, Germany

[2] Charité-Universitätsmedizin Berlin, Institut für Experimentelle Pädiatrische Endokrinologie, Augustenburger Platz 1, D-13353 Berlin, Germany

* Correspondence:
Corresponding Author
Dr. Klaudia Brix, Professor of Cell Biology, Department of Life Science and Chemistry, Jacobs University Bremen, Campus Ring 1, 28759 Bremen, Germany; k.brix@jacobs-university.de

Keywords: Trace amine-associated receptor 1, GPCR, trafficking, KTC-1, Nthy-ori 3-1, green fluorescent protein.

Abstract

Trace amine-associated receptor 1 (Taar1) is a seven-transmembrane G protein-coupled receptor that has been identified as the putative receptor of thyronamines, endogenous thyroid hormone metabolites. Expression of Taar1 in heterologous systems has repeatedly reported intracellular localisation of Taar1, as opposed to the expected cell surface expression. However, we have shown Taar1 to be localised at the apical plasma membrane of mouse thyroid epithelial cells *in situ*, as well as on the primary cilia of Fisher rat cells *in vitro*. Therefore, this study was designed to investigate mouse Taar1 trafficking in thyrocytes further. To this end, *in vitro* models were established by stably expressing mouse Taar1 tagged with an enhanced green fluorescent protein, which was linked to the C-terminus of Taar1 by a 12-amino-acid peptide (mTaar1-EGFP), in human thyroid epithelial Nthy-ori 3-1 and carcinoma KTC-1 cell lines. Transport studies by temperature shift and colocalisation experiments with compartment-specific markers showed mTaar1-EGFP to localise predominantly as a membrane protein to vesicles in the perinuclear region of the transduced cells. However, a subset of mTaar1-EGFP was observed to reach the plasma membrane, being present particularly on ciliary extensions of polarised KTC-1 cells. SDS-

PAGE and immunoblotting analyses indicated mTaar1-EGFP to predominantly occur in dimeric and tetrameric form in both thyroid cell lines. The results suggest that an *in vitro*-cell model was established that recapitulates Taar1 trafficking in thyrocytes and will enable studying thyronamine-triggered Taar1 signalling in future, thus extending our general understanding of the potential significance of Taar1-thyronamine interactions for thyroid auto-regulation.

(247 words)

Introduction

Trace amine-associated receptor 1 (human TAAR1 / mouse Taar1) is a G protein-coupled receptor (GPCR) that has been identified to be susceptible to activation by a variety of biogenic amines (Borowsky et al. 2001, Bunzow et al. 2001); for review, see (Grandy 2007). Despite being expressed in various human and mouse peripheral tissues (Borowsky et al. 2001, Bunzow et al. 2001), TAAR1/Taar1 has been primarily investigated for its role in regulation of neuromodulation in the central nervous system. As such, it has been assessed as a potential target for pharmacological intervention to treat neurological and psychiatric disorders (Wolinsky et al. 2007, Lindemann et al. 2008, Revel et al. 2011); reviewed in (Xie and Miller 2009, Jing and Li 2015, Pei et al. 2016). Hence, TAAR1 trafficking and subcellular localisation has been of interest ever since its discovery, in order to understand its physiological role as well as help characterise it pharmacologically. The weak cell surface expression of TAAR1/Taar1 *in vitro* proved to be a challenge (Miller 2011). Bunzow et al. were first to report the expression of rat Taar1 chimera with an N-terminal tag consisting of an 8-amino acid M1 flag-tag, preceded by a 16-amino acids signal sequence derived from the influenza haemagglutinin virus, thus targeting the HA-M1 flag-tagged Taar1, in principle, for transport along the secretory route (Bunzow et al. 2001). Stably expressed in HEK 293 cells, the M1 flag-tagged rat Taar1 appeared to be distributed as puncta intracellularly, as opposed to the M1 flag-tagged human dopamine 1 receptor, expressed as a control G_s-coupled protein receptor, which localised at the surface of HEK 293 cells. This led the authors to speculate that Taar1 may require a chaperone to promote trafficking to the cell surface that is absent in HEK 293 cells, or else that Taar1 functioned predominantly as an intracellular GPCR. The latter conjecture was further supported by the notion that Taar1 ligands, such as endogenous biogenic amines, which are synthesised in the cytoplasm, may be translocated into vesicles (Bunzow et al. 2001). Similarly, a rhesus monkey Taar1 with an enhanced green fluorescence protein (EGFP) tag fused to its N-terminus was transiently expressed in HEK 293 cells, resulting in a

predominantly intracellular fluorescence signal distribution, despite an infrequent cell surface localisation (Miller et al. 2005). The same group subsequently showed that rhesus monkey Taar1 associated with the total membrane fraction, but not with the plasma membrane fraction (Xie et al. 2008). Although the molecular mechanism underlying TAAR1 failing to reach the cell surface remains undisclosed, it was shown that engineering an extra residue with a further N-linked glycosylation site to the N-terminus of the human TAAR1 enabled its trafficking to and localisation at the cell surface in HEK 293 and U2OS cells (Barak et al. 2008). This was achieved by creating a construct that consisted of a triple influenza haemagglutinin (HA) tag, followed by a sequence coding for the first 9 amino acids of the human β2 adrenergic receptor (β2AR), which contains an N-linked glycosylation consensus motif on site 6, fused in frame to a sequence coding for the human TAAR1, either with or without an EGFP tag on its C-terminus. That study presented surface localisation of the TAAR1 chimera modified with the β2AR N-terminal sequence, but not the non-modified protein, in HEK 293 cells (Barak et al. 2008).

All in all, TAAR1/Taar1 trafficking studies remain limited for the difficulty in expressing it stably in heterologous systems (Grandy 2007). Although the prevalent view is that it retains an intracellular localisation in several different cellular model systems, the exact transport pathways of TAAR1, its main subcellular localisation along the secretory route, and whether it has the ability, or the need, to dimerise or oligomerise with itself, or with other GPCRs, for productive transport to the cell surface remain an important field for investigations. Moreover, our recent discovery that Taar1 localises to the apical plasma domain of thyroid epithelial cells *in situ*, and rat Taar1 is present at the primary cilia of Fischer rat thyroid (FRT) cells *in vitro* (Szumska et al. 2015), challenges the notion of Taar1 being a predominantly intracellular receptor, at least in polarised thyroid epithelial cells, which were never addressed by trafficking studies before. Primary cilia are plasma membrane appendages on the apical pole of well-differentiated epithelial cells that anchor and, thereby, provide a signalling platform to GPCRs (Gerdes et al. 2009, Louvi and Grove 2011). Hence, our observation of endogenous Taar1 localisation to primary cilia might suggest a signalling role of this GPCR in rodent thyrocytes (Szumska et al., 2015). Importantly, ciliary Taar1 localisation suggests that Taar1 follows the classical transport route of secretory proteins, namely from its synthesis site at the endoplasmic reticulum (ER), through the ER-Golgi intermediate complex (ERGIC), the Golgi apparatus, and the trans-Golgi network (TGN), to finally reach the plasma membrane, which is the canonical localisation for GPCRs where they can encounter extracellular ligands (Duvernay et al. 2005).

This study was therefore designed to test the proposal of Taar1 being transported along the secretory pathway and pulse-chase was performed to elucidate the trafficking of mouse Taar1 from the TGN onwards while it is heterologously and stably expressed in human Nthy-ori 3-1 and KTC-1 thyroid cell lines, the latter bearing characteristics of well-polarised epithelial cells. To this end, a construct coding for mouse Taar1 tagged with EGFP on its C-terminus was used to stably express mTaar1-EGFP in normal human thyroid epithelial (Nthy-ori 3-1) and human papillary thyroid carcinoma (KTC-1) cell lines in order to establish an *in vitro* model to study Taar1 trafficking in thyrocytes. Nthy-ori 3-1 is a well-studied human thyroid follicular epithelial cell line, which retains functional differentiation in that it is capable of iodide-trapping and thyroglobulin (TG) secretion (Lemoine et al. 1989). KTC-1, on the other hand, are poorly differentiated papillary thyroid carcinoma cells that, despite not expressing *TSHR*, thyroid peroxidase (*TPO*) and sodium iodide symporter (*NIS*), retain high transcript levels of *TG*, *TTF-1* and paired box gene 8 (*PAX8*) relative to other thyroid cancer cell lines (Kurebayashi et al. 2000, Schweppe et al. 2008, Suzuki et al. 2011). Additionally, these cells maintain a certain degree of epithelial polarity, supported by the prevalence of tight junction proteins, such as claudin-1, E-cadherin and occludin, in the lateral plasma membrane of the cells (Tedelind et al. 2011). Therefore, both cell lines were deemed appropriate as models for a functionally differentiated versus polarised, structurally differentiated human thyrocytes.

Immunocytochemical analysis revealed mTaar1-EGFP to localise to ciliary membranes in polarised KTC-1 cells, stably *mTaar1-EGFP*-expressing. Surface localisation of mTaar1-EGFP was also observed in stably *mTaar1-EGFP*-expressing Nthy-ori 3-1 cells. This may suggest that mouse *Taar1* contains a cell surface targeting sequence. mTaar1-EGFP was additionally observed in vesicular structures. Moreover, biochemical analyses indicated homodimerisation and tetramerisation of mTaar1-EGFP *in vitro*. Therefore, oligomerisation might either be a prerequisite of Taar1 transport to the plasma membrane, or it may serve as a requirement of keeping it at this site for canonical GPCR signalling.

Materials and Methods

Vector construction

32

Plasmids coding for mouse Taar1, Taar5 or Taar8b, with an HA-tag fused to the N-terminus, cloned into a pcDps expression vector (*p*HA-mTaar1, *p*HA-mTaar5 and *p*HA-mTaar8b) were described previously (Mühlhaus et al. 2014, Dinter et al. 2015).

These plasmids were used as templates to amplify mouse *Taar1*, *Taar5* or *Taar8b* cDNA sequences minus the stop codon, provided with overhangs complementary to the *XhoI* and *BamHI* restriction sequences. They were ligated into the linearised *p*EGFP-N1 (Clontech, Heidelberg, Germany) expression vector using T4 DNA ligase (Thermo Scientific) in the presence of ATP-containing reaction buffer (Thermo Fisher) for 15 min at room temperature, following which it was immediately used to transform competent *E.coli* DH5α cells. Kanamycin-resistant clones were used to isolate plasmid DNA using NucleoSpin® Plasmid EasyPure (740727. Macherey-Nagel) or GeneJET Plasmid Midiprep Kit (K0482, Thermo Fisher Scientific). The resultant plasmids coded for chimeric proteins with full-length mouse Taar1, Taar5 or Taar8b, covalently connected to the EGFP tag by a 12 amino acid long spacer peptide linker (*p*mTaar1-EGFP, *p*mTaar5-EGFP and *p*mTaar8b-EGFP, respectively). Primer sequences, PCR settings, construct maps and sequence alignments are provided as supplementary data. Sequences were confirmed using standard pEGFP-N1 forward and reverse primers at Eurofins Genomics, Ebersberg, Germany.

Similarly, the sequence coding for full length mouse Taar1 lacking the stop codon was inserted into a modified puc2CL6Ipwo lentiviral vector (Hanenberg et al. 1996, Hein et al. 2014) at *XhoI* and *AgeI* sites of insertion (5'-end and 3'-end, respectively), to obtain a construct coding for the chimeric protein consisting of full length mouse Taar1, covalently connected to the EGFP tag by a 12 amino acid long spacer peptide linker (mTaar1-EGFP in puc2CL6Ipwo). Sequences were confirmed using oSF031Fwd (5'- CGGCGCGCCAGTCCTCCG) and oSF031Rev (5'-TAGACAAACGCACACCGG) sequencing primers at Eurofins Genomics.

Cell culture

Fisher rat thyroid (FRT) cells were grown at 37°C and 5% CO_2 in F-12 Coon's media (F-6636, Sigma), containing 31.9 mM $NaHCO_3$, supplemented with 5% Foetal Bovine Serum (FBS; F7524, Sigma), 10 µg/ml insulin (I6634, Sigma), 5 µg/ml transferrin (11107-018, Invitrogen, Darmstadt, Germany), 10 ng/ml somatostatin (S1763, Sigma), 10 ng/ml glycyl-histidyl-lysine (Sigma), and 10 nM hydrocortisone (H-0135, Sigma). KTC-1 (Kurebayashi et al. 2000) and Nthy-ori 3-1 (Lemoine

et al. 1989) (Nthy-ori for short) cells were cultured in RPMI 1640 medium, containing 2 mM glutamine (BE12-702F, Lonza, Verviers, Belgium), supplemented with 10% FBS, 100 U/ml penicillin and 0.1 mg/ml streptomycin (P0781, Sigma), at 37°C and 5% CO_2 in a moisturised atmosphere (unless specified otherwise). HEK 293T cells (ACC 635, DSMZ, Braunschweig, Germany), were cultured in Dulbecco's modified Eagle's medium (DMEM; BE12-604F, Lonza), containing 2 mM glutamine and 10% FBS.

For trafficking studies, KTC-1 and Nthy-ori cells stably expressing mTaar1-EGFP (consequently referred to as KTC-Z and Nthy-Z, respectively, as explained below were grown on sterile cover slips in 10 cm Petri dishes until confluent, then incubated overnight at 18°C in Gibco's CO_2-independent culture medium (18045, Thermo Fisher Scientific) with 10% FBS and 1 µg/ml puromycin, following which they were shifted to 37°C. Cells were fixed in 4% PFA in 200 mM HEPES, pH 7.4, at t= 0 min, 15 min, 30 min, 45 min, 1.0 hr, 1.5 min, 2.0 hr, 3.0 hr and 4.0 hr, respectively, post temperature shift, and immunolabelled with compartment-specific markers, as described below.

Transient transfection

Cells were incubated in 1 ml 0.25% trypsin in EDTA (T4549, Sigma) solution at 37°C until they detached. They were washed in PBS, then 1 × 10^6 cells were resuspended in 150 µl cytomix solution (120 mM KCl, 10 mM KH_2PO_4, 5 mM $MgCl_2$, 25 mM HEPES, 2 mM EGTA, 2 mM ATP (A-2383, Sigma), and 5 mM oxidised glutathione (G4626, Sigma), pH 7.2) (van den Hoff et al. 1992) with 10 µg DNA. FRT cells were pulsed twice at 700V for 200 µs using a multiporator (Eppendorf). Following 10 min recovery on ice, cells were seeded onto sterilised cover slips in 6-well plates, at a density of approximately 5 × 10^5 cells per 2 ml media per well. Cells were fixed in 4% paraformaldehyde (PFA) in 200 mM HEPES, pH 7.4, for 10 min at room temperature, at 48 hr post transfection.

Lentiviral transduction

Transduction was performed as described previously (Hanenberg et al. 1996, Halenius et al. 2011, Hein et al. 2014). In brief, HEK 293T cells were transfected with 6 µg of each of the following plasmids: puc2CL6IP-mTaar1-EGFP, pCDNL-BH and vesicular stomatitis virus G, with 45 µl

polyethylenimine, branched (PEI; 408727 Sigma-Aldrich) solution (1mg/ml) as a transfection reagent. The virion-rich supernatant of HEK 293T cells was collected 48 hr post-transfection and filtered through a 0.45 µm filter before being applied to 70% confluent KTC-1 and Nthy-ori cells. Following transduction, KTC-1 And Nthy-ori cells were selected with 1 µg/ml puromycin (0240.2, Carl Roth, Karlsruhe, Germany) in medium.

Henceforth, the acronyms KTC-Z and Nthy-Z will be used when referring to transduced, mTaar1-EGFP-expressing KTC-1 and Nthy-ori cells, respectively. KTC-Z and Nthy-Z cells were cultured in RPMI 1640 medium with 10% FBS, in the presence of penicillin and streptomycin, and additionally supplied with 1 µg/ml puromycin.

Cytochemistry and indirect immunofluorescence

Following fixation, cells were washed 3 × 5 min by incubation with calcium- and magnesium-free PBS (CMF-PBS) consisting of 0.15 M NaCl, 2.7 mM KCl, 1.5 mM NaH_2PO_4, 8.1 mM Na_2HPO_4, pH 7.4.

Cover slips were incubated with primary antibodies diluted in 0.1% bovine serum albumin (BSA; 3854, Carl Roth) in CMF-PBS overnight at 4°C. For compartment-specific immunolabelling, mouse anti-human GM130 (1:100; 610822, BD Transduction Laboratories), mouse anti-rat acetylated α-tubulin (1:100; T7451, Sigma-Aldrich), and mouse anti-human LAMP-2 (H4B4, DSHB) antibodies were used. In order to label cell surface glycoproteins, cells were treated with 10 µg/ml of biotin-conjugated Concanavalin A (ConA) from *Canavalia ensiformis* (C2272, Sigma-Aldrich) for 30 min at 4°C.

After washing with 0.1% BSA in CMF-PBS, cells were incubated with Alexa 546-conjugated secondary antibodies (1:250; Molecular Probes, Karlsruhe, Germany), or with Alexa Fluor® 546-conjugated streptavidin (S-11225, Molecular Probes) for ConA label detection, for 1 h at 37°C together with 5 µM of the nuclear counterstain Draq5™ (Biostatus Limited, Shepshed, UK). Specific antibodies were omitted in negative controls.

The cells on coverslips were mounted with embedding medium consisting of 33% glycerol, 14% Mowiol in 200mM Tris-HCl, pH 8.5 (Hoechst AG, Frankfurt, Germany). The slides were analysed with a confocal laser scanning microscope equipped with Argon and Helium-Neon lasers (LSM 510 Meta; Carl Zeiss Jena GmbH, Jena, Germany). Images were obtained at a pinhole setting of

1 Airy unit and at a resolution of 1024 × 1024 pixels. Micrographs were analysed with the LSM 510 software, release 3.2 (Carl Zeiss Jena GmbH).

Cell lysate preparation, SDS-PAGE and immunoblotting

Cells were washed thrice in ice cold PBS, following which they were scraped off the 10 cm Petri dishes and collected in 500 µl lysis buffer, consisting of 50mM Tris (pH 6.8) with 0.2% TX-100 and supplemented with protease inhibitors (0.2 µg/ml aprotonin, 10 µM E-64 and 1 µM pepstatin A and 2 mM EDTA). The cell suspension was then incubated for 1 hr at 4°C with constant rotation, then, lysates were cleared by centrifugation for 10 min at 10,000 g at 4°C. The supernatant was collected and protein content was determined according to the Neuhoff assay (Neuhoff et al. 1979).

Protein samples were prepared in Laemmli sample buffer (Laemmli 1970) (50mM Tris-HCl (pH 7.6), 2.5% sodium dodecyl sulphate (SDS), 125mM dithiotreitol (DTT), 50% glycerine, 125 µg bromophenol blue) and heated for 5 min at 95°C prior to loading onto 12.5% SDS-polyacrylamide gels, which were then semi-dry blotted onto nitrocellulose membranes (Kyhse-Andersen 1984). Pre-stained protein standards covering a broad range of 11-245 kDa (#P7712S, NEB) were used as molecular mass markers.

Unspecific binding sites were blocked in 5% blotting grade milk powder (T1452, Roth) in PBS-special buffer (pH 7.5) containing 0.3% Tween-20 (9127.2, Roth) (PBS-T) solution overnight at 4°C, except for samples subjected to biotinylation, which were blocked in a 3% BSA in PBS-T solution instead. Membranes were incubated in primary antibodies, i.e. rabbit anti-GFP (ab209, Abcam) or mouse anti-GFP (#1814460, Roche) diluted in PBS-T were used overnight at 4°C, washed in PBS-T buffer 6 × 5 min on a shaker at room temperature, then incubated with goat anti-rabbit or goat anti-mouse (respectively), horseradish (HRP)-conjugated IgG secondary antibody for one hour while constantly rotating at room temperature. Alternatively, the membranes were incubated in streptavidin-peroxidase (S-5512, Sigma) in PBS-T. Following the washing steps, membranes were incubated with SuperSignal™ West Pico PLUS Chemiluminescent Substrate (34580, Thermo Scientific, Rockford, IL, USA) for 2 min at room temperature, and scanned using C-DiGit Blot Scanner from Li-COR Biosciences and the Image Studio Lite software version 5.2 (Lincoln, NE, USA).

Cell surface biotinylation

Cell surface biotinylation was performed according to a modified protocol described elsewhere (Brix et al. 1998). In brief, KTC-1, KTC-Z, Nthy-ori and Nthy-Z cells were cultured in biotin-free medium (DMEM + 10% FBS, additionally with 1 µg/ml puromycin for transduced "Z" cells) continuously for 14 days prior to commencing the experiments. Cells were grown in 10 cm Petri dishes until ~70% - 90% confluent. The cells were then washed in cold PBS 2 × 30 min, then incubated with 200 µg/ml biotinamidohexanoic acid 3-sulfo-N-hydroxysuccinimide ester sodium salt (B1022, Sigma-Aldrich Chemie GmbH, Steinheim, Germany) in PBS solution for 1 hr at 4°C with gentle shaking. Non-biotinylated controls were incubated in parallel in PBS only. The cells were then briefly rinsed in PBS, then washed with 10mM L-lysine (L5501, Sigma-Aldrich, Switzerland) in PBS solution 4 × 10 min to quench unbound biotin. Finally, the cells were incubated in lysis buffer (50 mM Tris, pH 6.8, with 0.2% TX-100, containing protease inhibitors as specified above), and collected in 2 ml microcentrifuge tubes to complete cell lysis and protein extraction, as described above. Cell lysates were subsequently used for SDS-PAGE and immunoblotting (see above).

Molecular mass calculation

The predicted molecular masses of mouse Taar1, the chimeric mTaar1-EGFP, and human TAAR1 were calculated using the SIB Swiss Institute of Bioinformatics ExPASy "Compute pI/Mw tool" (https://web.expasy.org/compute_pi/).

Results

Having previously shown Taar1 to localise at the apical plasma membrane of mouse thyroid epithelial cells *in situ*, as well as on ciliary appendages of FRT cells *in vitro* (Szumska et al. 2015), this study was designed to investigate Taar1 subcellular localisation and trafficking in human thyroid epithelial and carcinoma cells *in vitro*.

FRT cells are normal rat thyroid epithelial cells, characterised by maintaining highly polarised states, and featuring a single cilium at their apical plasma membrane. FRT cells grow in a tight monolayer before eventually forming domes and follicle-like structures once confluence is

reached. However, they lack the thyroid transcription factor-1 (TTF-1), do not express the Tshr and produce little thyroglobulin (Tg), they hence lack the functional properties of a typical thyrocyte (Zurzolo et al. 1991, Mascia et al. 1997, Tonoli et al. 2000).

The mouse Taar1 is a 332 amino acids long, 7-transmembrane GPCR, with extracellular N-terminus and a cytoplasmic C-terminal tail (Figure 1A). In the present study, N-terminally HA-tagged or C-terminally EGFP-tagged mouse Taar1, Taar5 or Taar8b chimeras were transiently co-expressed in FRT cells. A schematic diagram highlighting the position of either tags relative to the protein's transmembrane orientation is given in (Figure 1B).

Co-expression of related but differently tagged Taar molecules results in trafficking of Taar1 to cilia of FRT cells

Taar proteins have been classified into 3 phylogenetic subgroups (Lindemann et al. 2005). Consequently, Taar5 and Taar8b were chosen as representatives of the two other phylogenetic subgroups, besides Taar1. Contrary to Taar1, cell surface expression has been reported for both Taar5 and Taar8b in transiently expressing HEK 293 cells (Mühlhaus et al. 2014, Dinter et al. 2015). However, only Taar1 has been shown to be expressed in thyroid epithelial cells (Szumska et al. 2015). When singly and transiently expressed in FRT cells, mTaar1-EGFP signal appeared in a predominantly reticular and vesicular distribution in steady state (Figure 2A).

Next, we sought to test for Taar heterodimerisation and its effect on Taar trafficking to the cell surface. To this end, an EGFP-tagged Taar was paired with an HA-tagged Taar for co-expression studies. Our results show that co-expressing mTaar1-EGFP with HA-Taar8b results in their colocalisation at patchy plasma membrane sub-domains (Figure 3A). Furthermore, co-expressing mTaar5-EGFP and HA-Taar8b resulted in their colocalisation on what resembled ciliary extensions (Figure 3B). Collectively, these observations suggest that Taar co-expression, presumably resulting in oligomerisation, promotes trafficking to the cell surface, or that high protein amounts are required to trigger efficient transport in vesicles destined to reach the plasma membrane. Indeed, FRT cells expressing mTaar5-EGFP only, revealed surface localisation in addition to reticular localisation (Figure 2B), indicating Taar5 to traffic more efficiently to the plasma membrane than Taar1.

Therefore, to test the hypothesis of cells requiring translation of sufficiently high protein amounts to favour oligomerisation-driven cell surface transport and to be able to perform biochemical

analyses, stable mTaar1-EGFP expression was favoured over transient expression. This was achieved by transducing human KTC-1 and Nthy-ori thyroid cell lines to express mTaar1-EGFP.

<u>Chimeric mTaar1-EGFP is abundant in dimeric and tetrameric form in KTC-Z and Nthy-Z cells</u>

The predicted molecular mass of mouse Taar1 equals 37.6 kDa, and mTaar1-EGFP is 65.8 kDa, disregarding potential post-translational modifications like through usage of N-glycosylation sites. Similarly, the predicted molecular mass of human TAAR1 is 39.1 kDa.

Proteins of whole cell lysates of KTC-Z and Nthy-Z, versus the non-transduced KTC-1 and Nthyr-ori controls, respectively, were separated on 12.5% SDS-PAGE and immunolabelled with GFP-specific antibodies. Immunolabelling revealed anti-GFP positive bands prominently at an apparent molecular mass of 155 kDa and 276 kDa in Nthy-Z and KTC-Z lanes only. These molecular masses, when divided by 65.8, the predicted molecular mass of the monomeric chimera, yielded 2.35 and 4.19, respectively, suggesting mTaar1-EGFP exists in SDS-resistant dimeric and tetrameric forms (Figure 4). The said molecular masses represent an average of apparent molecular mass values, determined from the exponential equation of retardation factor (R_f) values plotted against the molecular masses of the protein ladder.

Additionally, a band at ~27 kDa was seen in mTaar1-EGFP-expressing cells only, corresponding to the size of EGFP, indicating cleavage of the EGFP tag by mTaar1-EGFP degradation which additionally seems to yield a protein of ~52 kDa. Therefore, the anti-GFP immunoblot was subsequently stripped and re-incubated with anti-Taar1 antibodies and the two immunoblots compared (Figure 5). The band at 52 kDa was identified with both anti-GFP and anti-Taar1 antibodies in Nthy-Z cell and KTC-Z cell lysate, respectively, suggesting degradation products of the chimeric protein. In addition to the bands positive for anti-GFP, the anti-Taar1 immunoblot revealed a band at ~41 kDa in both mTaar1-EGFP-expressing and non-expressing cells most likely represents endogenous TAAR1 (Figure 5B), as well as an anti-Taar1-positive band at ~72 kDa in Nthy-Z and Nthy-ori cell lysates, which may represent the endogenous TAAR1 homodimer (2 × 39.1 = 78.2 kDa).

Alternatively, Nthy-Z and KTC-Z cells, as well as their non-mTaar1-EGFP-expressing Nthy-ori and KTC-1 controls, were subjected to cell surface biotinylation with long chain biotin, i.e. biotinamidohexanoic acid 3-sulfo-N-hydroxysuccinimide ester sodium salt was used at 4°C, that is, under endocytosis-blocking conditions. Lysates from cell surface biotinylated cells, as well as lysates from non-biotinylated controls, were run on 12.5% SDS-PAGE and either immunolabelled

with GFP-specific antibodies, or incubated with HRP-conjugated streptavidin. The results are demonstrated in (Figure 6), showing that the proportion of biotinylated proteins corresponding in size to the 276 kDa and 155 kDa mTaar1-EGFP tetramer and dimer, respectively, were prevalent in Nthy-Z and KTC-Z cells. This provides indirect evidence that a subset of mTaar1-EGFP dimers and tetramers are localised on the cell surface.

Transport of mTaar1-EGFP in transduced, polarised thyroid epithelial cells results in its targeting to and localisation at cilia

When steadily incubated at 37°C, Nthy-Z and KTC-Z exhibit a reticular pattern of mTaar1-EGFP distribution (Figure 7A-B), besides an occasional cell surface localisation in sub-confluent cultures (Figure 7A).

In order to further elucidate mTaar1-EGFP trafficking in these cell lines, Nthy-Z and KTC-Z cells were grown on cover slips to >70% confluence and incubated at 18°C to inhibit anterograde trafficking of proteins along the secretory pathways from the *trans*-Golgi network onwards. Cells were incubated for a minimum of 8 hours, and up to 17 hours, at 18°C prior to shifting back to 37°C to restore the microtubule polymerisation/depolymerisation dynamics from the perinuclearly located microtubule-organising centre, therefore re-enabling post-TGN vesicle trafficking (Gierke et al. 2012). Following incubation at 18°C, mTaar1-EGFP was abundant in the perinuclear region, i.e. in the ER, as indicated by the green mTaar1-EGFP signal surrounding the nuclei and outlining the nuclear envelope, as well as in the Golgi, as evident from colocalisation of the mTaar1-EGFP signal with that of the *cis*-Golgi marker GM130 (Figure 8). Moreover, mTaar1-EGFP was observed as puncta in the cytoplasm of both KTC-Z and Nthy-Z cells (Figure 8A-B, arrows), which may represent vesicles at the ER-exit sites of the ER-Golgi intermediate compartment (ERGIC) or secretory vesicles in transit to the cell surface. Ciliary localisation of mTaar1-EGFP was maintained even at 18°C in the polarised KTC-Z cells, as evident from the colocalisation with the ciliary marker acetylated-α-tubulin (Piperno et al. 1987, Szumska et al. 2015) (Figure 9). The latter observation suggests that the half-life $t_{1/2}$ of Taar1 exceeds 17 hours. In addition, the results suggest that cilia once established in KTC-Z cells are not affected by temperature shifts, which is consistent with the understanding that microtubules of primary cilia are rendered cold-induced disassembly stable by the binding of MAP6 proteins (Dacheux et al. 2015). To see whether mTaar1-EGFP reached lysosomal compartments for degradation, cells were immunolabelled with LAMP-2. Partial colocalisation of mTaar1-EGFP with the lysosomal marker LAMP-2 was occasionally observed in KTC-Z cells, which was most distinct at 30 min post shift from 18°C to

37°C (Figure 10), indicating targeting of the chimeric GPCR-EGFP protein for lysosomal degradation, at least in some proportion of the total expressed chimeric protein.

The ER, Golgi, and vesicular distribution of mTaar1-EGFP prevailed in both cell lines for the duration of the experiment, i.e. up to 4 hours post shifting the cells back to 37°C. A distinct cell surface localisation of mTaar1-EGFP was observed through co-localisation with ConA-stained cell surface constituents in some Nthy-Z cells, especially at 45 min following TGN release onwards (Figure 11). It should be noted that the chimeric protein persisted in KTC-Z cells upon recovery from the 18°C transport block, particularly on ciliary extensions (Figure 12), consistent with cilia being resistant to cold temperature conditions, as mentioned.

Discussion

Previously conducted studies by other groups, involving heterologous expression of Taar1 in various cellular model systems, demonstrated Taar1 to retain an intracellular localisation pattern, which led to speculations that Taar1 functions as a GPCR signalling from within intracellular compartments, rather than from the cell surface (Bunzow et al. 2001). Alternatively, this may suggest Taar1 to require interaction with another protein to facilitate trafficking to the cell surface, a phenomenon known for many of the GPCRs (Panetta and Greenwood 2008, Milligan 2009, Smith and Milligan 2010). Indeed, TAAR1 has been shown to form functional dimers with TAAR2 in human leukocytes (Babusyte et al. 2011), as well as with the human dopamine receptor when co-expressed in HEK 293 cells (Espinoza et al. 2011). Moreover, the majority of studies reporting on TAAR1/Taar1 trafficking and subcellular localisation to date involved introducing modifications to the N-terminus of the TAAR1 sequence, often to promote its transport to the plasma membrane (Bunzow et al. 2001, Miller et al. 2005, Barak et al. 2008). We hereby present a model in which the N-terminus of Taar1 remained unaltered; however, a covalently linked EGFP tag was introduced at the protein's C-terminus.

FRT cells co-expressing mTaar1-EGFP and HA-Taar8b were shown to localise the GPCRs in a patchy pattern reminiscent of lipid raft-like microdomains, as opposed to a predominantly reticular distribution in cells expressing mTaar1-EGFP only. These results thus indicate that Taar1 heterodimerisation with another protein of the Taar-family enhances its trafficking to the cell surface. In support of that proposal, co-expression of mTaar5-EGFP with HA-Taar8b resulted in ciliary localisation of the molecules. However, FRT cells expressing mTaar5-EGFP only, also exhibited its localisation at the plasma membrane, namely in what resembles lipid raft-like

41

microdomains or ciliary extensions, suggesting that Taar5 traffics to the surface of well-polarised thyroid epithelial cells more readily than Taar1. The latter may be attributed to the fact that mTaar5 contains the amino acid sequence "FRKALKLLL", in its C-terminus, which corresponds to the $F(X)_6LL$ C-terminal motif that was identified to promote GPCR trafficking to the cell surface (Duvernay et al. 2009). This particular motif is absent in the C-terminus of mouse Taar1 and Taar8b.

Although mTaar1-EGFP signal was largely observed as puncta or in a reticular pattern, as well as in the Golgi, a subset of mTaar1-EGFP signal was observed on the surface of both Nthy-Z and KTC-Z cells, indicating that mTaar1-EGFP does, after all, successfully traffic to the cell surface. However, because the ratio of cell surface to perinuclear mTaar1-EGFP signal is very low, some of the surface localised mTaar1-EGFP can go undetected in fluorescence microscopy because the relative contribution of mTaar1-EGFP from within perinuclear organelles appears to obscure the much weaker signal derived from cell surface located chimeras.

The trafficking of mTaar1-EGFP to lipid raft-like microdomains or ciliary extensions in transfected FRT and in the stably expressing KTC-Z cells supports our previously reported observations that endogenous Taar1 localises on cilia of FRT cells, and on the apical plasma membrane domain of mouse thyroid epithelial cells *in situ* (Szumska et al. 2015). This fact is strongly suggestive of Taar1 serving a role in thyroid regulation, because the apical plasma membrane domain of thyrocytes faces the thyroid follicle lumen into which the cilia extend and where thyroglobulin, the precursor protein of thyroid hormones, is stored in high concentrations. Therefore, exposing the Taar1 to the extracellular environment opens up the possibility that Taar1 could potentially serve as a sensor to intraluminal molecular alterations. Such changes in the composition of the thyroid follicle lumen are readily achieved upon thyrocyte stimulation with TSH, hence, thyroglobulin degradation may result in the generation of thyronamine precursors, which eventually may be rendered into thyronamines upon cellular uptake and cytosolic conversion before re-export into the lumen, where they can, in principle, act as intra-thyroidally generated Taar1 agonists (Szumska et al. 2015). This suggestion of an intra-follicular mechanism of Taar1 ligand generation and Taar1 signalling from apically located cilia may contribute to regulating thyroid function in a non-canonical form (Szumska et al., 2015; commented in Brix et al., in press). Support of this hypothesis comes from our recent investigations describing the thyroid phenotype of Taar1-deficient mice, which is mild but affects TSH receptor localisation in particular (Qatato/Szumska et al., submitted).

Conclusion

This study was conducted by expressing a mouse Taar1 chimera with a C-terminal EGFP tag fused via a short linker peptide. We conclude that KTC-1 and Nthy-ori cells stably expressing mTaar1-EGFP provide a suitable model to study Taar1 trafficking and localisation in thyrocytes. We report that chimeric mTaar1-EGFP, when expressed in rat and human thyrocytes *in vitro*, is transported to the cell surface and is preferentially targeted to the primary cilia of polarised thyrocytes. We also report that mTaar1-EGFP forms homo-oligomers, whereby it is predominantly found in the dimeric and tetrameric forms, in stably expressing KTC-1 and Nthy-ori cells. We propose these cellular models to be suited for signalling studies that are beyond the scope of the present investigation, and will be conducted in future.

The current study mainly focused on the anterograde trafficking of mTaar1-EGFP from the trans-Golgi network to the cell surface. For future studies, we will rely on these established cellular models to further elucidate mTaar1 oligomerisation and its effect on the receptor's transport to the plasma membrane and to cilia in particular, as well as measure mTaar1 turnover rates, i.e. analyse its re-entry by endocytosis and subsequent fates like receptor recycling or endo-lysosomal degradation. Moreover, we intend to perform functional assays to study mTaar1 signalling *in vitro*, and its implication in regulation of thyroid function. In line with this notion, we have recently discovered that Taar1 is needed to maintain the basolateral localisation of the Tshr *in vivo*, suggesting that Taar1 functionally serves as a co-regulator in the hypothalamic-pituitary-thyroid feedback loop (Qatato/Szumska et al., submitted).

Author Contributions

MQ, WD, and ZH performed experiments. MQ and KBr devised the study. HB contributed plasmids and contributed to devising experiments. KBr and SSp supervised the experimental work. All authors contributed to data interpretation. MQ and KBr drafted the manuscript. All authors read and approved the final manuscript

Acknowledgement

The authors would like to thank kindly provided by Dr. Dr. Dagmar Führer (Universitätsklinikum Essen, Germany) for providing Nthy-ori 3-1 cells, and Dr. Junichi Kurebayashi for providing KTC-

References

Babusyte, A., M. Kotthoff, J. Fiedler and D. Krautwurst (2011). "Biogenic amines activate blood leukocytes via trace amine-associated receptors TAAR1 and TAAR2." J Leukoc Biol **93**(3): 387-394.

Borowsky, B., N. Adham, K. A. Jones, R. Raddatz, R. Artymyshyn, K. L. Ogozalek, et al. (2001). "Trace amines: identification of a family of mammalian G protein-coupled receptors." Proc Natl Acad Sci U S A **98**(16): 8966-8971.

Brix, K., W. Summa, F. Lottspeich and V. Herzog (1998). "Extracellularly occurring histone H1 mediates the binding of thyroglobulin to the cell surface of mouse macrophages." J Clin Invest **102**(2): 283-293.

Bunzow, J. R., M. S. Sonders, S. Arttamangkul, L. M. Harrison, G. Zhang, D. I. Quigley, et al. (2001). "Amphetamine, 3,4-methylenedioxymethamphetamine, lysergic acid diethylamide, and metabolites of the catecholamine neurotransmitters are agonists of a rat trace amine receptor." Mol Pharmacol **60**(6): 1181-1188.

Dacheux, D., B. Roger, C. Bosc, N. Landrein, E. Roche, L. Chansel, et al. (2015). "Human FAM154A (SAXO1) is a microtubule-stabilizing protein specific to cilia and related structures." J Cell Sci **128**(7): 1294-1307.

Dinter, J., J. Muhlhaus, C. L. Wienchol, C. X. Yi, D. Nurnberg, S. Morin, et al. (2015). "Inverse agonistic action of 3-iodothyronamine at the human trace amine-associated receptor 5." PLoS One **10**(2): e0117774.

Duvernay, M. T., C. Dong, X. Zhang, F. Zhou, C. D. Nichols and G. Wu (2009). "Anterograde Trafficking of G Protein-Coupled Receptors: Function of the." Mol Pharmacol **75**(4): 751-761.

Duvernay, M. T., C. M. Filipeanu and G. Wu (2005). "The regulatory mechanisms of export trafficking of G protein-coupled receptors." Cellular Signalling **17**(12): 1457-1465.

Espinoza, S., A. Salahpour, B. Masri, T. D. Sotnikova, M. Messa, L. S. Barak, et al. (2011). "Functional Interaction between Trace Amine-Associated Receptor 1 and Dopamine D2 Receptor." Mol Pharmacol **80**(3): 416-425.

Gerdes, J. M., E. E. Davis and N. Katsanis (2009). "The vertebrate primary cilium in development, homeostasis, and disease." Cell **137**(1): 32-45.

Gierke, S., P. Kumar and T. Wittmann (2012). "Analysis of microtubule polymerization dynamics in live cells." Methods Cell Biol **97**: 15-33.

Grandy, D. K. (2007). "Trace Amine-Associated Receptor 1 – Family Archetype or Iconoclast?" Pharmacol Ther **116**(3): 355-390.

Halenius, A., S. Hauka, L. Dolken, J. Stindt, H. Reinhard, C. Wiek, et al. (2011). "Human cytomegalovirus disrupts the major histocompatibility complex class I peptide-loading complex and inhibits tapasin gene transcription." J Virol **85**(7): 3473-3485.

Hanenberg, H., X. L. Xiao, D. Dilloo, K. Hashino, I. Kato and D. A. Williams (1996). "Colocalization of retrovirus and target cells on specific fibronectin fragments increases genetic transduction of mammalian cells." Nat Med **2**(8): 876-882.

Hein, Z., H. Uchtenhagen, E. T. Abualrous, S. K. Saini, L. Janssen, A. Van Hateren, et al. (2014). "Peptide-independent stabilization of MHC class I molecules breaches cellular quality control." J Cell Sci **127**(Pt 13): 2885-2897.

Jing, L. and J. X. Li (2015). "Trace amine-associated receptor 1: A promising target for the treatment of psychostimulant addiction." Eur J Pharmacol **761**: 345-352.

Kurebayashi, J., K. Tanaka, T. Otsuki, T. Moriya, H. Kunisue, M. Uno, et al. (2000). "All-Trans-Retinoic Acid Modulates Expression Levels of Thyroglobulin and Cytokines in a New Human Poorly Differentiated Papillary Thyroid Carcinoma Cell Line, KTC-11." The Journal of Clinical Endocrinology & Metabolism **85**(8): 2889-2896.

Kyhse-Andersen, J. (1984). "Electroblotting of multiple gels: a simple apparatus without buffer tank for rapid transfer of proteins from polyacrylamide to nitrocellulose." J Biochem Biophys Methods **10**(3-4): 203-209.

Laemmli, U. K. (1970). "Cleavage of structural proteins during the assembly of the head of bacteriophage T4." Nature **227**(5259): 680-685.

Lemoine, N. R., E. S. Mayall, T. Jones, D. Sheer, S. McDermid, P. Kendall-Taylor, et al. (1989). "Characterisation of human thyroid epithelial cells immortalised in vitro by simian virus 40 DNA transfection." <u>Br J Cancer</u> **60**(6): 897-903.

Lindemann, L., M. Ebeling, N. A. Kratochwil, J. R. Bunzow, D. K. Grandy and M. C. Hoener (2005). "Trace amine-associated receptors form structurally and functionally distinct subfamilies of novel G protein-coupled receptors." <u>Genomics</u> **85**(3): 372-385.

Lindemann, L., C. A. Meyer, K. Jeanneau, A. Bradaia, L. Ozmen, H. Bluethmann, et al. (2008). "Trace amine-associated receptor 1 modulates dopaminergic activity." <u>J Pharmacol Exp Ther</u> **324**(3): 948-956.

Louvi, A. and E. A. Grove (2011). "Cilia in the CNS: the quiet organelle claims center stage." <u>Neuron</u> **69**(6): 1046-1060.

Mascia, A., M. De Felice, C. Lipardi, R. Gentile, G. Cali, M. Zannini, et al. (1997). "Transfection of TTF-1 gene induces thyroglobulin gene expression in undifferentiated FRT cells." <u>Biochimica et biophysica acta</u> **1354**(2): 171-181.

Milligan, G. (2009). "G protein-coupled receptor hetero-dimerization: contribution to pharmacology and function." <u>Br J Pharmacol</u> **158**(1): 5-14.

Mühlhaus, J., J. Dinter, D. Nürnberg, M. Rehders, M. Depke, J. Golchert, et al. (2014). "Analysis of Human TAAR8 and Murine Taar8b Mediated Signaling Pathways and Expression Profile." <u>Int J Mol Sci</u> **15**(11): 20638-20655.

Neuhoff, V., K. Philipp, H. G. Zimmer and S. Mesecke (1979). "A simple, versatile, sensitive and volume-independent method for quantitative protein determination which is independent of other external influences." <u>Hoppe Seylers Z Physiol Chem</u> **360**(11): 1657-1670.

Panetta, R. and M. T. Greenwood (2008). "Physiological relevance of GPCR oligomerization and its impact on drug discovery." <u>Drug Discovery Today</u> **13**(23): 1059-1066.

Pei, Y., A. Asif-Malik and J. J. Canales (2016). "Trace Amines and the Trace Amine-Associated Receptor 1: Pharmacology, Neurochemistry, and Clinical Implications." <u>Front Neurosci</u> **10**: 148.

Piperno, G., M. LeDizet and X. J. Chang (1987). "Microtubules containing acetylated alpha-tubulin in mammalian cells in culture." <u>J Cell Biol</u> **104**(2): 289-302.

Revel, F. G., J. L. Moreau, R. R. Gainetdinov, A. Bradaia, T. D. Sotnikova, R. Mory, et al. (2011). "TAAR1 activation modulates monoaminergic neurotransmission, preventing hyperdopaminergic and hypoglutamatergic activity." <u>Proc Natl Acad Sci U S A</u> **108**(20): 8485-8490.

Schweppe, R. E., J. P. Klopper, C. Korch, U. Pugazhenthi, M. Benezra, J. A. Knauf, et al. (2008). "Deoxyribonucleic Acid Profiling Analysis of 40 Human Thyroid Cancer Cell Lines Reveals Cross-Contamination Resulting in Cell Line Redundancy and Misidentification." J Clin Endocrinol Metab **93**(11): 4331-4341.

Smith, N. J. and G. Milligan (2010). "Allostery at G protein-coupled receptor homo- and heteromers: uncharted pharmacological landscapes." Pharmacol Rev **62**(4): 701-725.

Suzuki, K., N. Mitsutake, V. Saenko, M. Suzuki, M. Matsuse, A. Ohtsuru, et al. (2011). "Dedifferentiation of Human Primary Thyrocytes into Multilineage Progenitor Cells without Gene Introduction." PLoS One **6**(4).

Szumska, J., M. Qatato, M. Rehders, D. Fuhrer, H. Biebermann, D. K. Grandy, et al. (2015). "Trace Amine-Associated Receptor 1 Localization at the Apical Plasma Membrane Domain of Fisher Rat Thyroid Epithelial Cells Is Confined to Cilia." Eur Thyroid J **4**(Suppl 1): 30-41.

Tedelind, S., S. Jordans, H. Resemann, G. Blum, M. Bogyo, D. Führer, et al. (2011). "Cathepsin B trafficking in thyroid carcinoma cells." Thyroid Res **4**(Suppl 1): S2.

Tonoli, H., V. Flachon, C. Audebet, A. Calle, T. Jarry-Guichard, M. Statuto, et al. (2000). "Formation of three-dimensional thyroid follicle-like structures by polarized FRT cells made communication competent by transfection and stable expression of the connexin-32 gene." Endocrinology **141**(4): 1403-1413.

van den Hoff, M. J., A. F. Moorman and W. H. Lamers (1992). "Electroporation in 'intracellular' buffer increases cell survival." Nucleic Acids Res **20**(11): 2902.

Wolinsky, T. D., C. J. Swanson, K. E. Smith, H. Zhong, B. Borowsky, P. Seeman, et al. (2007). "The Trace Amine 1 receptor knockout mouse: an animal model with relevance to schizophrenia." Genes Brain Behav **6**(7): 628-639.

Xie, Z. and G. M. Miller (2009). "Trace amine-associated receptor 1 as a monoaminergic modulator in brain." Biochemical pharmacology **78**(9): 1095-1104.

Zurzolo, C., R. Gentile, A. Mascia, C. Garbi, C. Polistina, L. Aloj, et al. (1991). "The polarized epithelial phenotype is dominant in hybrids between polarized and unpolarized rat thyroid cell lines." J Cell Sci **98 (Pt 1)**: 65-73.

Figures

mTaar1 (332 aa)
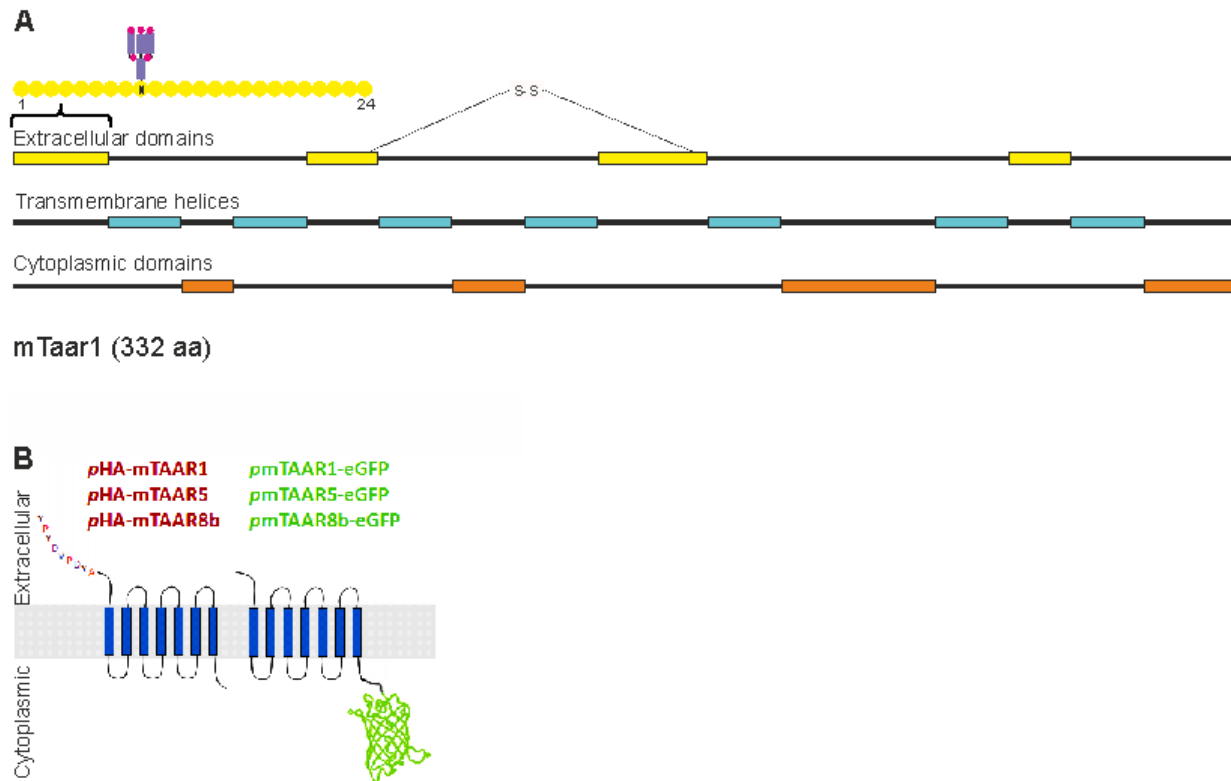
Figure 1: (A) A schematic diagram of the structural topology of the mouse Taar1, a 332 amino acid long protein, consisting of 7 transmembrane domains (blue), 4 extracellular domains (yellow), and 4 cytoplasmic domans (orange). A putative N-linked glycosylation site on the ninth residue and a disulphide bond connecting the second and third extracellular domains are indicated. The diagram is designed according to annotations in the UniProt entry Q923Y8 (TAAR1_MOUSE). (B) A schematic diagram showing the position of the tag in the different Taar chimeric protein, whereby plasmids *p*HA-mTaar1, *p*HA-mTaar5 and *p*HA-mTaar8b code for an HA-tag fused to the extracellular N-terminus of the 7-transmembrane Taar protein, as opposed to the *p*mTaar1-EGFP, *p*mTaar5-EGFP, and *p*mTaar8b-EGFP, which encode the respective Taar protein with a fused EGFP-tag on the cytoplasmic C-terminus of the Taar protein.
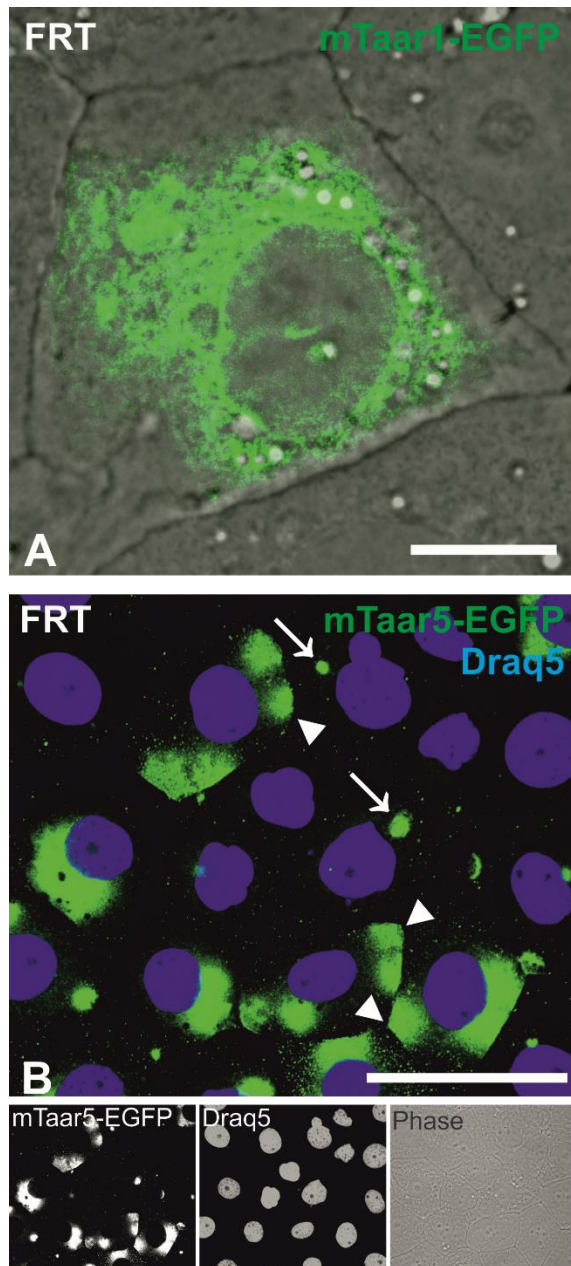
Figure 2: (A) mTAAR1-eGFP has a reticular localisation in FRT cells, indicating mTaar1-EGFP (green) to be primarily confined to the endoplasmic reticulum when singly expressed in FRT cells. Image overlaid with phase contrast. . (B) FRT cells expressing mTaar5-EGFP (green), which frequently localises at cilia (arrows) and associated with lipid raft-like microdomains (arrowheads). Bottom panels provide single fluorescence channels for mTaar5-EGFP (left) and Draq5™ as nuclear counter-stain (middle), and phase contrast (right). Scale bar represents 10 µm in (A) and 50 µm in (B).
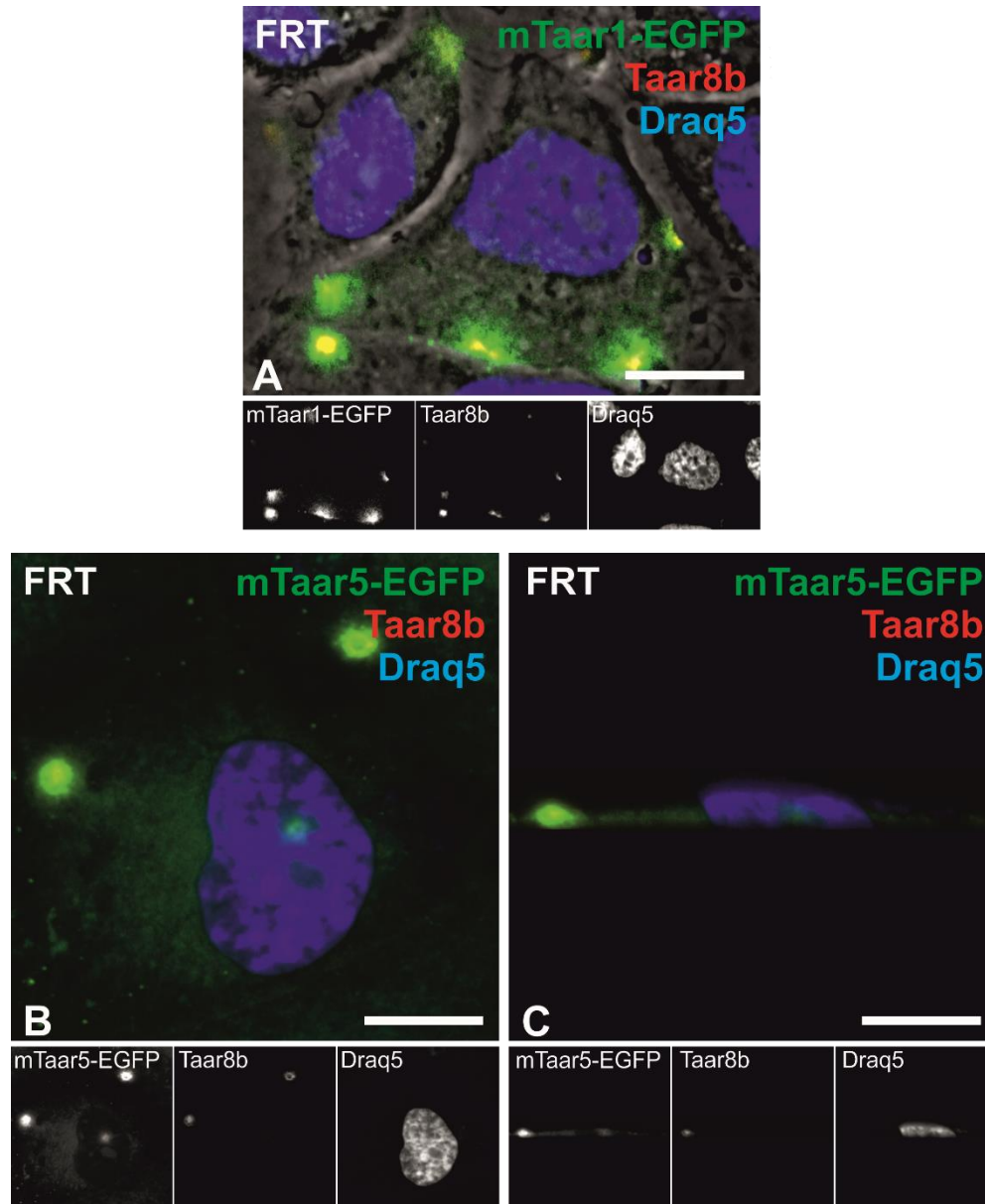
Figure 3: Co-expressing Taars in FRT cells enhances trafficking to lipid raft-like microdomains and the ciliary membrane. FRT cell co-expressing mTaar1-EGFP (green) and HA-Taar8b, labelled with Taar8-specific antibodies (red) show colocalisation at lipid raft-like microdomains (yellow), image is overlaid with phase contrast to outline the cell (A). FRT cell co-expressing mTaar5-EGFP (green) and HA-Taar8b, labelled with Taar8-specific antibodies (red) show colocalisation at the cilium (yellow), viewed from the top in (B) and as side view in (C), demonstrating the protrusion of the cilium from the cell. Single channel fluorescence are provided in the bottom panels, left to right: mTaar1-EGFP, Taar8b, and Draq5™ as nuclear counter-stain (A), and mTaar5-EGFP, Taar8b, and Draq5™ in (C). Scale bars represent 10 μm.
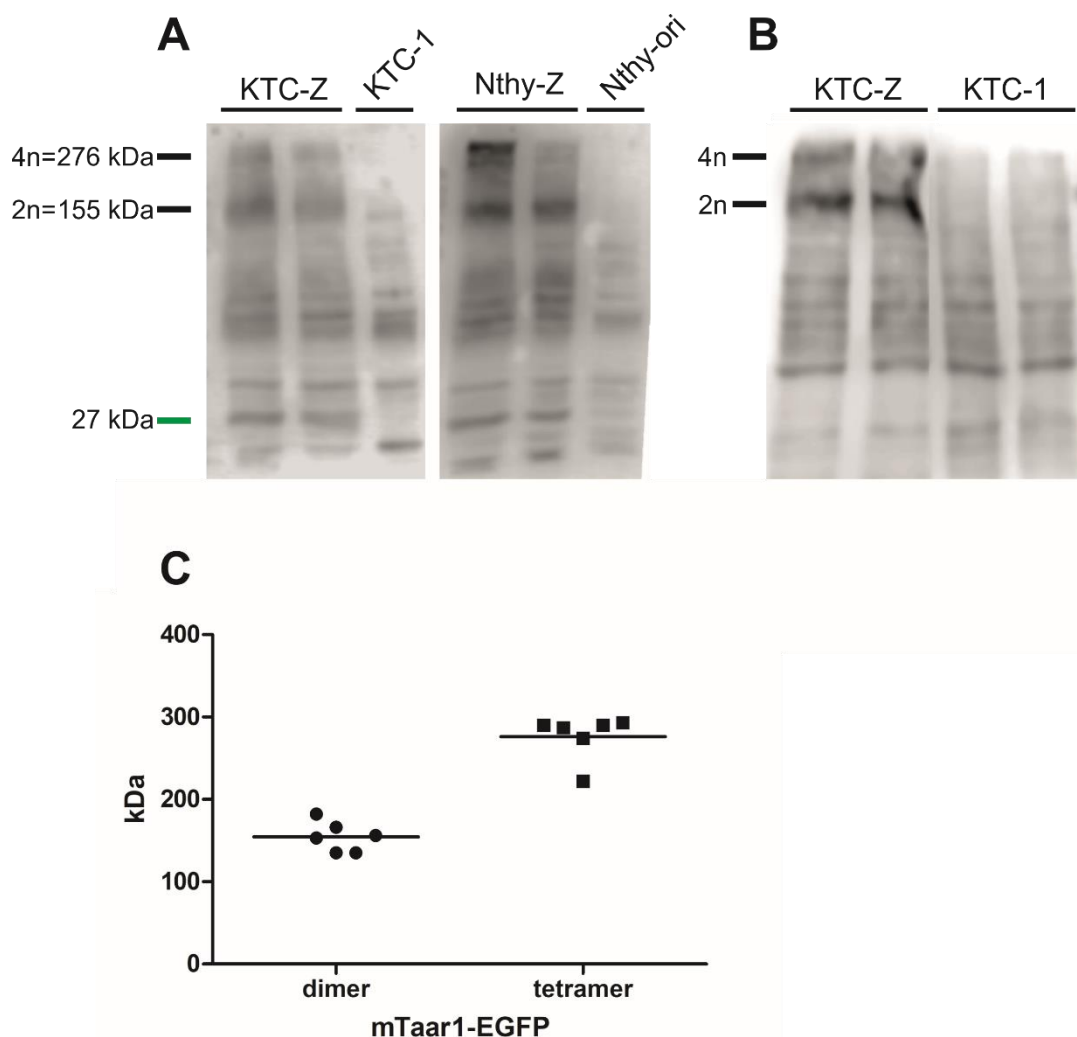
Figure 4: mTaar1-EGFP forms dimers and tetramers in stably expressing KTC-Z and Nthy-Z cells. Cells lysates prepared from stably mTaar1-EGFP-expressing KTC-Z and Nthy-Z cells were separated by 12.5% SDS-PAGE alongside lysates from non-transduced KTC-1 and Nthy-ori cells used as negative controls. Membranes immunolabelled with polyclonal rabbit-anti-GFP (abcam) (A), and monoclonal mouse-anti-GFP (Roche) (B) show two prominent GFP-specific bands at approximately 276 kDa and 155 kDa. In (A), an additional band of 27 kDa is seen, equivalent to the molecular mass of EGFP. The molecular masses were measured from 6 separate anti-GFP immunoblots (C), to give an average of 276 kDa and 155 kDa. These values, when divided by 65.8 kDa (the predicted molecular mass of the mTaar1-EGFP chimera), yield 4.19 and 2.36, indicating tetrameric and dimeric complexes, respectively.
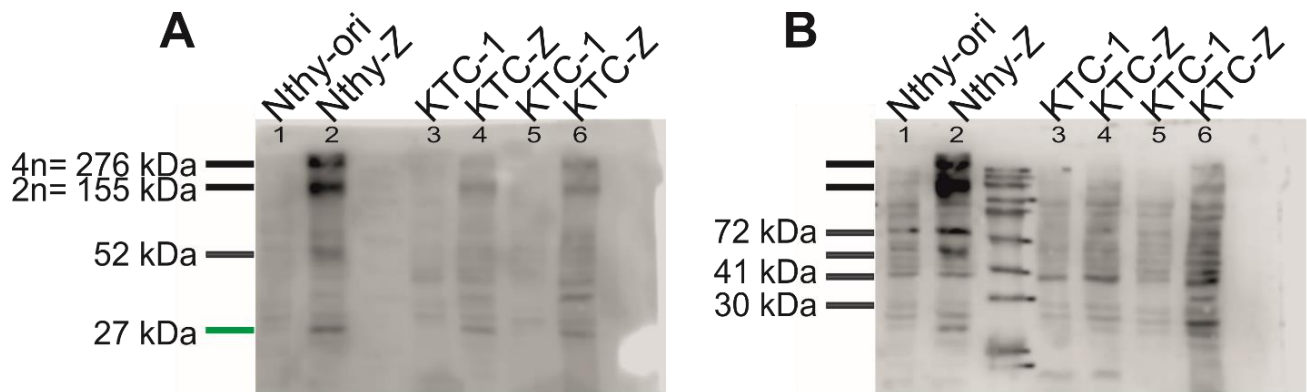
Figure 5: Comparison of GFP-positive immunoblot (A) to mouse Taar1-positive immunoblot (B). In (A), the major GFP-immunopositive bands representing the tetrameric and dimeric mTaar1-EGFP at the apparent molecular mass of 275 kDa and 155 kDa are seen, respectively (lanes 2, 4 and 6 in A). In addition, a fainter bands at 52 kDa (lane 2), which may either be the monomeric mTaar1-EGFP, or a degradation product. These bands can also be traced on the Taar1 immunoblot (B) for Nthy-Z and KTC-Z cells, but not their negative controls. The Taar1 immunoblot also shows Taar1-immunopositive bands at 72 kDa in Nthy-ori (lane 1) and Nthy-Z (lane 2) cells, and at 41 kDa in all cell lines, which may represent the dimeric and monomeric form of the endogenous TAAR1, respectively.
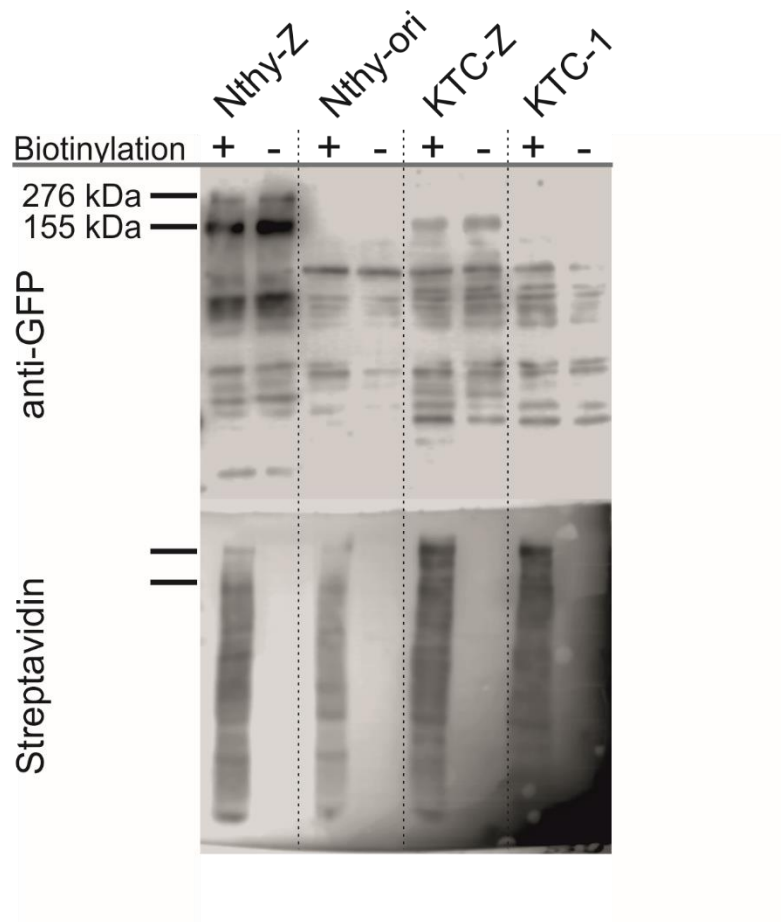
Figure 6: A subset of mTaar1-EGFP dimers and tetramers reaches the surface of Nthy-Z and KTC-Z cells. Nthy-Z and KTC-Z cells were subjected to cell surface biotinylation (+) or not (-), and cell lysates separated on 12.5% SDS-PAGE and either immunolabelled with GFP-specific antibodies (top), or labelled with streptavidin conjugated to HRP (bottom). Streptavidin-positive bands equivalent to the GFP-positive bands at 276 kDa and 155 kDa can be traced on the streptavidin blot, suggesting that dimeric and tetrameric mTaar1-EGFP may be among those surface biotinylated proteins. The fact that the streptavidin bands are fainter in Nthy-Z cells, compared to the strong GFP-positive bands, suggests that only a small subset of mTaar1-EGFP may be localised on the surface. On the other hand, a stronger streptavidin signal is seen in KTC-Z cells, suggesting that more mTaar1-EGFP may be reaching the cell surface in KTC-Z than in Nthy-Z cells.
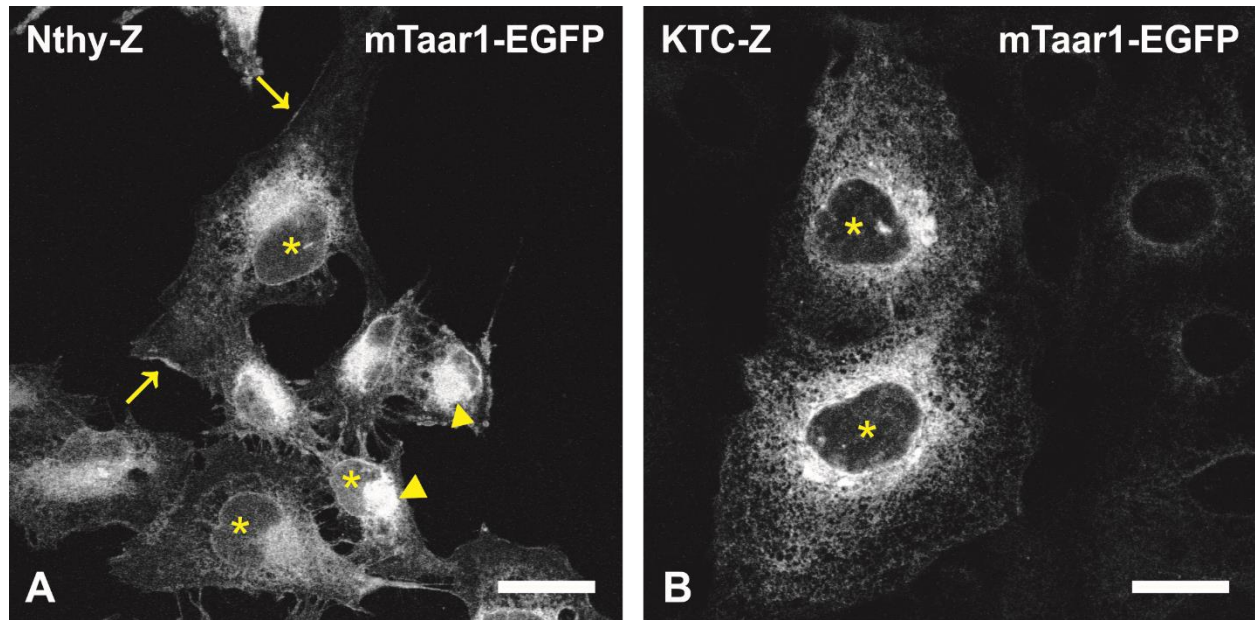
Figure 7: mTaar1-EGFP is predominantly localised in the perinuclear regions of Nthy-Z and KTC-Z cells at 37°C. mTaar1-EGFP signal can be seen spread out in a reticular pattern, as well as outlining the nuclei (*) in both Nthy-Z (A) and KTC-Z (B) cells. Additionally, mTaar1-EGFP can be seen on the surface of Nthy-Z cells (arrows), and in the Golgi (arrowheads). Scale bars represent 20 μm.
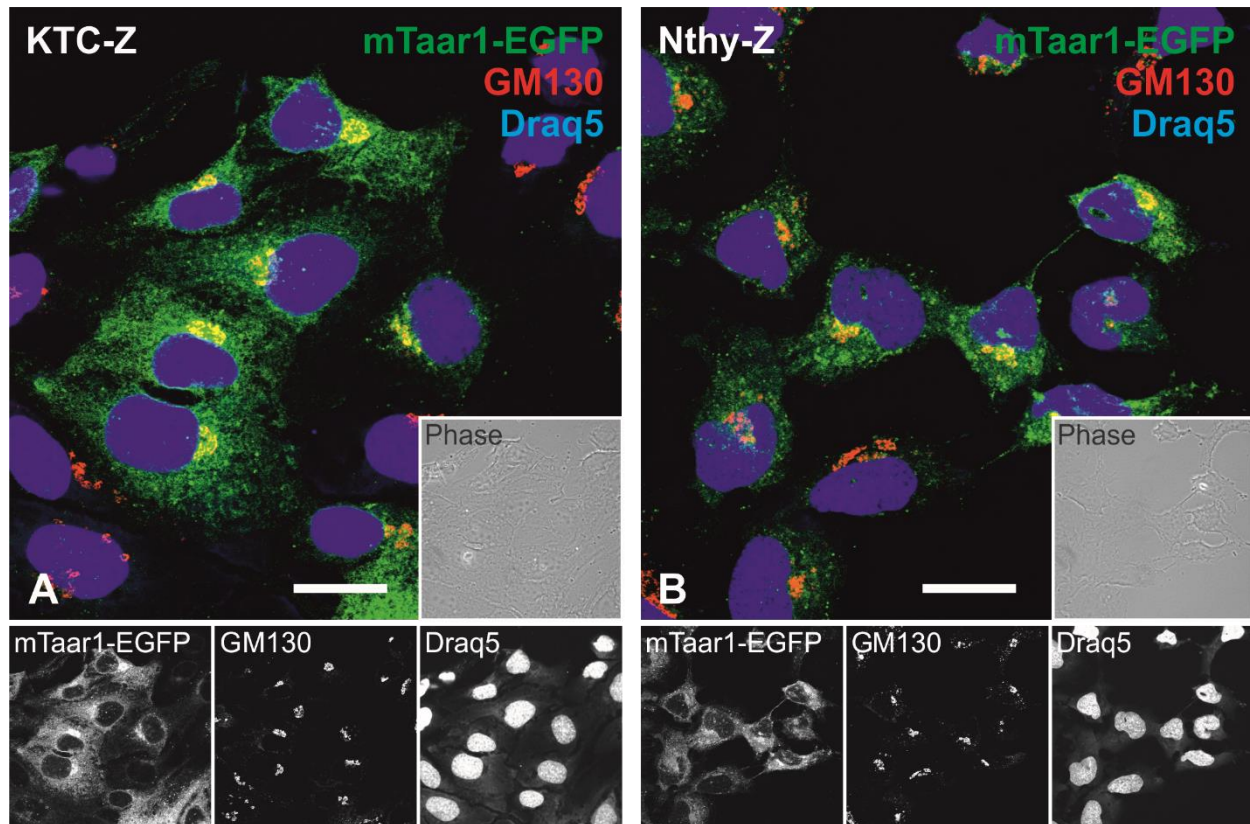
Figure 8: mTaar1-EGFP is localised in the Golgi and as puncta in Nthy-Z and KTC-Z cells directly following incubation at 18°C. Fixed cells were labelled with antibodies against the *cis*-Golgi marker GM130 (red). The presence of mTaar1-EGFP (green) in the Golgi of both Nthy-Z (A) and KTC-Z (B) cells is evident from its colocalisation (yellow) with GM130. mTaar1-EGFP is also seen distributed in a reticular pattern and as puncta (arrows), which may represent ER-Golgi intermediate compartments or ER exit sites. Single channel fluorescence are provided in the bottom panels, left to right: mTaar1-EGFP, GM130, and Draq5™ as nuclear counter-stain. Scale bars represent 20 μm.
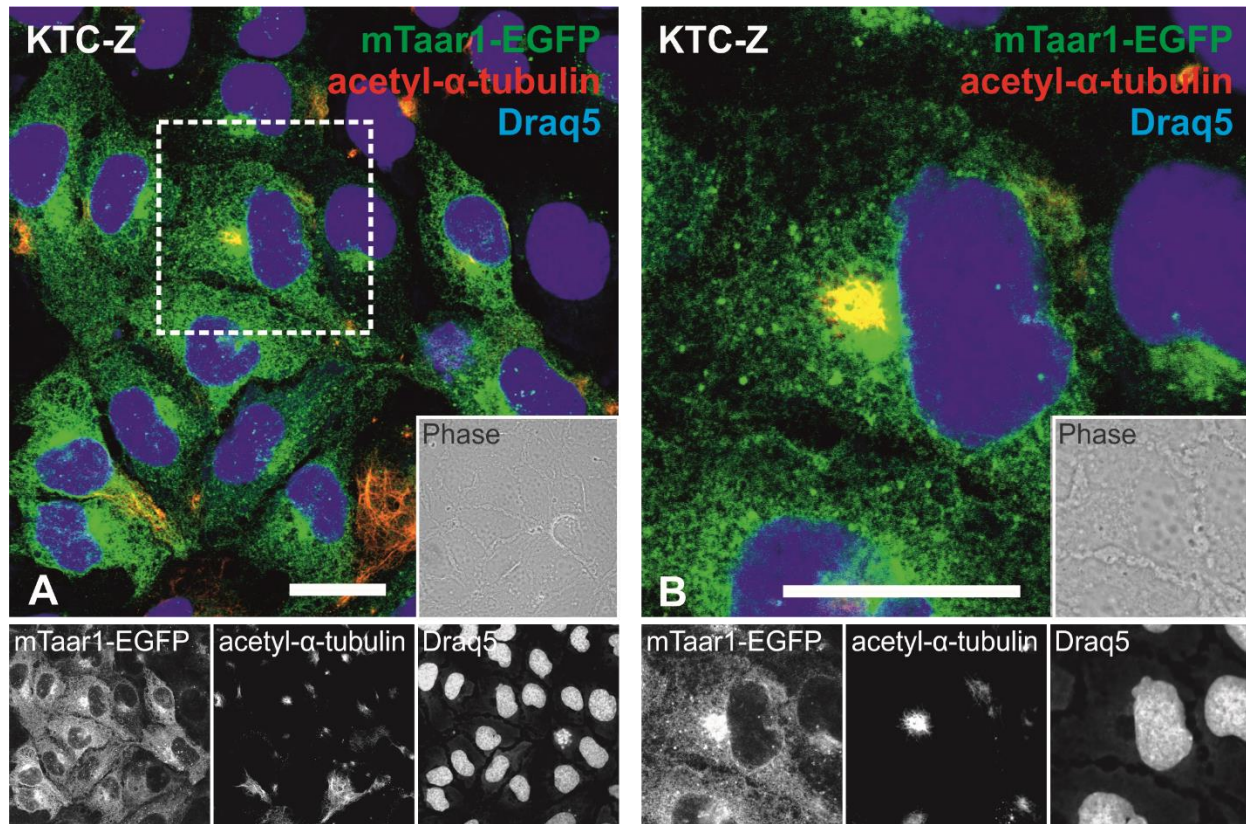
Figure 9: mTaar1-EGFP is localised in the ciliary membrane of KTC-Z cells directly following incubation at 18°C. Fixed cells were labelled with antibodies against the ciliary marker acetylated-α-tubulin (red). Square in (A) outlines the cell magnified in (B). The presence of mTaar1-EGFP (green) on the cilia of KTC-Z cells is evident from its colocalisation (yellow) with acetylated-α-tubulin. Single channel fluorescence are provided in the bottom panels, left to right: mTaar1-EGFP, acetylated-α-tubulin, and Draq5™ as nuclear counter-stain. Scale bars represent 20 μm.
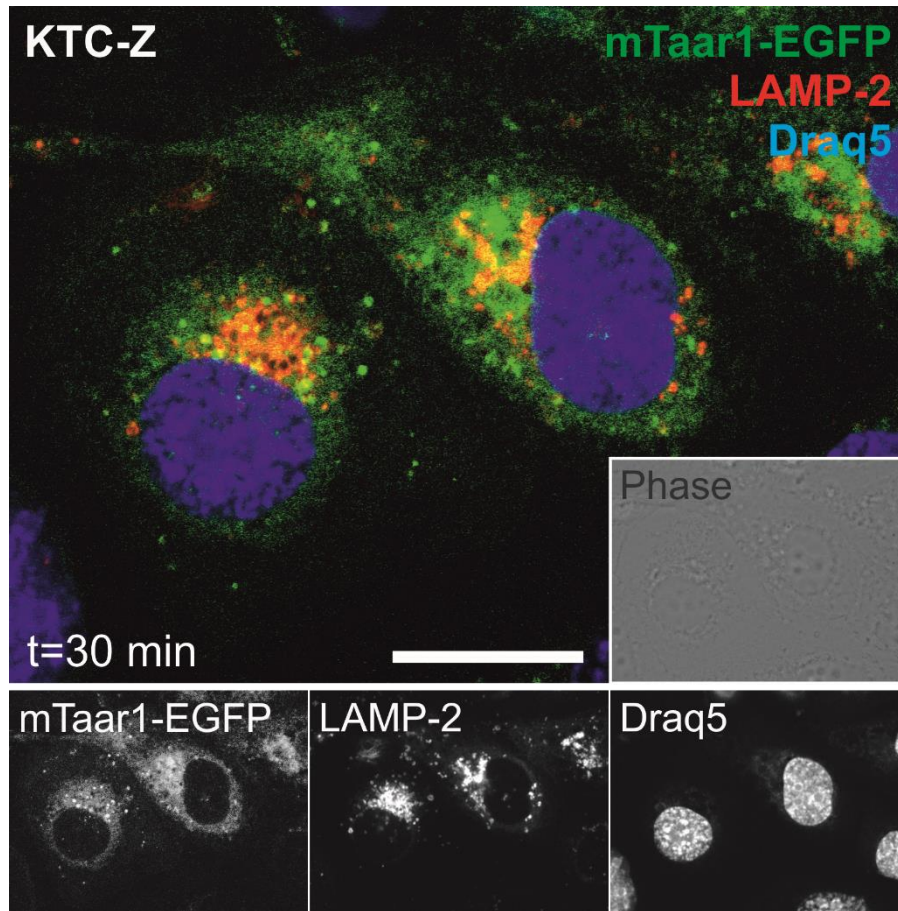
Figure 10: mTaar1-EGFP partially colocalised with LAMP-2 in the lysosomes of KTC-Z cells. Cells were fixed and immunolabelled with the lysosomal marker LAMP-2. mTaar1-EGFP (green) partially colocalised with LAMP-2 (red) in lysosomal compartments (yellow) at 30 min past shift from 18°C to 37°C. Single channel fluorescence are provided in the bottom panels, left to right: mTaar1-EGFP, LAMP-2, and Draq5™ as nuclear counter-stain. Scale bar represents 20 μm.

Figure 11: mTaar1-EGFP colocalises with concanavalin A staining on the surface of Nthy-Z cells. Fixed cells were stained with lectin concanavalin A (ConA). mTaar1-EGFP (green) colocalised with ConA (red) on the cell surface (arrows) at 45 min (A) and 1.5 hr (B) past shift from 18°C to 37°C. Single channel fluorescence are provided in the bottom panels, left to right: mTaar1-EGFP, ConA, and phase contrast. Scale bars represent 20 µm.

Figure 12: mTaar1-EGFP is localised on the cilia and surface of KTC-Z cells. Cells were fixed 4 hr past shift from 18°C to 37°C, and immunolabelled with acetylated-α-tubulin (A and B), or stained with lectin ConA (C). mTaar1-EGFP is localised on the cilium of a KTC-Z cell, as evident from its colocalisation with the ciliary marker acetylated-α-tubulin (yellow, arrow; A). In (B), a side-view of the same cell in (A) is provided, demonstrating the extension representing the cilium (arrow). In (C), mTaar1-EGFP is colocalised with ConA (arrowheads) on the surface of KTC-Z cells. Single channel fluorescence are provided in the bottom panels, left to right: mTaar1-EGFP, acetylated-α-tubulin and Draq5™ as nuclear counter-stain (A and B), and mTaar1-EGFP, ConA, and Draq5™ in (C). Scale bars represent 10 μm.

Supplementary Data

Primer	Sequence 5' → 3'
Taar1_for	G AT **C↓TC GAG** ATG CAT CTT TGC CAC GCT ATC AC
Taar1_rev	CGC **GGT AC↓C** GTC AAA AAT AGC TTA GAC CTA G
Taar5_for	G AT **C↓TC GAG** ATG AGA GCT GTC CTC CTC C
Taar5_rev	CGC **GGT AC↓C** GT GTC ATG GTA TAA ATC AAC AGT C
Taarr8b_for	GAT **C↓TC GAG** ATG ACC AGC AAC TTT TCC CAA C
Taar8b_rev	CGC **GGT AC↓C** GTC TCT GAA AAC AAA CTC ATG G

Table.1 Primers used to amplify the cDNA sequences for mouse Taar1, Taar5 and Taar8b. The forward (_for) primer sequences were preceded by an XhoI restriction site (5'...ctcgag...3'), whereas the reverse (_rev) primers were preceded by a KpnI restriction site (5'...ggtacc...3'). Primer overhangs are highlighted in red; the restriction sites are in bold, with the arrow indicating the position of cleavage. All primers were manufactured by Eurofins MWG Operon (Ebersberg, Germany). The PCR reaction consisted of 30 s denaturation at 95°C, 45 s of annealing at 48°C, and 1.5 min elongation at 72°C for a total of 30 cycles, preceded by 3 min of initial denaturation at 95°C, and followed by final elongation for 5 min at 72°C.
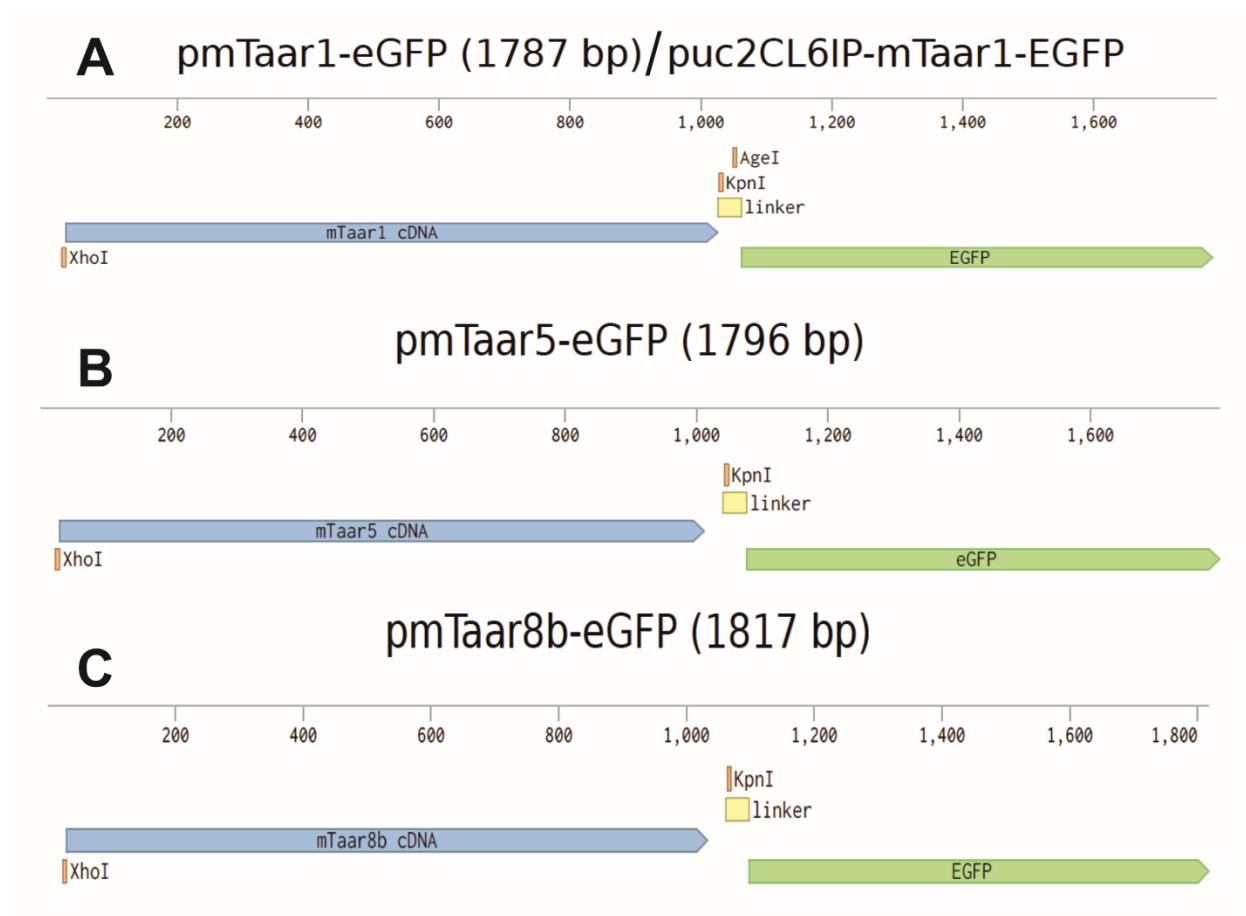
Figure S.1: Linear maps of plasmid construct coding for mTaar1-EGFP in either the *p*EGFP-N1 expression vector for transient transfection, or the puc2CL6IP vector for lentiviral transduction (A), mTAAR5-EGFP (B), mTAAR8b-EGFP (C). The constructs were designed using the online tool from Benchling Inc., San Francisco, USA (https://benchling.com/). Sequence alignments are provided below.

1. Sequence alignment for puc2CL6IP-mTaar1-EGFP using forward sequencing primer oSF031Fwd 5'- CGGCGCGCCAGTCCTCCG:

(from 1-300 bp)

Template Alignment: oSF130Fwd

12/18/2017 10:20:58 AM

Template Alignment: oSF130Fwd (from 2701-3000 bp)   12/18/2017 10:20:58 AM

ATATGGCCCAACCCTCAGCAGTTTCTTAAGACCCATCAGATGTTTCCAGGCTCCCCCAAGGACCTGAAATGACCCTGCGCCTTATTTGAATTAACCAATC

| 2,710 | 2,720 | 2,730 | 2,740 | 2,750 | 2,760 | 2,770 | 2,780 | 2,790 | 2,800 |

template sequence puc2CL6IP-mTaar1-EGFP

| 2,710 | 2,720 | 2,730 | 2,740 | 2,750 | 2,760 | 2,770 | 2,780 | 2,790 | 2,800 |

aligned sequence oSF130Fwd

AGCCTGCTTCTCGCTTCTGTTCGCGCGCTTCTGCTTCCCGAGCTCTATAAAAGAGCTCACAACCCCTCACTCGGCGCGCCAGTCCTCCGAcaGACTGAGT

| 2,810 | 2,820 | 2,830 | 2,840 | 2,850 | 2,860 | 2,870 | 2,880 | 2,890 | 2,900 |

template sequence puc2CL6IP-mTaar1-EGFP

| 2,810 | 2,820 | 2,830 | 2,840 | 2,850 | 2,860 | 2,870 | 2,880 | 2,890 | 2,900 |

aligned sequence oSF130Fwd

CGCCCGGGTACCGCggattagcggccgcaaCTCGAGATGcatctttgccacgctatcacaaacatttcccacagaaacagcgactggtcaagagaagtcc

| 2,910 | 2,920 | 2,930 | 2,940 | 2,950 | 2,960 | 2,970 | 2,980 | 2,990 | 3,000 |

XhoI   mTaar1 cDNA

template sequence puc2CL6IP-mTaar1-EGFP

------GGGGTCGCGGATTAGCGGCCGCAACTCGAGATGCATCTTTGCCACGCTATCACAAACATTTCCCACAGAAACAGCGACTGGTCAAGAGAAGTCC

| 2,910 | 2,920 | 2,930 | 2,940 | 2,950 | 2,960 | 2,970 | 2,980 | 2,990 | 3,000 |

aligned sequence oSF130Fwd

Template Alignment: oSF130Fwd (from 3001-3300 bp)   12/18/2017 10:20:58 AM

aagcttccctgtacagcttaatgtcactcataatcctggccactctggttggcaacttaatagtaataatttccatatcccatttcaagcaacttcatac

3,010   3,020   3,030   3,040   3,050   3,060   3,070   3,080   3,090   3,100

mTaar1 cDNA

template sequence puc2CL6IP-mTaar1-EGFP

AAGCTTCCCTGTACAGCTTAATGTCACTCATAATCCTGGCCACTCTGGTTGGCAACTTAATAGTAATAATTTCCATATCCCATTTCAAGCAACTTCATAC

3,010   3,020   3,030   3,040   3,050   3,060   3,070   3,080   3,090   3,100

aligned sequence oSF130Fwd

acccaccaactggctccttcactccatggccattgtcgactttctgctgggctgtctgataatgccctgcagcatggtgagaactgttgagcgctgttgg

3,110   3,120   3,130   3,140   3,150   3,160   3,170   3,180   3,190   3,200

mTaar1 cDNA

template sequence puc2CL6IP-mTaar1-EGFP

ACCCACCAACTGGCTCCTTCACTCCATGGCCATTGTCGACTTTCTGCTGGGCTGTCTGATAATGCCCTGCAGCATGGTGAGAACTGTTGAGCGCTGTTGG

3,110   3,120   3,130   3,140   3,150   3,160   3,170   3,180   3,190   3,200

aligned sequence oSF130Fwd

tattttggggaaatcctctgtaaagttcacaccagcaccgatatcatgctgagctccgcctccattttccacttagctttcatttccattgaccgctact

3,210   3,220   3,230   3,240   3,250   3,260   3,270   3,280   3,290   3,300

mTaar1 cDNA

template sequence puc2CL6IP-mTaar1-EGFP

TATTTTGGGGAAATCCTCTGTAAAGTTCACACCAGCACCGATATCATGCTGAGCTCCGCCTCCATTTTCCACTTAGCTTTCATTTCCATTGACCGCTACT

3,210   3,220   3,230   3,240   3,250   3,260   3,270   3,280   3,290   3,300

aligned sequence oSF130Fwd

https://benchling.com/maria/f/rvxenLsF-uploads/seq-CDL0QRqE-puc2cl6ip-mtaar1-egfp/edit#   11/31

Template Alignment: oSF130Rev (from 3601-3900 bp)   12/18/2017 10:19:17 AM

caatcaatcgtacgaatgttcaagttggattggaagggaaaagccaagcaccacaaagcaaggaaacaaaagccgcgaagaccttagggatcatggtggg

3,610   3,620   3,630   3,640   3,650   3,660   3,670   3,680   3,690   3,700

mTaar1 cDNA

template sequence puc2CL6IP-mTaar1-EGFP

CAATCAATCGTACGAATGTTCAAGTTGGATTGGAAGGGAAAAGCCAAGCACCACAAAGCAAGGAAACAAAAGCCGCGAAGACCTTAGGGATCATGGTGGG

3,610   3,620   3,630   3,640   3,650   3,660   3,670   3,680   3,690   3,700

aligned sequence oSF130Rev

cgttttcctcgtatgctggtgcccgttctttctctgcacggtcctggaccctttcctgggctatgttatcccaccctctctgaatgacgcactgtattgg

3,710   3,720   3,730   3,740   3,750   3,760   3,770   3,780   3,790   3,800

mTaar1 cDNA

template sequence puc2CL6IP-mTaar1-EGFP

CGTTTTCCTCGTATGCTGGTGCCCGTTCTTTCTCTGCACGGTCCTGGACCCTTTCCTGGGCTATGTTATCCCACCCTCTCTGAATGACGCACTGTATTGG

3,710   3,720   3,730   3,740   3,750   3,760   3,770   3,780   3,790   3,800

aligned sequence oSF130Rev

tttgggtacttgaattctgccctcaatccgatggtttatgcctttttctatccctggttcagaagagccttgaagatggttctccttggtaaaattttcc

3,810   3,820   3,830   3,840   3,850   3,860   3,870   3,880   3,890   3,900

mTaar1 cDNA

template sequence puc2CL6IP-mTaar1-EGFP

TTTGGGTACTTGAATTCTGCCCTCAATCCGATGGTTTATGCCTTTTTCTATCCCTGGTTCAGAAGAGCCTTGAAGATGGTTCTCCTTGGTAAAATTTTCC

3,810   3,820   3,830   3,840   3,850   3,860   3,870   3,880   3,890   3,900

aligned sequence oSF130Rev

https://benchling.com/maria/f/rvxenLsF-uploads/seq-CDL0QRqE-puc2cl6ip-mtaar1-egfp/edit#   13/31

Template Alignment: oSF130Fwd (from 3601-3900 bp)   12/18/2017 10:20:58 AM

caatcaatcgtacgaatgttcaagttggattggaagggaaaagccaagcaccacaaagcaaggaaacaaaagccgcgaagaccttagggatcatggtggg

| 3,610 | 3,620 | 3,630 | 3,640 | 3,650 | 3,660 | 3,670 | 3,680 | 3,690 | 3,700 |

mTaar1 cDNA

template sequence puc2CL6IP-mTaar1-EGFP

CAATCAATCGTACGAATGTTCAAGTTGGATTGGAAGGGAAAAGCCAAGCACCACAAAGCAAGGAAACAAAAGCCGCGAAGACCTTAGGGATCATGGTGGG

| 3,610 | 3,620 | 3,630 | 3,640 | 3,650 | 3,660 | 3,670 | 3,680 | 3,690 | 3,700 |

aligned sequence oSF130Fwd

cgttttcctcgtatgctggtgcccgttctttctctgcacggtcctggaccctttcctgggctatgttatcccaccctctctgaatgacgcactgtattgg

| 3,710 | 3,720 | 3,730 | 3,740 | 3,750 | 3,760 | 3,770 | 3,780 | 3,790 | 3,800 |

mTaar1 cDNA

template sequence puc2CL6IP-mTaar1-EGFP

CGTTTTCCTCGTATGCTGGTGCCCGTTCTTTCTCTGCACGGTCCTGGACCCTTTCCTGGGCTATGTTATCCCACCCTCTCTGAATGACGCACTGTATTGG

| 3,710 | 3,720 | 3,730 | 3,740 | 3,750 | 3,760 | 3,770 | 3,780 | 3,790 | 3,800 |

aligned sequence oSF130Fwd

tttgggtacttgaattctgccctcaatccgatggtttatgccttttttctatccctggttcagaagagccttgaagatggttctccttggtaaaattttcc

| 3,810 | 3,820 | 3,830 | 3,840 | 3,850 | 3,860 | 3,870 | 3,880 | 3,890 | 3,900 |

mTaar1 cDNA

template sequence puc2CL6IP-mTaar1-EGFP

TTTGGGTACTTGAATTCTGCCCTCAATCCGATGGTTTATGCCTTTTTTCTATCCCTGGTTCAGAAGAGCCTTGAAGATGGTTCTCCTTGGTAAAATTTTCC

| 3,810 | 3,820 | 3,830 | 3,840 | 3,850 | 3,860 | 3,870 | 3,880 | 3,890 | 3,900 |

aligned sequence oSF130Fwd

https://benchling.com/maria/f/rvxenLsF-uploads/seq-CDL0QRqE-puc2cl6ip-mtaar1-egfp/edit#   13/31

2. Sequence alignment for puc2CL6IP-mTaar1-EGFP using reverse sequencing primer oSF031Rev (5'-TAGACAAACGCACACCGG) sequencing primers:

(from 1-300 bp)   12/18/2017 10:19:17 AM
Template Alignment: oSF130Rev

Template Alignment: oSF130Rev (from 3301-3600 bp)   12/18/2017 10:19:17 AM

gtgctgtgtgtgacccctttgagatacaaagccaagatcaatatctccactattcttgtgatgatcctcgttagttggagccttcctgctgtttatgcatt

3,310   3,320   3,330   3,340   3,350   3,360   3,370   3,380   3,390   3,400

mTaar1 cDNA

template sequence puc2CL6IP-mTaar1-EGFP

GTGCTGTGTGTGACCCCTTTGAGATACAAAGCCAAGATCAATATCTCCACTATTCTTGTGATGATCCTCGTTAGTTGGAGCCTTCCTGCTGTTTATGCATT

3,310   3,320   3,330   3,340   3,350   3,360   3,370   3,380   3,390   3,400
aligned sequence oSF130Rev

tgggatgatcttcctggaactgaacttaaaaggagtggaagagctgtatcgcagtcaggtcagcgacctgggcggctgttctcccttctttagtaaagta

3,410   3,420   3,430   3,440   3,450   3,460   3,470   3,480   3,490   3,500

mTaar1 cDNA

template sequence puc2CL6IP-mTaar1-EGFP

TGGGATGATCTTCCTGGAACTGAACTTAAAAGGAGTGGAAGAGCTGTATCGCAGTCAGGTCAGCGACCTGGGCGGCTGTTCTCCCTTCTTTAGTAAAGTA

3,410   3,420   3,430   3,440   3,450   3,460   3,470   3,480   3,490   3,500
aligned sequence oSF130Rev

tctggggtactggcgttcatgacttccttctatatacctggatctgttatgttatttgtttactataggatatatttcatagctaaaggacaagcaaggt

3,510   3,520   3,530   3,540   3,550   3,560   3,570   3,580   3,590   3,600

mTaar1 cDNA

template sequence puc2CL6IP-mTaar1-EGFP

TCTGGGGTACTGGCGTTCATGACTTCCTTCTATATACCTGGATCTGTTATGTTATTTGTTTACTATAGGATATATTTCATAGCTAAAGGACAAGCAAGGT

3,510   3,520   3,530   3,540   3,550   3,560   3,570   3,580   3,590   3,600
aligned sequence oSF130Rev

Template Alignment: oSF130Rev (from 3601-3900 bp)   12/18/2017 10:19:17 AM

caatcaatcgtacgaatgttcaagttggattggaagggaaaagccaagcaccacaaagcaaggaaacaaaagccgcgaagaccttagggatcatggtggg

3,610   3,620   3,630   3,640   3,650   3,660   3,670   3,680   3,690   3,700

mTaar1 cDNA

template sequence puc2CL6IP-mTaar1-EGFP

CAATCAATCGTACGAATGTTCAAGTTGGATTGGAAGGGAAAAGCCAAGCACCACAAAGCAAGGAAACAAAAGCCGCGAAGACCTTAGGGATCATGGTGGG

3,610   3,620   3,630   3,640   3,650   3,660   3,670   3,680   3,690   3,700
aligned sequence oSF130Rev

cgttttcctcgtatgctggtgcccgttctttctctgcacggtcctggaccctttcctgggctatgttatcccaccctctctgaatgacgcactgtattgg

3,710   3,720   3,730   3,740   3,750   3,760   3,770   3,780   3,790   3,800

mTaar1 cDNA

template sequence puc2CL6IP-mTaar1-EGFP

CGTTTTCCTCGTATGCTGGTGCCCGTTCTTTCTCTGCACGGTCCTGGACCCTTTCCTGGGCTATGTTATCCCACCCTCTCTGAATGACGCACTGTATTGG

3,710   3,720   3,730   3,740   3,750   3,760   3,770   3,780   3,790   3,800
aligned sequence oSF130Rev

tttgggtacttgaattctgccctcaatccgatggtttatgcctttttctatccctggttcagaagagccttgaagatggttctccttggtaaaattttcc

3,810   3,820   3,830   3,840   3,850   3,860   3,870   3,880   3,890   3,900

mTaar1 cDNA

template sequence puc2CL6IP-mTaar1-EGFP

TTTGGGTACTTGAATTCTGCCCTCAATCCGATGGTTTATGCCTTTTTCTATCCCTGGTTCAGAAGAGCCTTGAAGATGGTTCTCCTTGGTAAAATTTTCC

3,810   3,820   3,830   3,840   3,850   3,860   3,870   3,880   3,890   3,900
aligned sequence oSF130Rev

Template Alignment: oSF130Rev (from 3901-4200 bp)   12/18/2017 10:19:17 AM

aaaaagattcatctaggtctaagctattttttgACGGTACcgcgggcccgGGATCCACCGGTCGCCACCATGGTGAGCAAGGGCGAGGAGCTGTTCACCGG

3,910   3,920   3,930   3,940   3,950   3,960   3,970   3,980   3,990   4,000

AgeI

mTaar1 cDNA   linker   EGFP

template sequence puc2CL6IP-mTaar1-EGFP

AAAAAGATTCATCTAGGTCTAAGCTATTTTTTGACGGTACCGCGGGCCCGGGATCCACCGGT--

3,910   3,920   3,930   3,940   3,950   3,960   3,970   3,980   3,990   4,000

aligned sequence oSF130Rev

GGTGGTGCCCATCCTGGTCGAGCTGGACGGCGACGTAAACGGCCACAAGTTCAGCGTGTCCGGCGAGGGCGAGGGCGATGCCACCTACGGCAAGCTGACC

4,010   4,020   4,030   4,040   4,050   4,060   4,070   4,080   4,090   4,100

EGFP

template sequence puc2CL6IP-mTaar1-EGFP

4,010   4,020   4,030   4,040   4,050   4,060   4,070   4,080   4,090   4,100

aligned sequence oSF130Rev

CTGAAGTTCATCTGCACCACCGGCAAGCTGCCCGTGCCCTGGCCCACCCTCGTGACCACCCTGACCTACGGCGTGCAGTGCTTCAGCCGCTACCCCGACC

4,110   4,120   4,130   4,140   4,150   4,160   4,170   4,180   4,190   4,200

EGFP

template sequence puc2CL6IP-mTaar1-EGFP

4,110   4,120   4,130   4,140   4,150   4,160   4,170   4,180   4,190   4,200

aligned sequence oSF130Rev

https://benchling.com/maria/f/rvxenLsF-uploads/seq-CDL0QRqE-puc2cl6ip-mtaar1-egfp/edit#   14/31

3. Sequence alignment for *p*mTaar1-EGFP (in *p*EGFP-N1) using forward sequencing primer pEGFPN1-Fwd (standard from Eurofin Genomics):

Template Alignment: pEGFP-N1_FWD (from 601-900 bp)   12/18/2017 10:09:46 AM

tgtatcgcagtcaggtcagcgacctgggcggctgttctcccttctttagtaaagtatctggggtactggcgttcatgacttccttctatatacctggatc

   610   620   630   640   650   660   670   680   690   700

mTaar1 cDNA

template sequence pmTaar1-eGFP

TGTATCGCAGTCAGGTCAGCGACCTGGGCGGCTGTTCTCCCTTCTTTAGTAAAGTATCTGGGGTACTGGCGTTCATGACTTCCTTCTATATACCTGGATC

   610   620   630   640   650   660   670   680   690   700

aligned sequence pEGFP-N1_FWD

tgttatgttatttgtttactataggatatatttcatagctaaaggacaagcaaggtcaatcaatcgtacgaatgttcaagttggattggaagggaaaagc

   710   720   730   740   750   760   770   780   790   800

mTaar1 cDNA

template sequence pmTaar1-eGFP

TGTTATGTTATTTGTTTACTATAGGATATATTTCATAGCTAAAGGACAAGCAAGGTCAATCAATCGTACGAATGTTCAAGTTGGATTGGAAGGGAAAAGC

   710   720   730   740   750   760   770   780   790   800

aligned sequence pEGFP-N1_FWD

caagcaccacaaagcaaggaaacaaaagccgcgaagaccttagggatcatggtgggcg-ttttcctcgtatgctggtgcccgttctttctctgcacggtc
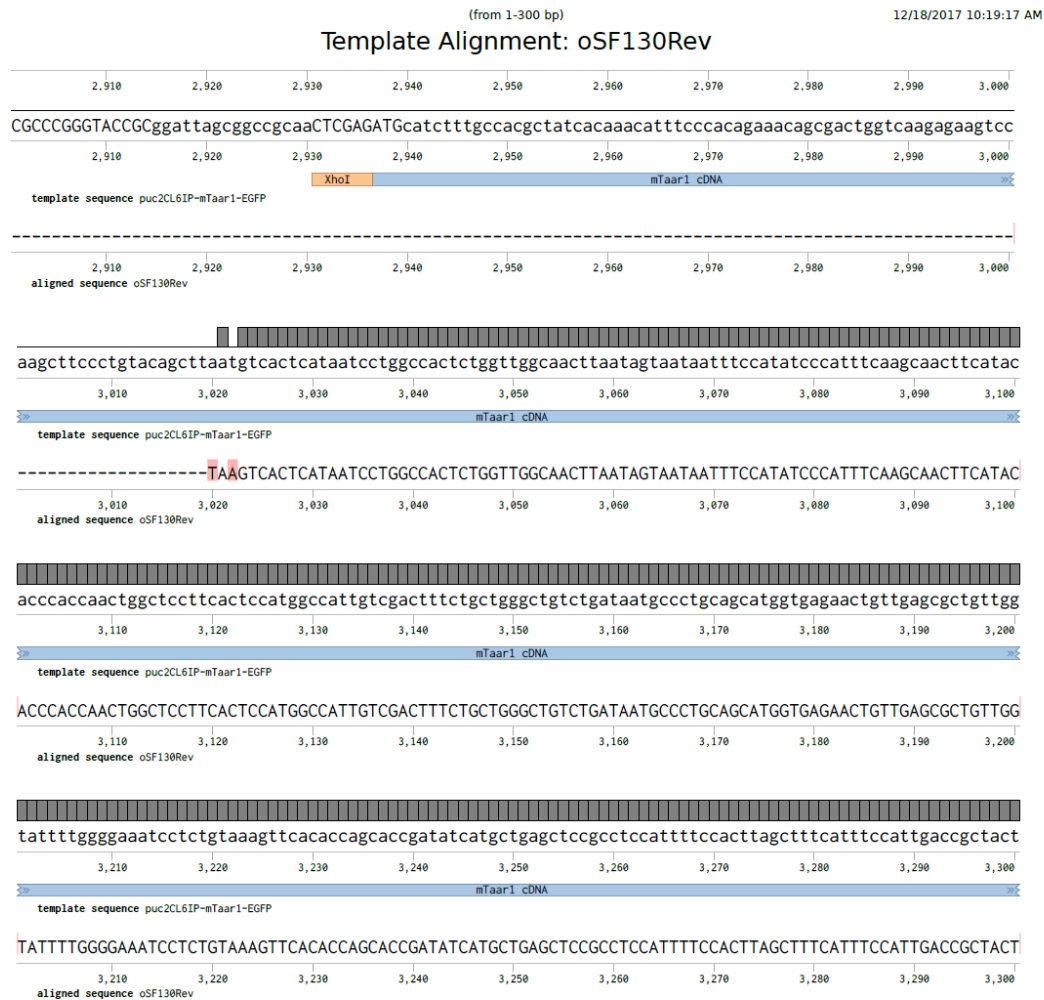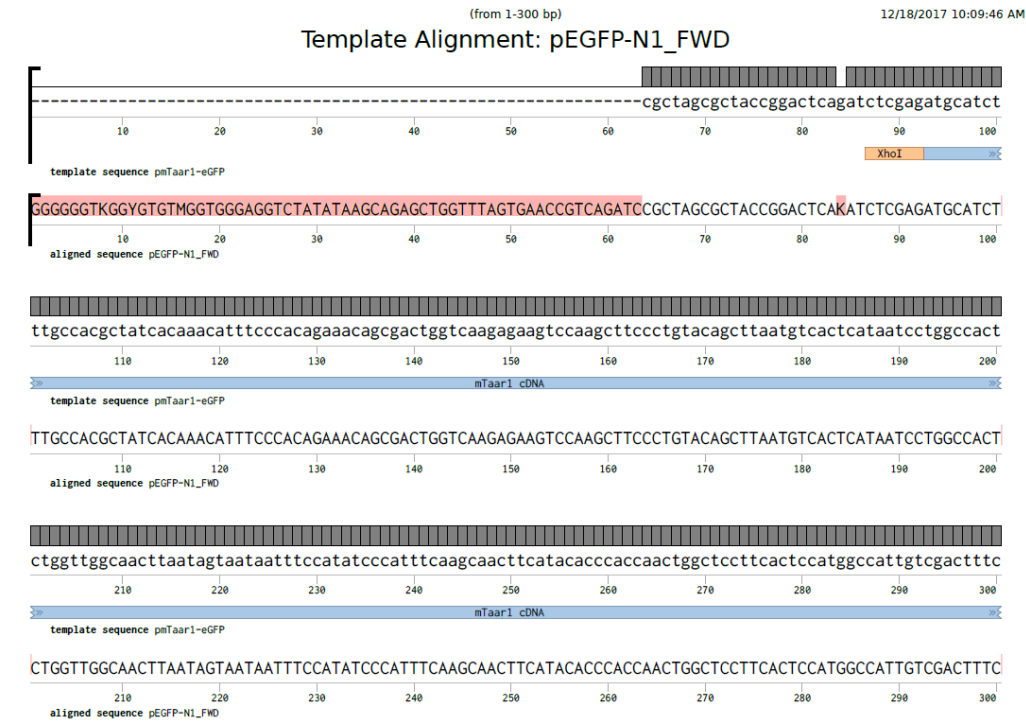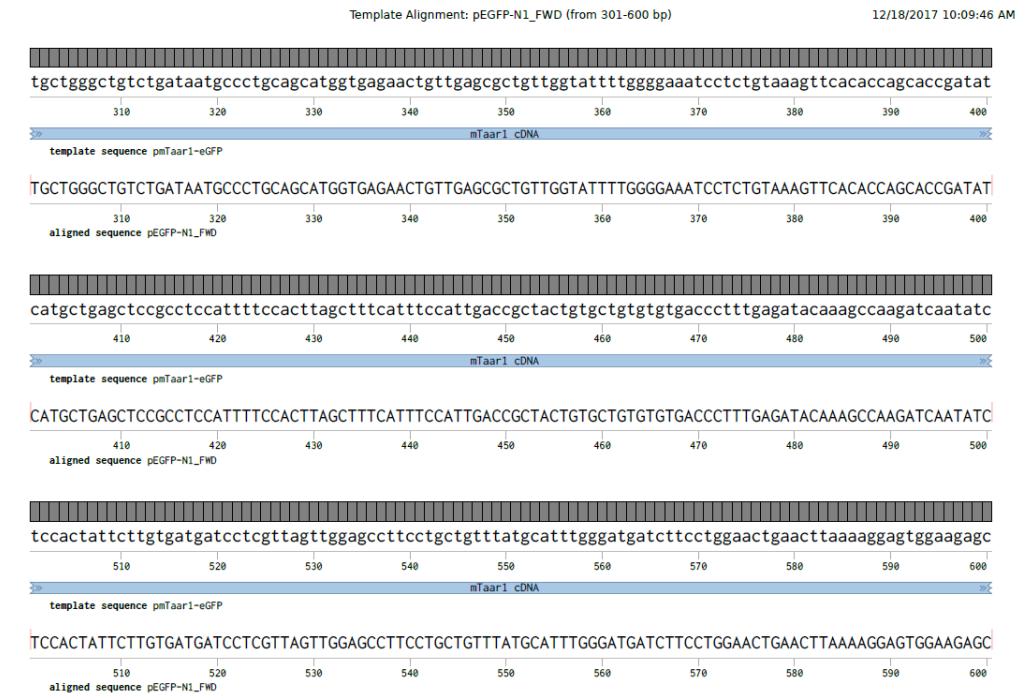
   810   820   830   840   850   860   870   880   890   900

mTaar1 cDNA

template sequence pmTaar1-eGFP

CAAGCACCACAAAGCAAGGAAACAAAAGCCGCGAAGACCTTAGGGATCATGGTGGGCGTTTTTCCTCGTATGCTGGTGCCCGTTCTTTCTCTGCACGGTC

   810   820   830   840   850   860   870   880   890   900

aligned sequence pEGFP-N1_FWD

Template Alignment: pEGFP-N1_FWD (from 901-1200 bp)   12/18/2017 10:09:46 AM

ctggaccctttcctgggctatgttatcccaccctctctgaatgacgcactgtattggtttgggtacttgaattctgccctcaatccgatggtttatgcct

   910   920   930   940   950   960   970   980   990   1,000

mTaar1 cDNA

template sequence pmTaar1-eGFP

CTGGACCCTTTTCCTGGCTATGTTATCCCACCCTCTCTGAATGACGCACTGTATTGGTTT-GGTACTTGGATTCTGCCCTCAATCCGATGG-TTATGCCC

   910   920   930   940   950   960   970   980   990   1,000

aligned sequence pEGFP-N1_FWD

ttttctatccctggttcagaagagccttgaagatggttctccttggtaaaattttccaaaaagattcatctaggtctaagctatttttgacggtaccgcg

  1,010   1,020   1,030   1,040   1,050   1,060   1,070   1,080   1,090   1,100

KpnI

mTaar1 cDNA   linker

template sequence pmTaar1-eGFP

TTTTCTATCCCTGGTCAGAGAG---CTTGAAGATGGTCTCT--

  1,010   1,020   1,030   1,040   1,050   1,060   1,070   1,080   1,090   1,100

aligned sequence pEGFP-N1_FWD

ggcccgggatccaccggtcgccaccatggtgagcaagggcgaggagctgttcaccggggtggtgcccatcctggtcgagctggacggcgacgtaaacggc

  1,110   1,120   1,130   1,140   1,150   1,160   1,170   1,180   1,190   1,200

AgeI

linker   EGFP

template sequence pmTaar1-eGFP

  1,110   1,120   1,130   1,140   1,150   1,160   1,170   1,180   1,190   1,200

aligned sequence pEGFP-N1_FWD

4. Sequence alignment for *p*mTaar1-EGFP (in *p*EGFP-N1) using reverse sequencing
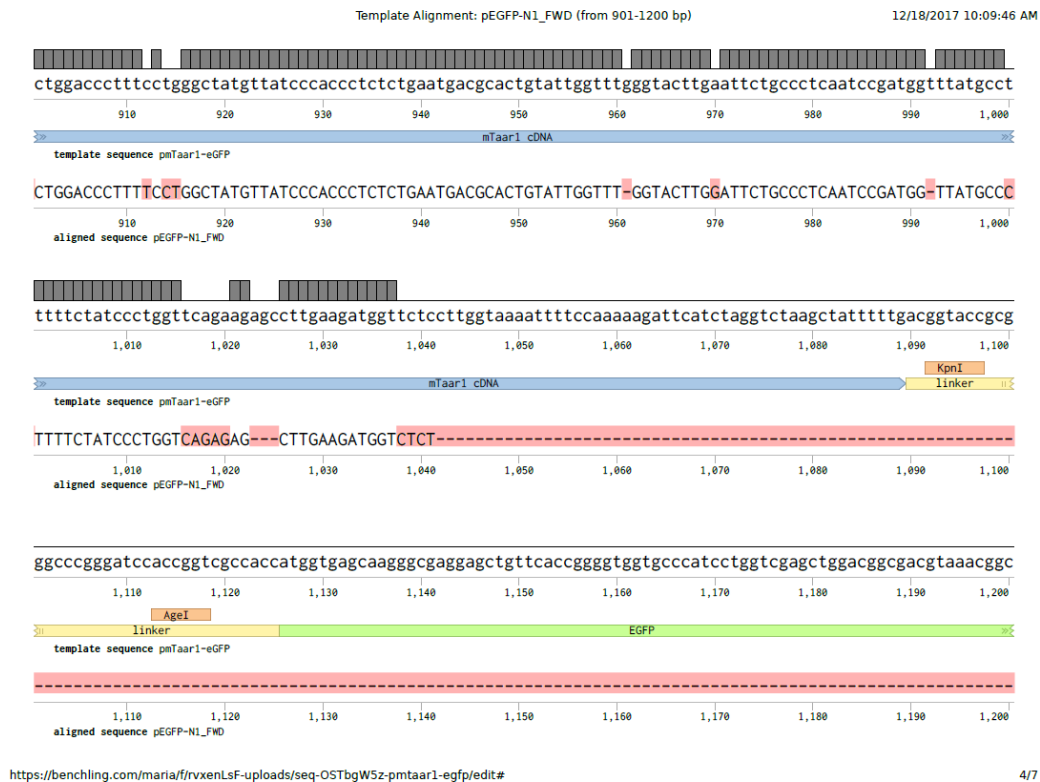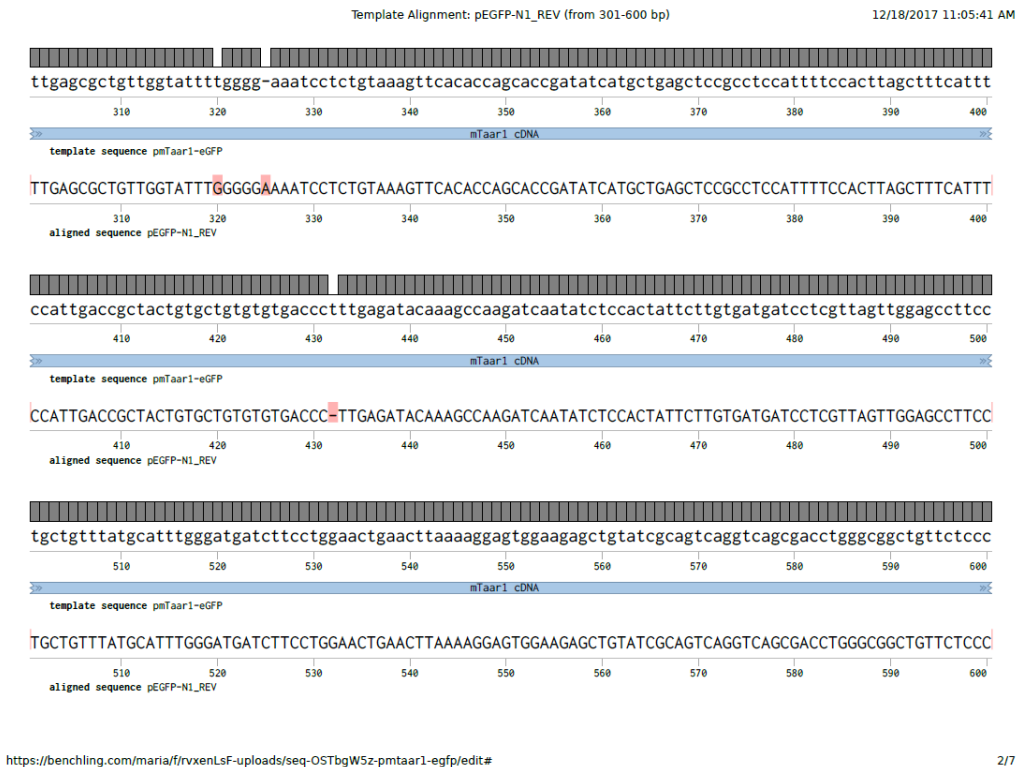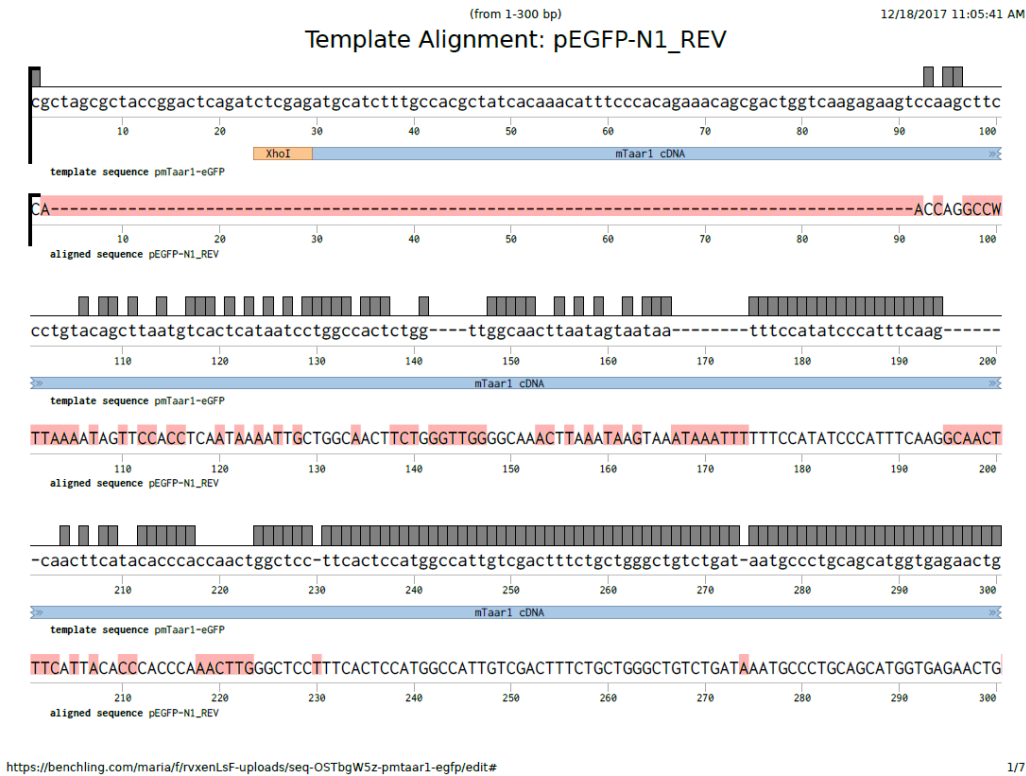   primer pEGFPN1-Rev (standard from Eurofin Genomics):

Template Alignment: pEGFP-N1_REV (from 601-900 bp)   12/18/2017 11:05:41 AM

ttctttagtaaagtatctggggtactggcgttcatgacttccttctatatacctggatctgttatgttatttgtttactataggatatatttcatagcta

610   620   630   640   650   660   670   680   690   700

mTaar1 cDNA

template sequence pmTaar1-eGFP

TTCTTTAGTAAAGTATCTGGGGTACTGGCGTTCATGACTTCCTTCTATATACCTGGATCTGTTATGTTATTTGTTTACTATAGGATATATTTCATAGCTA

610   620   630   640   650   660   670   680   690   700

aligned sequence pEGFP-N1_REV

aaggacaagcaaggtcaatcaatcgtacgaatgttcaagttggattggaagggaaaagccaagcaccacaaagcaaggaaacaaaagccgcgaagacctt

710   720   730   740   750   760   770   780   790   800

mTaar1 cDNA

template sequence pmTaar1-eGFP

AAGGACAAGCAAGGTCAATCAATCGTACGAATGTTCAAGTTGGATTGGAAGGGAAAAGCCAAGCACCACAAAGCAAGGAAACAAAAGCCGCGAAGACCTT
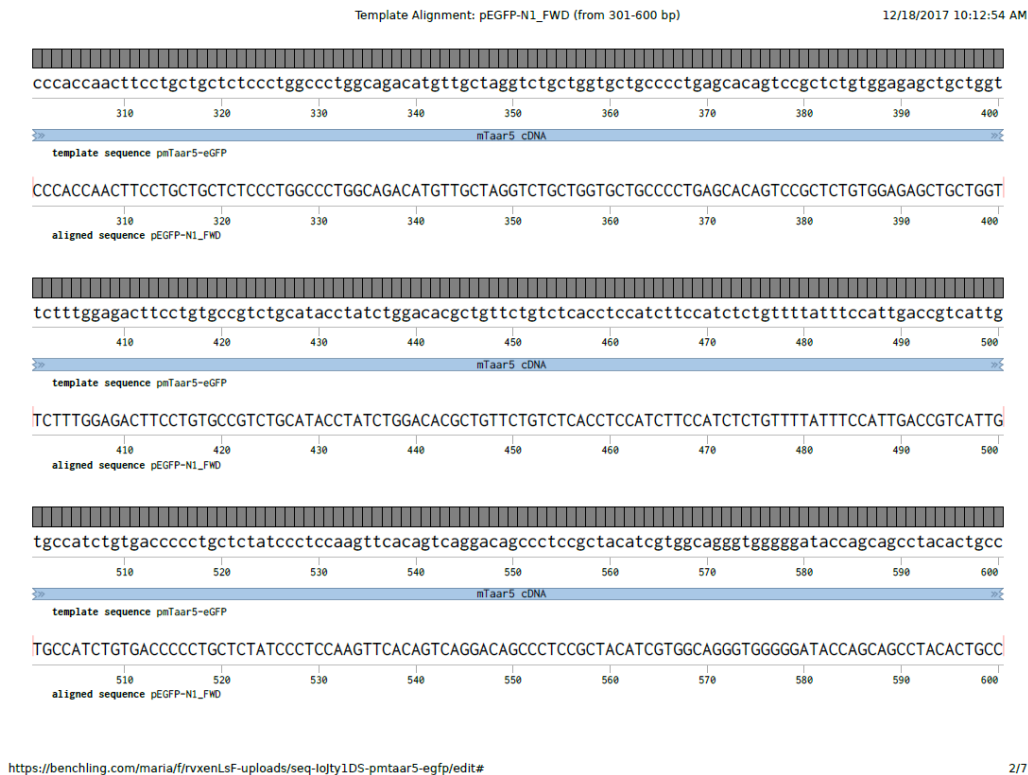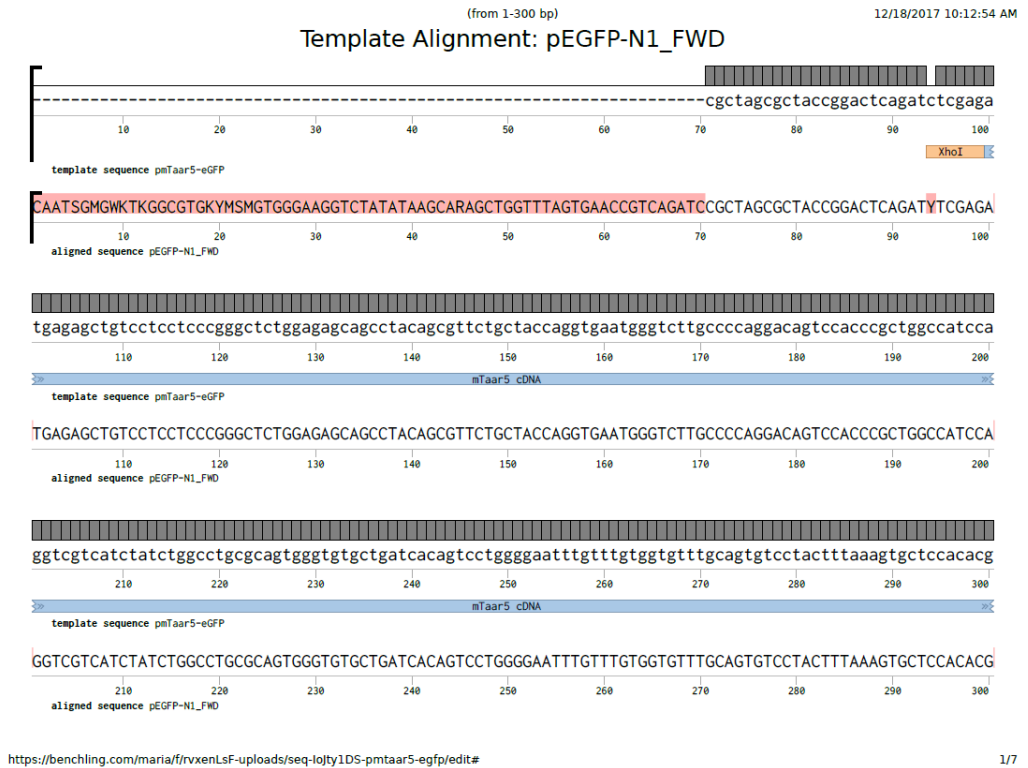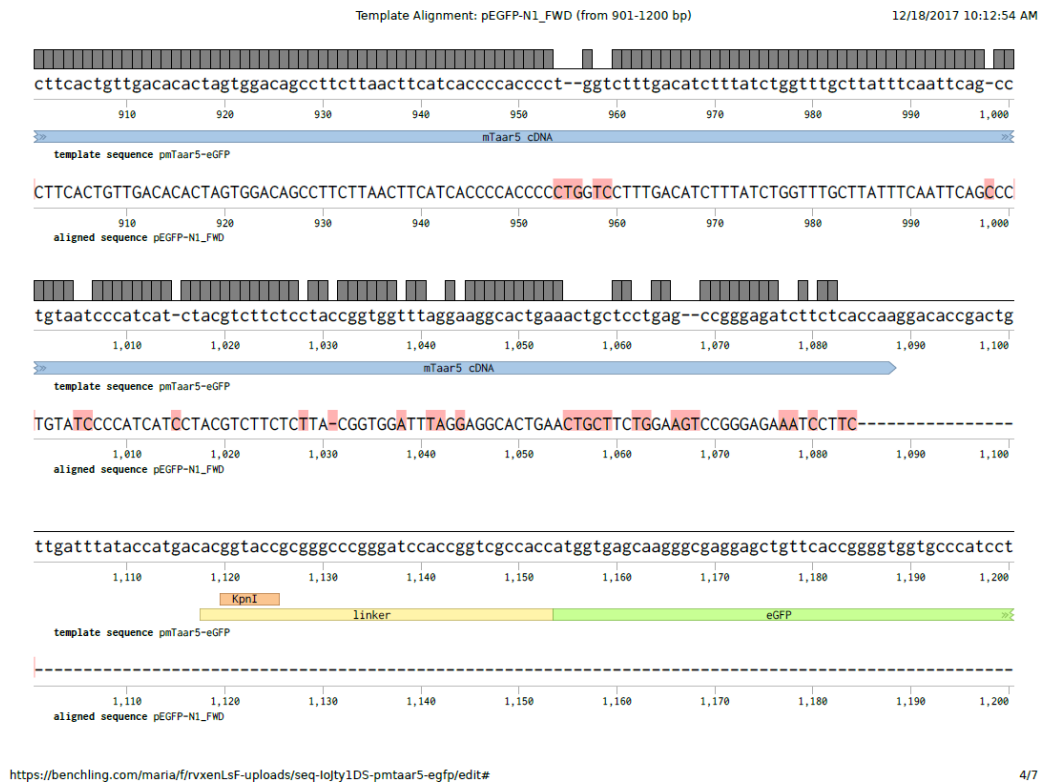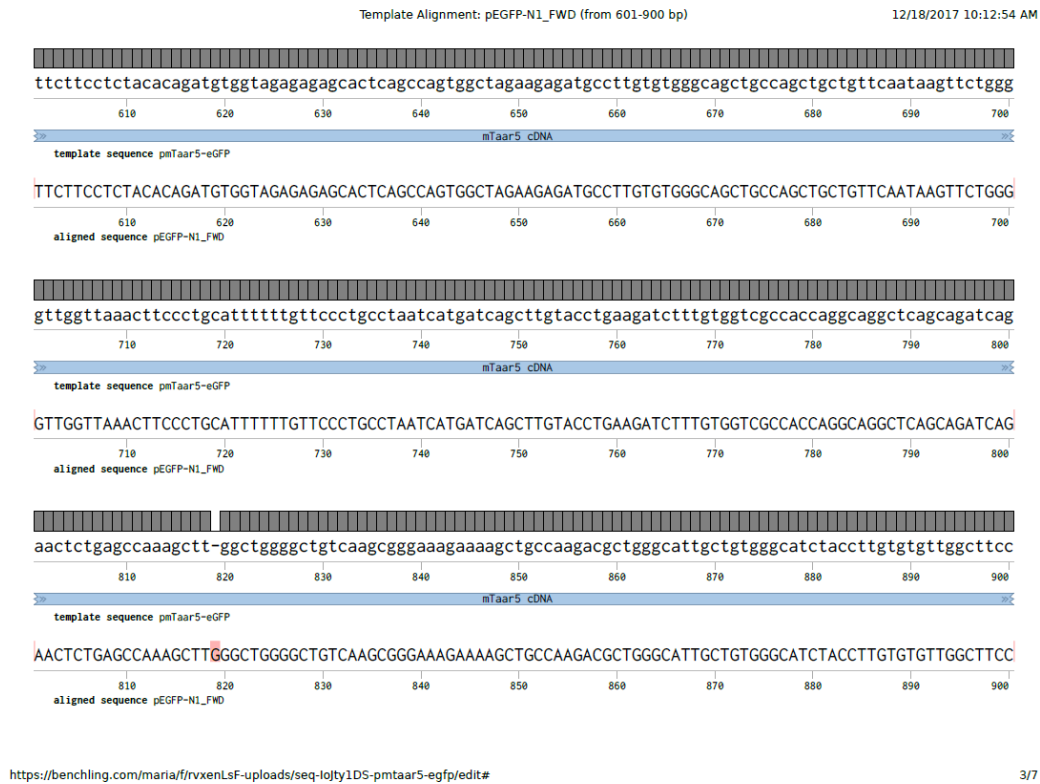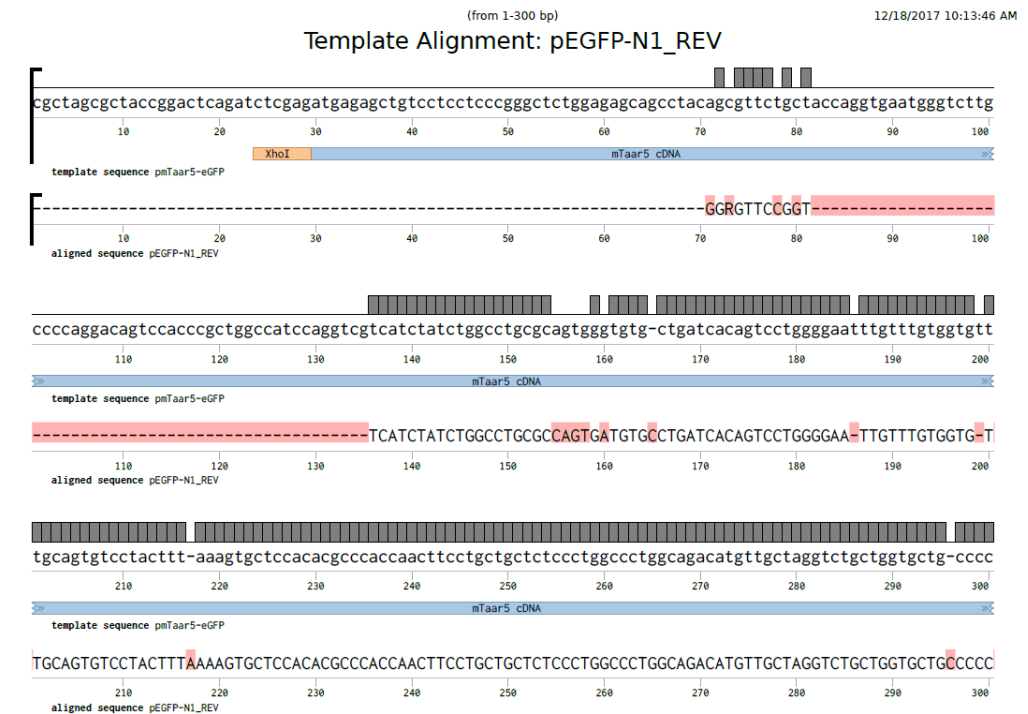
710   720   730   740   750   760   770   780   790   800

aligned sequence pEGFP-N1_REV

agggatcatggtgggcgttttcctcgtatgctggtgcccgttctttctctgcacggtcctggaccctttcctgggctatgttatcccaccctctctgaat

810   820   830   840   850   860   870   880   890   900

mTaar1 cDNA

template sequence pmTaar1-eGFP

AGGGATCATGGTGGGCGTTTTCCTCGTATGCTGGTGCCCGTTCTTTCTCTGCACGGTCCTGGACCCTTTCCTGGGCTATGTTATCCCACCCTCTCTGAAT

810   820   830   840   850   860   870   880   890   900

aligned sequence pEGFP-N1_REV

Template Alignment: pEGFP-N1_REV (from 901-1200 bp)   12/18/2017 11:05:41 AM

gacgcactgtattggtttgggtacttgaattctgccctcaatccgatggtttatgcctttttctatccctggttcagaagagccttgaagatggttctcc

910   920   930   940   950   960   970   980   990   1,000

mTaar1 cDNA

template sequence pmTaar1-eGFP

GACGCACTGTATTGGTTTGGGTACTTGAATTCTGCCCTCAATCCGATGGTTTATGCCTTTTTCTATCCCTGGTTCAGAAGAGCCTTGAAGATGGTTCTCC

910   920   930   940   950   960   970   980   990   1,000

aligned sequence pEGFP-N1_REV

ttggtaaaattttccaaaaagattcatctaggtctaagctattttttgacggtaccgcgggcccgggatccaccggtcgccaccatggtgagcaagggcga

1,010   1,020   1,030   1,040   1,050   1,060   1,070   1,080   1,090   1,100

KpnI   AgeI

mTaar1 cDNA   linker   EGFP

template sequence pmTaar1-eGFP

TTGGTAAAATTTTCCAAAAAGATTCATCTAGGTCTAAGCTATTTTTTGACGGTACCGCGGGCCCGGGATCCACCGGTCGCCACCATGGTGAGCAAGGGMGR

1,010   1,020   1,030   1,040   1,050   1,060   1,070   1,080   1,090   1,100

aligned sequence pEGFP-N1_REV

ggagctgttcaccggggtggtgcccatcctggtcgagctggacggcgacgtaaacggccacaagttcagcgtgtccggcgagggcgagggcgatgccacc

1,110   1,120   1,130   1,140   1,150   1,160   1,170   1,180   1,190   1,200

EGFP

template sequence pmTaar1-eGFP

GGAGCTGTTCACCGGGGTGGTGCCCATCCTGGTCGAGCTGGACGGCGACGTAAAC-GCCACAAGTC--------------------------------

1,110   1,120   1,130   1,140   1,150   1,160   1,170   1,180   1,190   1,200

aligned sequence pEGFP-N1_REV

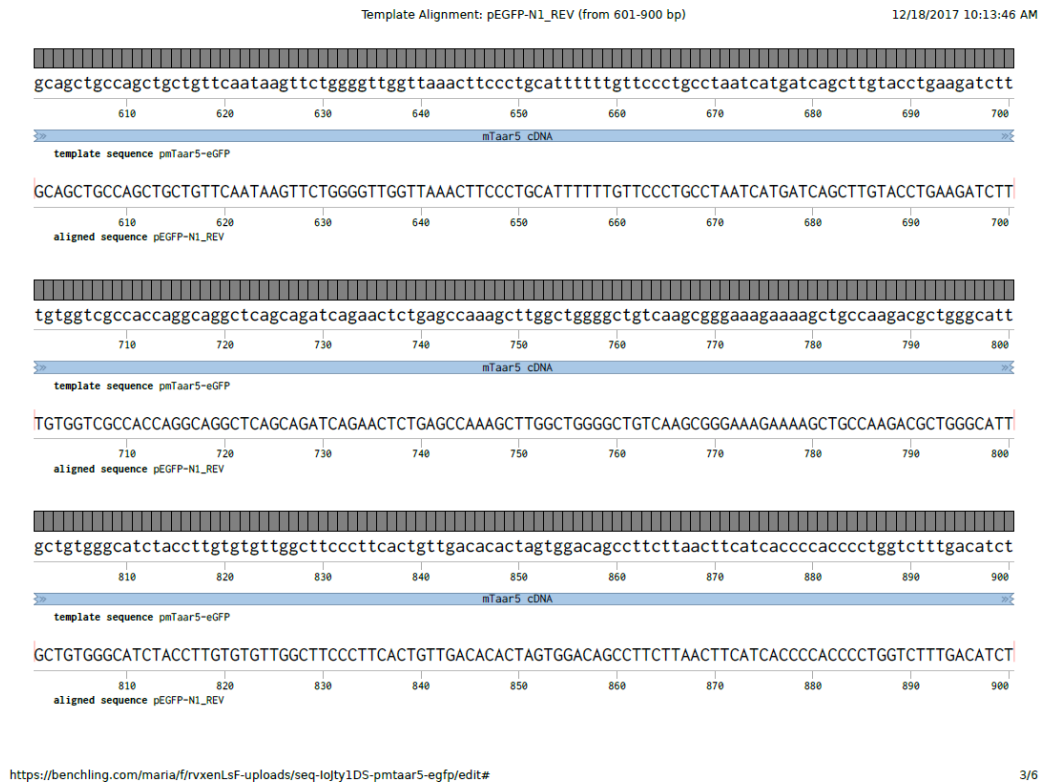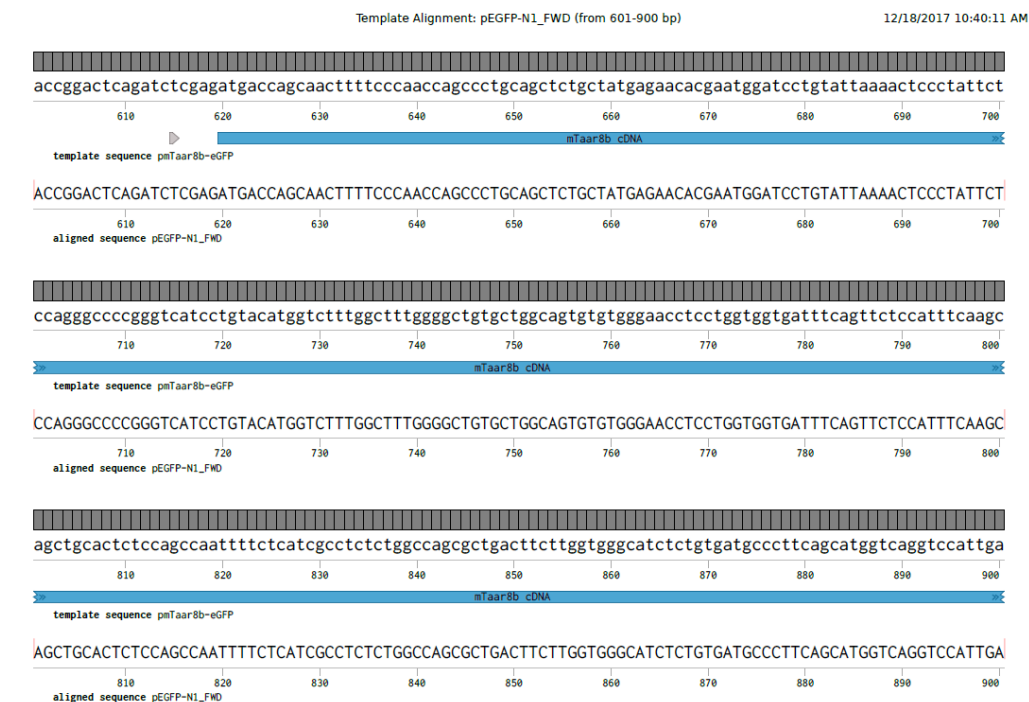5. Sequence alignment for *p*mTaar5-EGFP using forward sequencing primer pEGFPN1-Fwd:

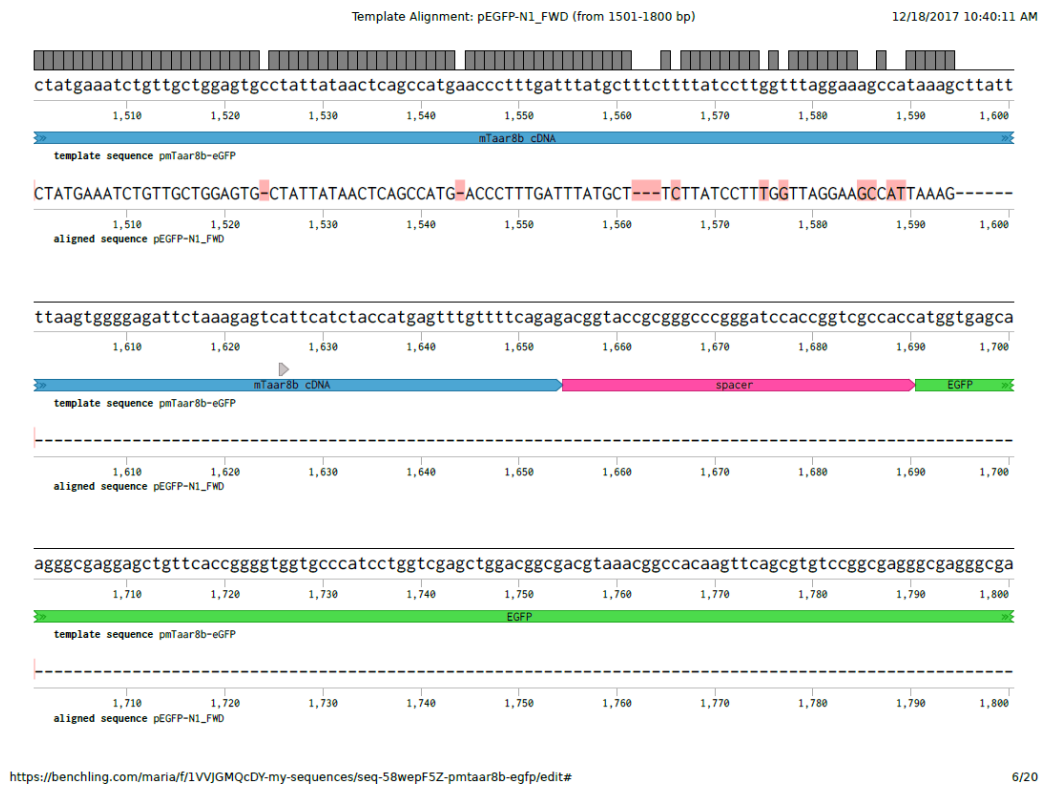Template Alignment: pEGFP-N1_FWD (from 601-900 bp)   12/18/2017 10:12:54 AM

ttcttcctctacacagatgtggtagagagagcactcagccagtggctagaagagatgccttgtgtgggcagctgccagctgctgttcaataagttctggg

610   620   630   640   650   660   670   680   690   700

mTaar5 cDNA

template sequence pmTaar5-eGFP

TTCTTCCTCTACACAGATGTGGTAGAGAGAGCACTCAGCCAGTGGCTAGAAGAGATGCCTTGTGTGGGCAGCTGCCAGCTGCTGTTCAATAAGTTCTGGG

610   620   630   640   650   660   670   680   690   700

aligned sequence pEGFP-N1_FWD

gttggttaaacttccctgcattttttgttccctgcctaatcatgatcagcttgtacctgaagatctttgtggtcgccaccaggcaggctcagcagatcag

710   720   730   740   750   760   770   780   790   800

mTaar5 cDNA

template sequence pmTaar5-eGFP

GTTGGTTAAACTTCCCTGCATTTTTTGTTCCCTGCCTAATCATGATCAGCTTGTACCTGAAGATCTTTGTGGTCGCCACCAGGCAGGCTCAGCAGATCAG

710   720   730   740   750   760   770   780   790   800

aligned sequence pEGFP-N1_FWD

aactctgagccaaagctt-ggctggggctgtcaagcgggaaagaaaagctgccaagacgctgggcattgctgtgggcatctaccttgtgtgttggcttcc

810   820   830   840   850   860   870   880   890   900

mTaar5 cDNA

template sequence pmTaar5-eGFP

AACTCTGAGCCAAAGCTTGGGCTGGGGCTGTCAAGCGGGAAAGAAAAGCTGCCAAGACGCTGGGCATTGCTGTGGGCATCTACCTTGTGTGTTGGCTTCC

810   820   830   840   850   860   870   880   890   900

aligned sequence pEGFP-N1_FWD

https://benchling.com/maria/f/rvxenLsF-uploads/seq-IoJty1DS-pmtaar5-egfp/edit#   3/7

Template Alignment: pEGFP-N1_FWD (from 901-1200 bp)   12/18/2017 10:12:54 AM

cttcactgttgacacactagtggacagccttcttaacttcatcaccccaccct--ggtctttgacatctttatctggtttgcttatttcaattcag-cc

910   920   930   940   950   960   970   980   990   1,000

mTaar5 cDNA

template sequence pmTaar5-eGFP

CTTCACTGTTGACACACTAGTGGACAGCCTTCTTAACTTCATCACCCCACCCCCTGGTCCTTTGACATCTTTATCTGGTTTGCTTATTTCAATTCAGCCC

910   920   930   940   950   960   970   980   990   1,000

aligned sequence pEGFP-N1_FWD

tgtaatcccatcat-ctacgtcttctcctaccggtggtttaggaaggcactgaaactgctcctgag--ccgggagatcttctcaccaaggacaccgactg

1,010   1,020   1,030   1,040   1,050   1,060   1,070   1,080   1,090   1,100

mTaar5 cDNA

template sequence pmTaar5-eGFP

TGTATCCCCATCATCCTACGTCTTCTCTTA-CGGTGGATTTAGGAGGCACTGAACTGCTTCTGGAAGTCCGGGAGAAATCCTTC----------------

1,010   1,020   1,030   1,040   1,050   1,060   1,070   1,080   1,090   1,100

aligned sequence pEGFP-N1_FWD

ttgatttataccatgacacggtaccgcgggcccgggatccaccggtcgccaccatggtgagcaagggcgaggagctgttcaccggggtggtgcccatcct

1,110   1,120   1,130   1,140   1,150   1,160   1,170   1,180   1,190   1,200

KpnI

linker   eGFP

template sequence pmTaar5-eGFP

1,110   1,120   1,130   1,140   1,150   1,160   1,170   1,180   1,190   1,200

aligned sequence pEGFP-N1_FWD

https://benchling.com/maria/f/rvxenLsF-uploads/seq-IoJty1DS-pmtaar5-egfp/edit#   4/7

6. Sequence alignment for *p*mTaar5-EGFP using reverse sequencing primer pEGFPN1-Rev:

Template Alignment: pEGFP-N1_REV (from 601-900 bp)   12/18/2017 10:13:46 AM

gcagctgccagctgctgttcaataagttctggggttggttaaacttccctgcatttttttgttccctgcctaatcatgatcagcttgtacctgaagatctt

610   620   630   640   650   660   670   680   690   700

mTaar5 cDNA

template sequence pmTaar5-eGFP

GCAGCTGCCAGCTGCTGTTCAATAAGTTCTGGGGTTGGTTAAACTTCCCTGCATTTTTTGTTCCCTGCCTAATCATGATCAGCTTGTACCTGAAGATCTT

610   620   630   640   650   660   670   680   690   700

aligned sequence pEGFP-N1_REV

tgtggtcgccaccaggcaggctcagcagatcagaactctgagccaaagcttggctggggctgtcaagcgggaaagaaaagctgccaagacgctgggcatt

710   720   730   740   750   760   770   780   790   800

mTaar5 cDNA

template sequence pmTaar5-eGFP

TGTGGTCGCCACCAGGCAGGCTCAGCAGATCAGAACTCTGAGCCAAAGCTTGGCTGGGGCTGTCAAGCGGGAAAGAAAAGCTGCCAAGACGCTGGGCATT

710   720   730   740   750   760   770   780   790   800

aligned sequence pEGFP-N1_REV

gctgtgggcatctaccttgtgtgttggcttcccttcactgttgacacactagtggacagccttcttaacttcatcaccccacccctggtctttgacatct

810   820   830   840   850   860   870   880   890   900

mTaar5 cDNA

template sequence pmTaar5-eGFP

GCTGTGGGCATCTACCTTGTGTGTTGGCTTCCCTTCACTGTTGACACACTAGTGGACAGCCTTCTTAACTTCATCACCCCACCCCTGGTCTTTGACATCT

810   820   830   840   850   860   870   880   890   900

aligned sequence pEGFP-N1_REV

https://benchling.com/maria/f/rvxenLsF-uploads/seq-IoJty1DS-pmtaar5-egfp/edit#   3/6

Template Alignment: pEGFP-N1_REV (from 901-1200 bp)   12/18/2017 10:13:46 AM

ttatctggtttgcttatttcaattcagcctgtaatcccatcatctacgtcttctcctaccggtggtttaggaaggcactgaaactgctcctgagccggga

910   920   930   940   950   960   970   980   990   1,000

mTaar5 cDNA

template sequence pmTaar5-eGFP

TTATCTGGTTTGCTTATTTCAATTCAGCCTGTAATCCCATCATCTACGTCTTCTCCTACCGGTGGTTTAGGAAGGCACTGAAACTGCTCCTGAGCCGGGA

910   920   930   940   950   960   970   980   990   1,000

aligned sequence pEGFP-N1_REV

gatcttctcaccaaggacaccgactgttgatttataccatgacacggtaccgcgggcccgggatccaccggtcgccaccatggtgagcaagggcgaggag

1,010   1,020   1,030   1,040   1,050   1,060   1,070   1,080   1,090   1,100

mTaar5 cDNA   KpnI   linker   eGFP

template sequence pmTaar5-eGFP

GATCTTCTCACCAAGGACACCGACTGTTGATTTATACCATGACACGGTACCGCGGGCCCGGGATCCACCGGTCGCCACCATGGTGAGCAAGGRMGAGGAG

1,010   1,020   1,030   1,040   1,050   1,060   1,070   1,080   1,090   1,100

aligned sequence pEGFP-N1_REV

ctgttcaccggggtggtgcccatcctggtcgagctggacggcgacgtaaacggccacaagttcagcgtgtccggcgagggcgagggcgatgccacctacg

1,110   1,120   1,130   1,140   1,150   1,160   1,170   1,180   1,190   1,200

eGFP

template sequence pmTaar5-eGFP

CTGTTCACCGGGGTGGTGCCCATCCTGGTCGAGCTGGACGGCGACGTAAACGGCCACAAGTC---AGCGGCCGGCCGGGGMARG----------------

1,110   1,120   1,130   1,140   1,150   1,160   1,170   1,180   1,190   1,200

aligned sequence pEGFP-N1_REV

https://benchling.com/maria/f/rvxenLsF-uploads/seq-IoJty1DS-pmtaar5-egfp/edit#   4/6

7. Sequence alignment for *p*mTaar8b-EGFP using forward sequencing primer pEGFPN1-Fwd:

Template Alignment: pEGFP-N1_FWD (from 1501-1800 bp)   12/18/2017 10:40:11 AM

ctatgaaatctgttgctggagtgcctattataactcagccatgaacccctttgatttatgctttcttttatccttggtttaggaaagccataaagcttatt

1,510   1,520   1,530   1,540   1,550   1,560   1,570   1,580   1,590   1,600

mTaar8b cDNA

template sequence pmTaar8b-eGFP

CTATGAAATCTGTTGCTGGAGTG-CTATTATAACTCAGCCATG-ACCCTTTGATTTATGCT---TCTTATCCTTTGGTTAGGAAGCCATTAAAG------

1,510   1,520   1,530   1,540   1,550   1,560   1,570   1,580   1,590   1,600

aligned sequence pEGFP-N1_FWD

ttaagtggggagattctaaagagtcattcatctaccatgagtttgttttcagagacggtaccgcgggcccgggatccaccggtcgccaccatggtgagca

1,610   1,620   1,630   1,640   1,650   1,660   1,670   1,680   1,690   1,700

mTaar8b cDNA   **spacer**   **EGFP**

template sequence pmTaar8b-eGFP

1,610   1,620   1,630   1,640   1,650   1,660   1,670   1,680   1,690   1,700

aligned sequence pEGFP-N1_FWD

agggcgaggagctgttcaccggggtggtgcccatcctggtcgagctggacggcgacgtaaacggccacaagttcagcgtgtccggcgagggcgagggcga

1,710   1,720   1,730   1,740   1,750   1,760   1,770   1,780   1,790   1,800

EGFP

template sequence pmTaar8b-eGFP

1,710   1,720   1,730   1,740   1,750   1,760   1,770   1,780   1,790   1,800

aligned sequence pEGFP-N1_FWD

Template Alignment: pEGFP-N1_FWD (from 901-1200 bp)   12/18/2017 10:40:11 AM

gagctgctggtactttggagatgcattttgtagccttcacagttgctgtgatgtggctttttgttactcttctgccctccacctgtgcttcatctcagtg

910   920   930   940   950   960   970   980   990   1,000

mTaar8b cDNA

template sequence pmTaar8b-eGFP

GAGCTGCTGGTACTTTGGAGATGCATTTTGTAGCCTTCACAGTTGCTGTGATGTGGCTTTTTGTTACTCTTCTGCCCTCCACCTGTGCTTCATCTCAGTG

910   920   930   940   950   960   970   980   990   1,000

aligned sequence pEGFP-N1_FWD

gacaggtacattgctgtcacagaccctctggtctatcccaccaagttcacagtgtctgtgtctggaatttgcatcagcatctcctggattctgcccctgg

1,010   1,020   1,030   1,040   1,050   1,060   1,070   1,080   1,090   1,100

mTaar8b cDNA

template sequence pmTaar8b-eGFP

GACAGGTACATTGCTGTCACAGACCCTCTGGTCTATCCCACCAAGTTCACAGTGTCTGTGTCTGGAATTTGCATCAGCATCTCCTGGATTCTGCCCCTGG

1,010   1,020   1,030   1,040   1,050   1,060   1,070   1,080   1,090   1,100

aligned sequence pEGFP-N1_FWD

tatacagcagtgcagtgttctacacaggcatcagtgctaaggggattgaaagcttagtaagtgctctgaattgtgtaggggggctgccaaatcgttgtcaa

1,110   1,120   1,130   1,140   1,150   1,160   1,170   1,180   1,190   1,200

mTaar8b cDNA

template sequence pmTaar8b-eGFP

TATACAGCAGTGCAGTGTTCTACACAGGCATCAGTGCTAAGGGGATTGAAAGCTTAGTAAGTGCTCTGAATTGTGTAGGGGGCTGCCAAATCGTTGTCAA

1,110   1,120   1,130   1,140   1,150   1,160   1,170   1,180   1,190   1,200

aligned sequence pEGFP-N1_FWD

8. Sequence alignment for *p*mTaar8b-EGFP using reverse sequencing primer pEGFPN1-Rev:

Template Alignment: pEGFP-N1_REV (from 601-900 bp)   12/18/2017 10:55:46 AM

https://benchling.com/maria/f/1VVJGMQcDY-my-sequences/seq-58wepF5Z-pmtaar8b-egfp/edit#   3/20

Template Alignment: pEGFP-N1_REV (from 901-1200 bp)   12/18/2017 10:55:46 AM

https://benchling.com/maria/f/1VVJGMQcDY-my-sequences/seq-58wepF5Z-pmtaar8b-egfp/edit#   4/20

78

Template Alignment: pEGFP-N1_REV (from 1201-1500 bp)   12/18/2017 10:55:46 AM

atcgttgtcaatcaagactgggttttgatagattttcttctattttttcatacctacccttgttatgatcattctttacagcaaaatattttttggtagcca

1,210   1,220   1,230   1,240   1,250   1,260   1,270   1,280   1,290   1,300

mTaar8b cDNA

template sequence pmTaar8b-eGFP

ATCGTTGTCAATCAAGACTGGGTTTTGATAGATTTTCTTCTATTTTTTCATACCTACCCTTGTTATGATCATTCTTTACAGCAAAATATTTTTTGGTAGCCA

1,210   1,220   1,230   1,240   1,250   1,260   1,270   1,280   1,290   1,300

aligned sequence pEGFP-N1_REV

aacagcaagctgtaaaaattgaaacttctgtaagtgacaacagaggtgaatcatcctcagagagtcacaaagccagagtggccaagagagagaggaaggc

1,310   1,320   1,330   1,340   1,350   1,360   1,370   1,380   1,390   1,400

mTaar8b cDNA

template sequence pmTaar8b-eGFP

AACAGCAAGCTGTAAAAATTGAAAMWTMWRTAAGTGACAACAGAGGTGAATCATCCTCAGAGAGTCACAAAGCCAGAGTGGCCAAGAGAGAGAGGAAGGC

1,310   1,320   1,330   1,340   1,350   1,360   1,370   1,380   1,390   1,400

aligned sequence pEGFP-N1_REV

tgcaaaaaccttgggggtcactgtggtggcttttatggtctcgtggctcccatacacaattgactcattggttgatgctttcgtgggcttcattactcct

1,410   1,420   1,430   1,440   1,450   1,460   1,470   1,480   1,490   1,500

mTaar8b cDNA

template sequence pmTaar8b-eGFP

TGCAAAAACCTTGGGGGTCACTGTGGTGGCTTTTATGGTCTCGTGGCTCCCATACACAATTGACTCATTGGTTGATGCTTTCGTGGGCTTCATTACTCCT

1,410   1,420   1,430   1,440   1,450   1,460   1,470   1,480   1,490   1,500

aligned sequence pEGFP-N1_REV

Template Alignment: pEGFP-N1_REV (from 1501-1800 bp)   12/18/2017 10:55:46 AM

gcctatgtctatgaaatctgttgctggagtgcctattataactcagccatgaaccctttgatttatgctttctttttatccttggtttaggaaagccataa

1,510   1,520   1,530   1,540   1,550   1,560   1,570   1,580   1,590   1,600

mTaar8b cDNA

template sequence pmTaar8b-eGFP

GCCTATGTCTATGAAATCTGTTGCTGGAGTGCCTATTATAACTCAGCCATGAACCCTTTGATTTATGCTTTCTTTTTATCCTTGGTTTAGGAAARCCATAA

1,510   1,520   1,530   1,540   1,550   1,560   1,570   1,580   1,590   1,600

aligned sequence pEGFP-N1_REV

agcttattttaagtggggagattctaaagagtcattcatctaccatgagtttgttttcagagacggtaccgcgggcccgggatccaccggtcgccaccat

1,610   1,620   1,630   1,640   1,650   1,660   1,670   1,680   1,690   1,700

mTaar8b cDNA   spacer

template sequence pmTaar8b-eGFP

AGCTTATTTTWWKTGGGGAGATTCTAAAGAGTCATTCATCTACCATGAGTTTGTTTTCAGAGACGGTACCGCGGGMCCGGGATCCACCGGTCGCCACCAT

1,610   1,620   1,630   1,640   1,650   1,660   1,670   1,680   1,690   1,700

aligned sequence pEGFP-N1_REV

ggtgagcaagggcgaggagctgttcaccggggtggtgcccatcctggtcgagctggacggcgacgtaaacggccacaagttcagcgtgtccggcgagggc

1,710   1,720   1,730   1,740   1,750   1,760   1,770   1,780   1,790   1,800

EGFP

template sequence pmTaar8b-eGFP

GGTGAGCTA---

1,710   1,720   1,730   1,740   1,750   1,760   1,770   1,780   1,790   1,800

aligned sequence pEGFP-N1_REV

4.5 Canonical TSH regulation in the thyroid resulting in regular cathepsin-mediated thyroglobulin processing requires Taar1 expression

Maria Qatato [1#], Joanna Szumska [1#], Vladislav Skripnik [1], Eddy Rijntjes [2], Josef Köhrle [2], and Klaudia Brix [1*]

[1]Department of Life Sciences and Chemistry, Jacobs University Bremen, Bremen, Germany
[2]Institut für Experimentelle Endokrinologie, Charité – Universitätsmedizin Berlin, corporate member of Freie Universität Berlin, Humboldt-Universität zu Berlin, and Berlin Institute of Health, Berlin, Germany
[#]These authors contributed equally to this manuscript.

* Correspondence:
Corresponding Author
k.brix@jacobs-university.de

Keywords: cathepsins, morphometry, thyroglobulin, thyroid stimulating hormone receptor, trace amine-associated receptor 1

Submitted to Frontiers in Pharmacology; under review.

Abstract

Trace amine-associated receptor 1 (Taar1) has been suggested as a putative receptor of thyronamines. These are aminergic messengers with potential physiological roles related to metabolic and neurological effects of their contingent precursors, the thyroid hormones. Recently, we found Taar1 to be localized at the primary cilia of rodent thyroid epithelial cells *in vitro* and *in situ*. Thus, Taar1 is present in a location of thyroid follicles where it might be involved in regulation of thyroglobulin utilization from luminal storage forms through its cathepsin-mediated proteolytic processing, eventually yielding TH and derivatives thereof.

In this study, Taar1-deficient male mice (*taar1^{-/-}*) were used to determine whether and how Taar1 function would entail alterations in thyroid states of young and adult animals. Analyses of blood serum revealed largely unaltered T_4 and T_3 concentrations upon Taar1 deficiency, however, accompanied by elevated TSH concentrations. Interestingly, TSH receptors, typically localized at the basolateral plasma membrane domain of wild type controls, were located at vesicular membranes in thyrocytes of *taar1^{-/-}* mice. In addition, determination of epithelial extensions in *taar1^{-/-}* thyroids showed prismatic cells, which might indicate activation states higher than in the wild type. However, gross degradation of thyroglobulin was comparable to

controls. Still, deregulated thyroglobulin turnover in *taar1*^{-/-} mice was indicated by luminal accumulation of covalently cross-linked thyroglobulin storage forms. These findings were in line with decreased proteolytic activities of thyroglobulin-solubilizing and -processing proteases, due to upregulated cystatins acting as their endogenous inhibitors *in situ.*

In conclusion, Taar1-deficient mice are hyperthyrotropinemic, as based on elevated TSH but unaltered T_4 and T_3 concentrations in blood serum, and are characterized by non-canonical TSH receptor localization in intracellular compartments, which is accompanied by altered thyroglobulin turnover due to a disbalanced proteolytic network in the angio-follicular units.

These finding are of significance considering the rising popularity of using TAAR1 agonists or antagonists as neuro-modulating pharmacological drugs. Our study highlights the importance of further evaluating potential thyroid-related off-target effects, which may not only affect the thyroid hormone-generating thyroid gland, but may emanate to other thyroid hormone target organs like the CNS that is vitally dependent on their proper supply.

1   Introduction

Trace amine-associated receptor 1 (Taar1) is a G protein coupled receptor (GPCR) that was shown to be involved in regulation of dopaminergic neurotransmission in rodents (Wolinsky et al., 2007; Lindemann et al., 2008; Espinoza et al., 2011; Revel et al., 2011; Revel et al., 2012a; Leo et al., 2014; Harmeier et al., 2015). Subsequently, Taar1 was considered as a drug target for treatment of alcohol and drug addiction, as well as Parkinson's disease and schizophrenia (Bradaia et al., 2009; Galley et al., 2012; Revel et al., 2012b; Lynch et al., 2013; Alvarsson et al., 2015; reviewed in Grandy, 2007, 2014; Grandy et al., 2016; Berry et al., 2017). In the context of neuro-modulation, *taar1*^{-/-} mouse models were developed to study schizophrenia particularly, but also other neuropsychiatric disorders. The *taar1*^{-/-} mouse model exhibited elevated sensitivity to amphetamines in comparison to wild type (WT) littermates, which manifested in enhanced locomotor activity. This was correlated with higher dopamine and norepinephrine release in the striatum upon amphetamine treatment, as well as a significant increase in striatal expression of high-affinity dopamine receptors, all of which are regarded as characteristic symptoms of schizophrenia (Wolinsky et al., 2007; Lindemann et al., 2008). Otherwise, the *taar1*^{-/-} mouse proved comparable to WT controls in terms of development and growth, as well as tissue morphogenesis, as far as this was investigated.

Hence, Taar1 and the *taar1*^{-/-} mouse models have been studied mainly in the context of the central nervous system (CNS). So far, there was no focus on investigating the thyroid gland of *taar1*^{-/-} mice. However, we have previously shown Taar1 to be expressed in thyroid epithelial cells, where it localizes to primary cilia (Szumska et al., 2015). Because the thyroid gland produces thyroid hormones (TH), which play a crucial role in brain development, and which were shown to be deregulated in various neuropsychiatric disorders (Bauer et al., 2008), including depression, Parkinson's disease, and schizophrenia, we decided that studying the thyroid phenotype of *taar1*^{-/-} mice was important to better understand TH-mediated endocrine regulation at large, and with regard to maintenance of CNS functions.

Taar1 at primary cilia of the apical plasma membrane of thyroid epithelial cells is exposed to the pH neutral and oxidizing milieu of the thyroid follicle lumen, in which thyroglobulin (Tg) is stored. The apical plasma membrane domain of thyrocytes is the site of Tg secretion, upon which it is iodinated to preform TH, and is then stored in the lumen of thyroid follicles in covalently cross-linked form. In addition, partial degradation by Tg-processing cathepsins B, K, and L for solubilization and initial TH liberation, and subsequent endocytosis of Tg happen at the apical plasma membrane domain, too, *i.e.* in direct vicinity of the Taar1-bearing cilia of thyrocytes (Brix et al., 1996; Tepel et al., 2000; Jordans et al., 2009; reviewed in Dauth et al., 2011). Currently, the site(s) of thyronamine production remain(s) controversial as both the thyroid gland (Hackenmueller et al., 2012), the gastrointestinal mucosa and other potential tissues (Hoefig et al., 2016) have been proposed to provide these aminergic ligands, which were shown to activate TAAR1 *in vitro* (Scanlan et al., 2004). Thus, it is plausible that the thyroid follicle lumen may be providing ligands that activate Taar1 at cilia of the apical plasma membrane domain of thyrocytes (Szumska et al., 2015), thereby implicating that Taar1 could be involved in the regulation of thyroid gland functions, namely Tg degradation and, consequently, TH liberation. Therefore we investigated in this study morphological features of thyroid follicles, Tg processing, TSH receptor (Tshr) localization as well as resulting serum thyroid hormone status in male *taar1*^{-/-} mice *vs.* wild type (WT) controls.

Classical regulation of the thyroid gland involves the hypothalamic-pituitary-thyroid (HPT) axis, whereby low TH concentrations trigger a negative feedback resulting in thyroid releasing hormone (TRH) release from the hypothalamus to trigger thyroid stimulating hormone (TSH) release from the pituitary gland. Circulating TSH binds to its receptors (human TSHR / mouse Tshr) expressed at the basolateral plasma membrane of thyrocytes. Ligand binding on TSHR induces $G_{q\alpha}$ and $G_{s\alpha}$ signaling pathways. Activation of $G_{q\alpha}$ induces non-genomic effects of TSH stimulation that culminate in relocation of Tg-processing cathepsins to the apical plasma membrane, where they are released into the thyroid follicle lumen to initiate Tg solubilization and TH liberation (Brix et al., 1996; Linke et al., 2002). This is completed by re-internalization of partially degraded Tg molecules for lysosomal degradation and exhaustive TH liberation (Friedrichs et al., 2003; Jordans et al., 2009). In contrast and subsequently, the long-term effect of TSH stimulation entails enhanced secretion of *de novo* synthesized Tg into the follicular lumen (reviewed in: Brix et al., 2001; Dauth et al., 2011). Thus, any disturbances in TSH regulation of thyrocytes will potentially translate into alterations in levels of Tg-processing proteases and, therefore, the degree of Tg processing and degradation, which would eventually affect TH concentrations in the blood serum. Accordingly, this study included investigations on the Tshr to determine the effect of Taar1 deficiency on thyroid function in male mice.

2   Materials and Methods

2.1   Animals, Thyroid Tissue Sampling, and Cryo-sectioning

Male *taar1*^{-/-} and C57BL6/J wild type (WT) mice were kept in the animal facility of Jacobs University Bremen, Germany. The founder *taar1*^{-/-} mice were provided by Dr. David K. Grandy (Oregon Health & Science University, Portland, OR, USA), and genotyped as previously described (Szumska et al., 2015). Mice were housed under standard conditions, with a 12h/12h

light/dark cycle and *ad libitum* water and food. Testing was conducted in accordance with institutional guidelines in S1-laboratories of Jacobs University Bremen (SfAFGJS Az. 513-30-00/2-15-32 and Az. 0515_2040_15).

Young (5 - 8 months old) and adult (10 - 15 months old) male mice were euthanized by CO_2 inhalation. Perfusion was carried out through the heart with 0.9% NaCl including 0.4 IU heparin per mL. The resected thyroid gland tissue was either snap-frozen in liquid nitrogen and stored at -80°C until used, or fixed in 4% paraformaldehyde (PFA) in 200 mM HEPES, pH 7.4, and left overnight at 4°C. Cryo-preservation was carried out by incubation in 0.5 M, and then 1 M sucrose solution in phosphate-buffered saline (PBS), pH 7.4, for 24h each at 4°C. PFA-fixed tissue samples were embedded in Tissue Freezing Medium (Jung, through Leica Microsystems, Nussloch, Germany) and stored at -20°C until sectioning on a cryostat (Leica CM1900, Leica Microsystems) into 5 µm-thick transverse sections and thaw-mounting on microscope slides.

2.2   Indirect Immunofluorescence

Residual embedding solution was washed out by overnight-incubation in calcium- and magnesium-free PBS (CMF-PBS), composed of 0.15 M NaCl, 2.7 mM KCl, 1.5 mM NaH_2PO_4, 8.1 mM Na_2HPO_4 at pH 7.4, at 4°C, followed by blocking with 3% bovine serum albumin (BSA; Carl Roth GmbH, Karlsruhe, Germany) in CMF-PBS for 1 hour at 37°C. The sections were then incubated with primary antibodies diluted in 0.1% BSA in CMF-PBS, overnight at 4°C (see Table 1). After washing with 0.1% BSA in CMF-PBS, the sections were incubated with Alexa 488- or Alexa 546-conjugated secondary antibodies for 1 hour at 37°C (1:200; Molecular Probes, Karlsruhe, Germany) together with 5 µM of the nuclear counter-stain Draq5™ (Biostatus Limited, Shepshed, Leicestershire, UK). Epithelial cells were stained with HCS CellMask™ Orange for 1 hour at 37°C (1:1000, Molecular Probes, H32713). Glycosylated tissue components were stained with the biotinylated lectin Concanavalin A from *C. ensiformis* (ConA; Sigma-Aldrich, C2272) at 10µg/mL for 30 min at 4°C, followed by incubation with Alexa Fluor® 546-conjugated streptavidin (Molecular Probes, Karlsruhe, Germany, S-11225) as the secondary ConA detection label. Specific antibodies were omitted in negative controls. After washing with CMF-PBS and deionized water, the sections were mounted with embedding medium consisting of 33% glycerol, and 14% Mowiol in 200 mM Tris-HCl, pH 8.5 (Hoechst AG, Frankfurt, Germany).

2.3   Image Acquisition and Analysis

Immuno- and lectin-labeled thyroid tissue cryo-sections were inspected with a confocal laser scanning microscope equipped with Argon and Helium-Neon lasers (LSM 510 Meta; Carl Zeiss Jena GmbH, Jena, Germany). Images were obtained at a pinhole setting of 1 Airy unit and at a resolution of 1024 × 1024 pixels. Micrographs were analyzed with the LSM 510 software, release 3.2 (Carl Zeiss Jena GmbH).

The epithelial extensions, follicle areas, follicle luminal areas, cell numbers per 1000 $µm^2$ of tissue area, as well as the fluorescence intensities of anti-cystatin C- and D-, and ConA-positive signals were analyzed with the aid of the open source software Cell Profiler (version 2.1.1.;

available from the Broad Institute at www.cellprofiler.org, (Lamprecht et al., 2007), following our established pipelines described elsewhere (Weber et al., 2015).

2.4   Tissue Lysate Preparation

Resected deep-frozen thyroid tissue was homogenized on ice in lysis buffer (0.5% Triton X-100 in PBS, pH 7.4), and incubated at 4°C for 30 min. Lysates were cleared by centrifugation at 4°C and 13,000 g for 5 min. Quantitative protein determination was performed by the Neuhoff method (Neuhoff et al., 1979) using BSA dissolved in 0.5% Triton X-100 in PBS as a standard.

2.5   SDS-PAGE, Immunoblotting, and Silver Staining

Protein lysates were separated through SDS-PAGE on 12.5% self-cast vertical polyacrylamide gels along with a Page Ruler Prestained Protein ladder (Thermo Scientific, #26616), and transferred onto nitrocellulose membranes by semi-dry blotting. Unspecific binding sites were blocked by incubation with 5% blotting grade milk powder in PBS, supplemented with 0.3% Tween (PBS-T) for 16 hours at 4°C. Afterwards, membranes were incubated for 2 hours at room temperature with antibodies specific for cathepsins B, D, and L, as well as β-tubulin for normalization, each diluted in PBS-T, respectively (see Table 1). Incubation with horseradish peroxidase-conjugated secondary antibodies (Southern Biotech, Birmingham, USA, #6160-05, #4050-05, 1:5000) was performed for 1 hour at room temperature, followed by incubation with the respective secondary horseradish peroxidase-conjugated antibody, and visualization by chemiluminescence ECL Western Blotting substrate onto XPosure films (Pierce via Thermo Scientific, Schwerte, Germany). Band densitometry analysis was performed using ImageJ version 1.48.

A total of 0.5 µg protein from thyroid lysate preparations were separated on horizontal SDS Gradient 8-18 ExcelGel (GE Healthcare, Upsala, Sweden). Gels were silver stained (Heukeshoven & Dernick, 1988), and band densitometry analysis was performed on Image Studio Lite version 5.2.

2.6   Cathepsin B Activity Assays

Cathepsin B activity assays were performed as described (Barrett, 1980; Brix et al., 1996; Mayer et al., 2009). In brief, protein samples prepared from thyroid tissues were assayed in triplicates by monitoring cleavage of 10 µM cathepsin B-specific substrate N-benzyloxycarbonyl-arginine-arginine-7-amido-4-methylcoumarin hydrochloride (Z-Arg-Arg-AMC*HCl; Bachem, Bubendorf, Switzerland, #I-1135) at pH 6.0, and for 60 min at 40°C. In negative controls, prepared for each sample, 10 µM E-64 were added at the start of the reaction time. Substrate cleavage was stopped by the addition of 2 M Tris-HCl (pH 9.0). The amounts of released AMC were quantified by measuring the fluorescence with a Tecan GENios Reader (Tecan Deutschland GmbH) using an excitation wavelength of 360 nm and emission reading at 465 nm.

2.7   Measurement of Serum TSH Concentrations

Blood was taken from right heart ventricles, and allowed to clot by placing on ice before sera were stored at -20°C upon clearance by centrifugation at 4°C at 13,000 g for 10 min. Blood

serum samples were used for evaluation of TSH concentrations by use of a mouse TSH-specific
ELISA kit (Cloud-Clone Corp. via Antibodies Online, # CEA463MU). Absorbance was
determined at 450 nm using a Tecan Infinite M1000 Pro instrument (Grödig, Salzburg, Austria).
According to the manufacturer's instructions, the detectable TSH concentrations range from
49.4 pg/ml to 4,000 pg/ml.

2.8   Measurement of Total T_4 and T_3 Serum Concentrations

Total T_3 and T_4 serum concentrations were measured by competitive radioimmunoassay (DRG
Instruments GmbH, Marburg, Germany, #4525, #4524) according to the manufacturer's
instructions and as described (Wirth et al., 2015). The coefficient of variation was ≤ 5 % for both
assays.

2.9   Statistical Analyses

Data are depicted as means ± standard deviations (SD). Statistical analyses were performed by
conducting univariate analysis of variance, followed by one-way ANOVA with a Bonferroni or
Dunnett's T3 as *post-hoc* test, using SPSS 24.0. *P*-values were determined by unpaired t test
with Welch's correction using GraphPad Prism 5.01 (GraphPad, San Diego, CA, USA). Data
sets were compared once for genotypic effect and once for age effect, therefore values of
$p<0.025$ were considered to be statistically significant, unless specified otherwise.

3   Results

Taar1 and the *taar1-/-* mouse models have been studied in relation to behavior and the central
nervous system, but were not yet investigated in detail with regard to the thyroid gland and
possible regulation of its functions as TH-generating endocrine organ. Since we have previously
shown that Taar1 is localized at primary cilia of thyroid epithelial cells *in vitro* and *in situ*
(Szumska et al., 2015), the present study asks whether Taar1 plays a role in thyroid
morphology. In addition, we were interested in testing whether Taar1 is required for thyroid
tissue morphogenesis, and for regulation of Tg processing and the resulting serum TH status,
as well as for Tshr localization, which are important aspects of thyroid gland function in
maintaining proper TH supply to peripheral and central target organs, including the CNS.

3.1   No morphological alterations were detectable regarding follicle size and follicle
count between WT and *taar1-/-* thyroids

To determine possible roles of Taar1 during development, which might be related to
differentiation of thyroid follicle cells and thyroid tissue morphogenesis, a morphometric
approach was chosen that allows determination of entire thyroid lobes and their constituency,
namely the thyroid follicles (Weber et al., 2015). Initial morphological assessment revealed no
significant difference in follicle areas, or the number of follicles per lobe in animals of either
genotype from both age groups, namely young and adult male *taar1-/-* mice in comparison with
WT controls (Figure 1). Similarly, when comparing the average number of cells constituting a
follicle, measured as the number of nuclei per 1000 µm² of follicle area, no significant difference
was found, although the number of cells constituting thyroid follicles tend to be slightly higher in

the young WT than in the other tested groups (Figure 2A). There were 4.81 ± 1.81 cells and 5.45 ± 2.24 cells per 1000 μm^2, which composed the follicles of young *taar1*^{-/-} and WT mice, respectively. Thus, the follicles of young *taar1*^{-/-} mice were rather comparable to follicles of adult mice of both genotypes, which generally have less cells occupying 1000 μm^2 follicle area than per young WT follicle (Figure 2A).

3.2 Lower follicle to cell volume ratios in *taar1*^{-/-} thyroids

The lack of Taar1 did not appear to have an effect on the tissue volume of either young or adult mouse thyroids, as indicated by comparable follicle sizes and follicle counts. However, the finding of slightly fewer cells per follicle area in *taar1*^{-/-} *vs.* WT thyroid glands prompted us to further investigate and compare the rate of cell death and the volume of epithelial cells in *taar1*^{-/-} *vs.* WT. The mechanism of cell death in the thyroid gland is not fully understood, but it resembles terminal differentiation and shedding of dead cells into the lumen where the remnants remain detectable for long time intervals (Friedrichs et al., 2003; Nilsson & Fagman, 2017). In keeping with this notion, activation of procaspase 3 was not observed in WT or *taar1*^{-/-} thyroid tissue (data not shown). However, the proportion of dead cells was determined by counting the luminal Draq5™-positive signal of nuclei representing such remnants of dead cells (Figure 2 B-B'), divided by the total count of cells (nuclei) comprising the respective follicle. The results showed a significant rise in cell death rate in young *taar1*^{-/-} follicular epithelia, equivalent to 3.5-fold that of young WT, besides a 2.8-fold increase in the cell death rate of adult *taar1*^{-/-} thyroid epithelia compared to the adult WT, while cell death rates were comparable in both young and adult WT follicular epithelia (Figure 2C). This data indicated increased thyroid epithelial cell death rates in young *taar1*^{-/-} over adult and WT mice, respectively.

Moreover, a trend towards higher epithelial extensions (EExt) was revealed in both young and adult *taar1*^{-/-} mice (5.27 μm ± 0.69 μm and 5.17 μm ± 0.40 μm, respectively) as compared to their WT counterparts (4.80 μm ± 0.91 μm and 4.38 μm ± 0.65 μm for young and adult WT, respectively) (Figure 3A). This increase in the EExt is consistent with a decrease in the luminal area in *taar1*^{-/-} follicles, where average luminal area in young *taar1*^{-/-} thyroid follicles is significantly smaller (2,287 μm^2 ± 334 μm^2), when compared to their WT counterparts (2,895 μm^2 ± 312 μm^2) (Figure 4A). While a similar trend towards smaller luminal areas was observed in the adult *taar1*^{-/-}, the difference is insignificant when compared to the adult WT.

The luminal areas were additionally investigated to provide a color-coded depiction of area distribution of follicular lumina per middle-section of a given thyroid lobe (Figure 4B). Such analyses highlighted the heterogeneity of the follicle populations per thyroid section, where the bigger follicles tend to localize on the thyroid lobe periphery, surrounding the smaller, more centrally located follicles. This distribution is maintained in both the young and adult populations of thyroid follicles in both genotypes.

Overall, an approximate 10% and 18% increase in EExt in young and adult *taar1*^{-/-} follicles, respectively, is indicative of a more prismatic thyrocyte shape (Figure 3B), suggesting a higher activation state (Friedrichs et al., 2003). Thus, higher thyrocyte activity states correlating to smaller thyroid follicle lumina could be associated with altered thyroglobulin (Tg) synthesis and secretion rates, or less colloid stored in the lumen, which, in turn, could be the outcome of

enhanced Tg degradation and/or more compacted Tg. Therefore, we next performed biochemical and morphological analyses of Tg, while also conducting investigations on Tg-processing proteases and the availability of the TSH receptor in thyroid tissue of both genotypes.

3.3   Taar1-deficiency has an age-dependent effect on thyroglobulin glycosylation, but no overall effect on its synthesis or state of proteolytic processing

Thyroglobulin is a complex, heavily glycosylated molecule, which makes up most of the protein content of thyroid tissue. We therefore sought to visualize and compare the processing pattern of thyroidal thyroglobulin and to analyze its glycosylation pattern in both young and adult WT and *taar1*^{-/-} thyroid tissue. The degree of Tg glycosylation was evaluated *via* quantification of fluorescence intensity of positive signal from thyroid cryosections stained with ConA (Figure 5 A-E), a lectin that recognizes α-D-mannosyl α-D-glucosyl groups (Goldstein et al., 1974). The results indicated that Tg tends to be more glycosylated in adult vs. young WT tissue, and less so in adult *taar1*^{-/-} vs. WT glands (Figure 5E).

The degree of glycosylation is typically positively correlated with the degree of protein stability; therefore, we next checked the degradation status of Tg with the aim to answer whether or not Tg from adult thyroids was less prone to degradation. A silver staining of SDS-PAGE separated proteins in thyroid lysates under reducing conditions shows no inter-genotypic differences in the amounts and gross degradation pattern of Tg (Figure 5F). However, overall degradation of thyroidal proteins appears to be enhanced in the adult mice, as compared to their young counterparts.

On the other hand, morphological assessment of Tg storage was enabled by immunolabeling WT and *taar1*^{-/-} thyroid cryosections of both young and adult mice with an antibody specific for Tg (see also (Weber et al., 2017)). The proportion of follicles with a homogeneous Tg-immunopositive signal, resembling intact cross-linked Tg was higher in young *taar1*^{-/-} thyroid cryosections (10.0% and 24.9% for WT and *taar1*^{-/-}, respectively), as opposed to the multi-layered, partially solubilized Tg, which makes it better accessible for antibody binding. This difference was no longer detected in the adult mice, with the percentage of cross-linked Tg-containing follicles amounting to 10.2% and 7.0% in the WT and *taar1*^{-/-}, respectively (Figure 6 A-D).

Furthermore, protein separation under non-reducing conditions revealed a trend toward less Tg multimers in the adult *taar1*^{-/-}, as shown by the relative intensity of bands pertaining to multimeric Tg to the total protein per lane (Figure 6 E and F, respectively). Because no difference in the amounts of Tg, a proxy for biosynthesis of Tg, was detected in thyroid lysates of WT and *taar1*^{-/-} thyroid tissue by reducing SDS-PAGE, a reduction in multimeric Tg forms in the lumen may reflect a difference in Tg storage capacity upon Taar1 deficiency.

Thus, the results show differences in Tg-glycosylation upon ageing in both WT and *taar1*^{-/-} mice, as well as in Tg storage in cross-linked form in adult *taar1*^{-/-}, in comparison to their WT counterparts. Hence, we next asked whether there was a difference in the efficiency with which

Tg was solubilized, a process that is enabled by cathepsin B- and L-mediated extracellular proteolysis of covalently cross-linked Tg (Friedrichs et al., 2003).

3.4 Altered proteolytic activity of Tg-processing cathepsins in the *taar1*^{-/-} thyroid

We first looked at whether or not Taar1 deficiency had any effect on the subcellular localization of cathepsins. Immunofluorescence revealed the subcellular localization of Tg-processing cathepsins B, D, and L to be unaltered, as they confine mainly to endo-lysosomal compartments in both WT and *taar1*^{-/-} thyroid tissue (Figure 7).

Furthermore, densitometric analysis of immunoblots showed both the pro- and mature forms of cathepsin B to be comparable in WT and *taar1*^{-/-} thyroid tissue (Figure 8 A-A3). However, a slight decrease in the single chain cathepsin L was noted in adult *taar1*^{-/-} thyroids, while retaining comparable levels of both the pro- and heavy chain of cathepsin L in both age groups of both genotypes (Figure 8 B-B3). Similarly, a slight reduction in cathepsin D proform was observed in adult *taar1*^{-/-} thyroid lysates (Figure 8 C-C1). Despite no differences in total cathepsin B protein levels, however, an age-effect was elucidated in the proteolytic activity of this protease, namely that it was significantly diminished in adult *taar1*^{-/-} thyroid lysates compared to their young counterparts (Figure 9 A), that latter also exhibiting lower proteolytic activity than in the WT controls.

The notion of reduced Tg-solubilizing capacity in Taar1 deficiency is further supported by an enhancement in the fluorescence intensity of cystatin C immunopositive signal in *taar1*^{-/-} thyroid cryo-sections (Figure 9 B-E), cystatin C being an endogenous inhibitor of cysteine proteases. Moreover, the related cystatin D was also localized intra-luminally in the peri-cellular space at the apical plasma membrane, where extracellular proteolysis for Tg solubilization and initial T_4 liberation occurs, with an approximate 36% increase in the fluorescence intensity of luminal cystatin D observed in the young, but not in adult, *taar1*^{-/-} thyroid cryo-sections, as compared to the WT (Figure 9 F-H).

Overall, subtle differences in the balance of proteolytic to anti-proteolytic activities are observed in the *taar1*^{-/-} mouse thyroid gland with declining potency to solubilize and degrade Tg by both, extra- and intra-cellular means. In order to see whether this had a systemic effect, we next looked at T_3, T_4 and TSH concentrations in the serum.

3.5 Lack of functional Taar1 leads to a mild case of hyperthyrotropinemia in young mice

Thyroid hormone serum concentrations were measured by radioimmunoassay, revealing an age-dependent increase in total T_4 concentrations in both genotypes, with a trend towards lower total T_4 in young *taar1*^{-/-} mice. Age-related increasing T_4 and stable T_3 serum concentrations were comparable in both genotypes (Figure 10 A-B). To complete the picture, serum TSH concentrations were measured *via* ELISA revealing a significant increase in serum TSH in young *taar1*^{-/-} mice (Figure 10C), pointing to a mild state of pituitary hypothyroidism, which was no longer detectable in adult animals.

Furthermore, the basolateral localization of Mct8, the major TH-exporting molecule of thyrocytes, was not altered in *taar1*^{-/-} *vs*. WT thyroid tissue (Figure 11 A-B), thus ruling out major differences in TH release from thyroid follicles as a cause of high TSH concentrations in the serum of young Taar1-deficient mice. Finally, we checked whether the TSH receptor (Tshr) localization was affected in the *taar1*^{-/-} thyroid tissue. Immunofluorescence inspection of thyroid sections from young mice labeled for Tshr showed a stark difference in the receptor's localization between the genotypes, where it was predominantly localized to vesicular compartments in *taar1*^{-/-} tissue, as opposed to the classical basolateral pattern of subcellular localization in the WT tissue (Figure 11 C-F).

4   Discussion

Members of the TAAR family of receptors such as TAAR1 have been proposed as targets mediating the actions of the thyroid hormone metabolite 3-T$_1$AM (Panas et al., 2010). Albeit several actions of 3-T$_1$AM are distinct from those of classical thyroid hormones, if administered in pharmacological doses, only few studies addressed the role of TAAR1/Taar1 and its ligand 3-T$_1$AM on the thyroid gland and the regulation of the HPT axis (Klieverik et al., 2009; Agretti et al., 2011; Schanze et al., 2017). Here we show that the thyroid gland of *taar1*^{-/-} mice is characterized by more prismatic epithelial cells and, consequently, smaller follicle lumen areas in which the cross-linked, compact form of Tg is stored. Such a phenotype is typically observed in TSH-activated thyroid glands, where peripheral TH demands are feeding back on the TH-generating cells to first, liberate TH for short-term supply of target organs, and second, trigger re-synthesis of Tg to fill up the stores of TH precursor molecules. A question that has been asked for a long time, refers to the mechanisms by which individual follicles are able to sense the amount of stored Tg, because an autonomy in thyroid follicle activity is observed for any given thyroid follicle in conditions of TH demand or proper TH supply alike (Roger et al., 1992; reviewed in Suzuki et al., 2011). An involvement in such regulatory processes by primary cilia at the apical plasma membrane domain of thyrocytes, and reaching out into the Tg stored within the thyroid follicle lumen, has been discussed before but was formally never proven (Herzog et al., 1992; reviewed in Brix et al., 2001).

Previously, we proposed that Taar1 at cilia of thyrocytes might play a role in auto-regulation of individual thyroid follicles when triggered by TH derivatives, namely the thyronamines (Szumska et al., 2015). In principle, thyronamines could be generated by intra-thyroidal means (Hackenmueller et al., 2012). Because Tg is processed extracellularly before it is re-internalized, and thus, undergoes limited proteolysis in the apical pericellular space (Brix et al., 1996; Friedrichs et al., 2003), thyronamine precursors could principally be liberated during this process (Szumska et al., 2015). These would then need to be taken up and modified to thyronamines for their subsequent delivery into the thyroid follicle lumen for triggering *e.g.* Taar1 signaling (Szumska et al., 2015). In order to test this hypothesis, it would be required to analyze the composition of the peri-cellular luminal content with regard to TH derivatives, in particular, thyronamine precursors, and thyronamines themselves. Such investigations might become feasible in future with more advanced imaging MALDI spectrometry at hand.

4.1   Canonical regulation of the thyroid gland upon Taar1 deficiency

Although thyroid-specific ligands remain unknown, it is clear that the Taar1 receptor has a role in thyroid gland regulation involving the HPT axis, because in the absence of functional Taar1, the localization and potentially the signaling outcome of ligand-triggered Tshr are affected. The metabolites of classical TH, particularly 3-T_1AM, have been shown to potently activate Taar1 *in vitro* (Scanlan et al., 2004), leading to speculations, that thyronamines in general could serve as the natural ligands for Taar1. However, that remains debatable, especially, when considering persistence of several effects of high doses of 3-T_1AM including thermoregulatory responses in *taar1*^{-/-} mice (Panas et al., 2010).

Recently, Schanze and colleagues have shown that the *in vivo* application of 3-T_1AM leads to the decrease in expression of the sodium-iodide symporter (*Nis*), *pendrin* and *Tg*, but did not alter *tshr* expression, nor did it affect TSH-induced signaling in the treated animals, leading the authors to conclude that stimulation with 3-T_1AM does not affect the HPT axis but interferes with functional characteristics of thyroid epithelial cells (Schanze et al., 2017). The results of this study may suggest that the 3-T_1AM-triggered effects are indeed not Taar1-mediated (Schanze et al., 2017). One could also argue, however, that this may be so simply because Taar1 is not present at the basolateral plasma membrane domain of thyrocytes, and cannot be activated by circulating 3-T_1AM. However, it is not known yet whether in thyrocytes Taar1 gets activated by either thyronamines or other TH metabolites such as 3-T_1AaM or 3-T_1Ac. Indeed, 3-T_1AM can be metabolized by thyrocytes to yield T_0AM and 3-T_1Ac, as shown by (Schanze et al., 2017) for PCCL3 cells, or might reach the thyroid follicular lumen by means of transcytotic transport as previously suggested (Szumska et al., 2015). While the latter proposal has not been tested experimentally, the present study supports the view that Taar1 is indeed involved in thyroid gland morphogenesis and in maintenance of its canonical function. Similar to the observations in *taar1*^{-/-} mice of this study, a smaller follicular lumen and higher epithelial heights have been observed after administration of 3-T_1AM for 7 days in male mice (Schanze, 2017). The results of the present study and those upon 3-T_1AM administration therefore suggest a role of both, Taar1 and circulating 3-T_1AM in maintaining thyroid follicle architecture and thyrocyte functionality.

The obvious abundance of the Tshr in intracellular compartments of *taar1*^{-/-} thyrocytes, as indicated by the predominantly vesicular Tshr-immunopositive signals, and as opposed to a mainly basolateral localization of Tshr in the WT, could be due to either poor targeting of the Tshr to the cell surface, which would lead to partial TSH resistance (Calebiro et al., 2005), or rather to an enhancement in Tshr internalization. The latter is the inevitable fate of an activated GPCR to be internalized into endo-lysosomal compartments, generally a β-arrestin-chaperoned and clathrin-mediated pathway, from where the receptor is either recycled back to the cell surface, or proceeds to be degraded by endo-lysosomal enzymes (reviewed in Luttrell & Lefkowitz, 2002). Receptor internalization has initially been regarded as a process exclusive for GPCR down-regulation (reviewed in Lohse, 1993); however, but is also essential for efficient receptor desensitization (reviewed in Calebiro, 2011).

In the case of the TSHR, it is co-internalized complexed to its ligand into subcellular compartments, even including retrograde trafficking to the *trans*-Golgi network (Godbole et al., 2017), from where it continues to persistently signal *via* the cAMP-related pathways (Frenzel et al., 20016; Calebiro et al., 2009; Calebiro et al., 2010; Werthmann et al., 2012; Godbole et al.,

2017). It is noteworthy that downstream cellular targets of cAMP signaling appear to be dependent on the subcellular site of signal origin (Rich et al., 2001; Godbole et al., 2017), i.e. GPCRs signaling from within intracellular compartments do not necessarily activate the same pathways as classically activated by cell surface-localized signaling GPCRs.

One must also consider the possibility of Tshr undertaking an alternative trafficking route, leading to less Tshr reaching the surface in the first place, resulting in a lesser proportion of Tshr being available for classical TSH stimulation. Either scenario may ultimately result in less efficient TH liberation *via* cathepsin-mediated Tg-proteolysis.

4.2   Taar1 is important for thyroid morphology and function

Our results show that the absence of functional Taar1 imposes no overt changes in the thyroid gland morphogenesis, nor does it affect the overall size of the gland. However, closer inspection revealed increased cell death rates in *taar1^{-/-}* thyrocytes, which, although statistically proven insignificant, show a trend toward more extended thyroid epithelia, resulting in significantly smaller follicular lumen area. Such changes were found to be more pronounced in the younger group of tested animals. Taar1 deficiency also presents subtle disturbances in the levels and proteolytic activity of Tg-processing cathepsins, resulting in persistence of more cross-linked Tg in the follicle lumen of young animals. Moreover, a correlation can be drawn between the increase in cell death rate in the *taar1^{-/-}* and the decrease in the amounts of cathepsin L single chain form, since cathepsin L is regarded as a survival factor for thyrocytes, whereupon cathepsin L-deficient thyroid follicles were marked by highly prominent cell remnants in the follicular lumen (Friedrichs et al., 2003). Whether unaltered Mct8 localization in the *taar1^{-/-}* thyrocytes relates to the observed trend towards lower T_4 serum concentration remains to be studied by functional assays in context with analysis of other TH transporters found in thyrocytes. Overall, the data of this study are therefore in line with previous characterizations of *taar1^{-/-}* mice, that did not exhibit a growth phenotype, or severe alterations in organogenesis, especially not with regard to classical TH target organs like the central nervous system or the liver (Wolinsky et al., 2007; Lindemann et al., 2008). The investigations herein highlight, however, that it will be critically important to better understand the process of Tg degradation and possible intra-thyroidal thyronamine generation in order to deduce thyroid follicle auto-regulatory mechanisms triggered by GPCRs like Taar1 at the cilia of thyrocytes *in situ*.

4.3   Taar1 is interconnected with Tg processing proteases

Decreased cathepsin B activity and smaller amounts of cathepsin L were observed in *taar1^{-/-}* follicles (this study). Judging by the fact that cathepsin B activity and the amount of cathepsin L were only mildly diminished in the *taar1^{-/-}* thyroids vs. WT, but higher cystatin levels prevailed, we conclude that Taar1 deficiency might have limited effects on the expression of thyrocyte-typical genes, but might rather affect proteostasis resulting in altered balances of proteolytic to anti-proteolytic activities in *taar1^{-/-}* *vs.* WT controls, thereby leading to a mildly misbalanced Tg turnover. In future, experiments are planned to correlate expression levels of Taar1 with those of Mct8 or other TH transporting proteins of thyrocytes in order to propose mechanistic links between various molecular players with obvious roles in thyroid functions

(Weber et al., 2017). The aim of such future studies would entail a better understanding of intra-thyroidal auto-regulation and how this is connected to TSH-regulation *via* the HPT axis.

4.4   Conclusions and perspectives

Our results show that the Tshr is predominantly localized in vesicular membranes of Taar1-deficient thyrocytes, rather than on the basolateral plasma membrane as in WT. Moreover, Taar1-deficient thyroid follicles are characterized by fewer cells per follicle area, owing to more prismatic epithelia and higher cell death rates, in addition to a decreased luminal area, in which the compacted cross-linked form of Tg is more prevalent than in the WT controls. These alterations are more evident in young (5-8 months) than in the adult (10-15 months) animals. No other thyroid-specific morphological changes were noted. However, serum TSH concentrations were slightly increased in young Taar1-deficient animals, with a tendency towards lower T_4 concentrations. These results support the hypothesis that Taar1 plays a regulatory role in thyroid homeostasis including the HPT axis, its function being important for Tshr localization and regulation of its signaling potential. We conclude that Taar1-deficient animals show a tendency towards lower serum T_4 concentrations, and eventually manifest a mild hypothyroid status, as indicated by the slightly elevated serum TSH concentrations. Most strikingly, the thyroid epithelia of young Taar1-deficient mice are characterized by a vesicular localization of the Tshr, which signifies that Taar1 signaling is necessary to maintain homeostatic Tshr signaling and canonical HPT-axis regulation (Figure 12). The results highlight the importance of evaluating Taar1-targeting drugs in pre-clinical studies for potential side effects they may have on thyroid gland homeostasis.

5   Conflict of Interest

The authors declare that the research was conducted in the absence of any commercial or financial relationships that could be construed as a potential conflict of interest.

6   Author Contributions

MQ, JS, VS, ER, and KB performed experiments. JK and KB devised the study and supervised the experimental work. All authors contributed to data interpretation and manuscript drafting. All authors read and approved the final manuscript.

7   Funding

8   Acknowledgments

9   References

Agretti, P., De Marco, G., Russo, L., Saba, A., Raffaelli, A., Marchini, M., et al. (2011). 3-Iodothyronamine metabolism and functional effects in FRTL5 thyroid cells. *J Mol Endocrinol, 47*(1), 23-32. doi:10.1530/jme-10-0168

Alvarsson, A., Zhang, X., Stan, T. L., Schintu, N., Kadkhodaei, B., Millan, M. J., et al. (2015). Modulation by Trace Amine-Associated Receptor 1 of Experimental Parkinsonism, L-DOPA Responsivity, and Glutamatergic Neurotransmission. *J Neurosci, 35*(41), 14057-14069. doi:10.1523/jneurosci.1312-15.2015

Barrett, A. J. (1980). Fluorimetric assays for cathepsin B and cathepsin H with methylcoumarylamide substrates. *Biochem J, 187*(3), 909-912.

Bauer, M., Goetz, T., Glenn, T., & Whybrow, P. C. (2008). The thyroid-brain interaction in thyroid disorders and mood disorders. *J Neuroendocrinol, 20*(10), 1101-1114. doi:10.1111/j.1365-2826.2008.01774.x

Berry, M. D., Gainetdinov, R. R., Hoener, M. C., & Shahid, M. (2017). Pharmacology of human trace amine-associated receptors: Therapeutic opportunities and challenges. *Pharmacol Ther, 189*, 161-180. doi: 10.1016/j.pharmthera.2017.07.002

Bradaia, A., Trube, G., Stalder, H., Norcross, R. D., Ozmen, L., Wettstein, J. G., et al. (2009). The selective antagonist EPPTB reveals TAAR1-mediated regulatory mechanisms in dopaminergic neurons of the mesolimbic system. *Proc Natl Acad Sci U S A, 106*(47), 20081-20086. doi:10.1073/pnas.0906522106

Brix, K., Lemansky, P., & Herzog, V. (1996). Evidence for extracellularly acting cathepsins mediating thyroid hormone liberation in thyroid epithelial cells. *Endocrinology, 137*(5), 1963-1974. doi:10.1210/endo.137.5.8612537

Brix, K., Linke, M., Tepel, C., & Herzog, V. (2001). Cysteine proteinases mediate extracellular prohormone processing in the thyroid. *Biol Chem, 382*(5), 717-725. doi:10.1515/bc.2001.087

Brix, K., Summa, W., Lottspeich, F., & Herzog, V. (1998). Extracellularly occurring histone H1 mediates the binding of thyroglobulin to the cell surface of mouse macrophages. *J Clin Invest, 102*(2), 283-293. doi:10.1172/jci1614

Calebiro, D. (2011). Thyroid-stimulating hormone receptor activity after internalization. *Ann Endocrinol (Paris), 72*(2), 64-67. doi:10.1016/j.ando.2011.03.008

Calebiro, D., de Filippis, T., Lucchi, S., Covino, C., Panigone, S., Beck-Peccoz, P., et al. (2005). Intracellular entrapment of wild-type TSH receptor by oligomerization with mutants linked to dominant TSH resistance. *Hum Mol Genet, 14*(20), 2991-3002. doi:10.1093/hmg/ddi329

Calebiro, D., Nikolaev, V. O., Gagliani, M. C., de Filippis, T., Dees, C., Tacchetti, C., et al. (2009). Persistent cAMP-signals triggered by internalized G-protein-coupled receptors. *PLoS Biol, 7*(8), e1000172. doi:10.1371/journal.pbio.1000172

Calebiro, D., Nikolaev, V. O., & Lohse, M. J. (2010). Imaging of persistent cAMP signaling by internalized G protein-coupled receptors. *J Mol Endocrinol, 45*(1), 1-8. doi:10.1677/jme-10-0014

Dauth, S., Arampatzidou, M., Rehders, M., Yu, D. M. T., Führer, D., & Brix, K. (2011). Thyroid Cathepsin K: Roles in Physiology and Thyroid Disease. *Clinical Reviews in Bone and Mineral Metabolism, 9*(2), 94-106. doi:10.1007/s12018-011-9093-7

Espinoza, S., Salahpour, A., Masri, B., Sotnikova, T. D., Messa, M., Barak, L. S., et al. (2011). Functional interaction between trace amine-associated receptor 1 and dopamine D2 receptor. *Mol Pharmacol, 80*(3), 416-425. doi:10.1124/mol.111.073304

Frenzel, R., Voigt, C., & Paschke, R. (2006). The Human Thyrotropin Receptor Is Predominantly Internalized by β-Arrestin 2. *Endocrinology, 147*(6), 3114-3122. doi:10.1210/en.2005-0687

Friedrichs, B., Tepel, C., Reinheckel, T., Deussing, J., von Figura, K., Herzog, V., et al. (2003). Thyroid functions of mouse cathepsins B, K, and L. *J Clin Invest, 111*(11), 1733-1745. doi:10.1172/jci15990

Galley, G., Stalder, H., Goergler, A., Hoener, M. C., & Norcross, R. D. (2012). Optimisation of imidazole compounds as selective TAAR1 agonists: discovery of RO5073012. *Bioorg Med Chem Lett, 22*(16), 5244-5248. doi:10.1016/j.bmcl.2012.06.060

Godbole, A., Lyga, S., Lohse, M. J., & Calebiro, D. (2017) Internalized TSH receptors en route to the TGN induce local G_S-protein signaling and gene transcription. *Nat Comm*, 8, 443. doi:10.1038/s41467-017-00357-2

Goldstein, I. J., Reichert, C. M., & Misaki, A. (1974). INTERACTION OF CONCANAVALIN A WITH MODEL SUBSTRATES*. *Annals of the New York Academy of Sciences, 234*(1), 283-296. doi:10.1111/j.1749-6632.1974.tb53040.x

Grandy, D. K. (2007). Trace amine-associated receptor 1-Family archetype or iconoclast? *Pharmacol Ther, 116*(3), 355-390. doi:10.1016/j.pharmthera.2007.06.007

Grandy, D. K. (2014). TAAR1 transforms thinking about a plant alkaloid that transformed the practice of medicine. *Int J Neuropsychopharmacol, 17*(10), 1545-1547. doi:10.1017/s1461145714000911

Grandy, D. K., Miller, G. M., & Li, J. X. (2016). "TAARgeting Addiction"--The Alamo Bears Witness to Another Revolution: An Overview of the Plenary Symposium of the 2015 Behavior,

Biology and Chemistry Conference. *Drug Alcohol Depend, 159*, 9-16.
doi:10.1016/j.drugalcdep.2015.11.014

Hackenmueller, S. A., Marchini, M., Saba, A., Zucchi, R., & Scanlan, T. S. (2012). Biosynthesis
of 3-Iodothyronamine (T(1)AM) Is Dependent on the Sodium-Iodide Symporter and
Thyroperoxidase but Does Not Involve Extrathyroidal Metabolism of T(4). *Endocrinology,
153*(11), 5659-5667. doi:10.1210/en.2012-1254

Harmeier, A., Obermueller, S., Meyer, C. A., Revel, F. G., Buchy, D., Chaboz, S., et al. (2015).
Trace amine-associated receptor 1 activation silences GSK3beta signaling of TAAR1 and D2R
heteromers. *Eur Neuropsychopharmacol, 25*(11), 2049-2061.
doi:10.1016/j.euroneuro.2015.08.011

Herzog V, Berndorfer, U., & Saber, Y. (1992). Isolation of insoluble secretory product from
bovine thyroid: extracellular storage of thyroglobulin in covalently cross-linked form. *J Cell Biol,
118*(5), 1071-1083. Heukeshoven, J, & Dernick, R. (1988). Improved silver staining procedure
for fast staining in PhastSystem Development Unit. I. Staining of sodium dodecyl sulfate gels.
Electrophoresis, 9(1), 28-32.

Hoefig, C. S., Zucchi, R., & Kohrle, J. (2016). Thyronamines and Derivatives: Physiological
Relevance, Pharmacological Actions, and Future Research Directions. *Thyroid, 26*(12), 1656-
1673. doi:10.1089/thy.2016.0178

Jordans, S., Jenko-Kokalj, S., Kuhl, N. M., Tedelind, S., Sendt, W., Bromme, D., et al. (2009).
Monitoring compartment-specific substrate cleavage by cathepsins B, K, L, and S at
physiological pH and redox conditions. *BMC Biochem, 10*, 23. doi:10.1186/1471-2091-10-23

Klieverik, L. P., Foppen, E., Ackermans, M. T., Serlie, M. J., Sauerwein, H. P., Scanlan, T. S., et
al. (2009). Central effects of thyronamines on glucose metabolism in rats. *J Endocrinol, 201*(3),
377-386. doi:10.1677/joe-09-0043

Lamprecht, M. R., Sabatini, D. M., & Carpenter, A. E. (2007). CellProfiler: free, versatile
software for automated biological image analysis. *Biotechniques, 42*(1), 71-75.

Leo, D., Mus, L., Espinoza, S., Hoener, M. C., Sotnikova, T. D., & Gainetdinov, R. R. (2014).
Taar1-mediated modulation of presynaptic dopaminergic neurotransmission: role of D2
dopamine autoreceptors. *Neuropharmacology, 81*, 283-291.
doi:10.1016/j.neuropharm.2014.02.007

Lindemann, L., Meyer, C. A., Jeanneau, K., Bradaia, A., Ozmen, L., Bluethmann, H., et al.
(2008). Trace amine-associated receptor 1 modulates dopaminergic activity. *J Pharmacol Exp
Ther, 324*(3), 948-956. doi:10.1124/jpet.107.132647

Linke, M., Jordans, S., Mach, L., Herzog, V., & Brix, K. (2002). Thyroid stimulating hormone
upregulates secretion of cathepsin B from thyroid epithelial cells. *Biol Chem, 383*(5), 773-784.
doi:10.1515/bc.2002.081

Lohse, M. J. (1993). Molecular mechanisms of membrane receptor desensitization. *Biochim Biophys Acta, 1179*(2), 171-188.

Luttrell, L. M., & Lefkowitz, R. J. (2002). The role of beta-arrestins in the termination and transduction of G-protein-coupled receptor signals. *J Cell Sci, 115*(Pt 3), 455-465.

Lynch, L. J., Sullivan, K. A., Vallender, E. J., Rowlett, J. K., Platt, D. M., & Miller, G. M. (2013). Trace amine associated receptor 1 modulates behavioral effects of ethanol. *Subst Abuse, 7*, 117-126. doi:10.4137/sart.s12110

Mayer, K., Vreemann, A., Qu, H., & Brix, K. (2009). Release of endo-lysosomal cathepsins B, D, and L from IEC6 cells in a cell culture model mimicking intestinal manipulation. *Biol Chem, 390*(5-6), 471-480. doi:10.1515/bc.2009.047

Neuhoff, V., Philipp, K., Zimmer, H. G., & Mesecke, S. (1979). A simple, versatile, sensitive and volume-independent method for quantitative protein determination which is independent of other external influences. *Hoppe Seylers Z Physiol Chem, 360*(11), 1657-1670.

Nilsson, M., & Fagman, H. (2017). Development of the thyroid gland. *Development, 144*(12), 2123-2140. doi:10.1242/dev.145615

Panas, H. N., Lynch, L. J., Vallender, E. J., Xie, Z., Chen, G. L., Lynn, S. K., et al. (2010). Normal thermoregulatory responses to 3-iodothyronamine, trace amines and amphetamine-like psychostimulants in trace amine associated receptor 1 knockout mice. *J Neurosci Res, 88*(9), 1962-1969. doi:10.1002/jnr.22367

Revel, F. G., Meyer, C. A., Bradaia, A., Jeanneau, K., Calcagno, E., Andre, C. B., et al. (2012a). Brain-specific overexpression of trace amine-associated receptor 1 alters monoaminergic neurotransmission and decreases sensitivity to amphetamine. *Neuropsychopharmacology, 37*(12), 2580-2592. doi:10.1038/npp.2012.109

Revel, F. G., Moreau, J. L., Gainetdinov, R. R., Bradaia, A., Sotnikova, T. D., Mory, R., et al. (2011). TAAR1 activation modulates monoaminergic neurotransmission, preventing hyperdopaminergic and hypoglutamatergic activity. *Proc Natl Acad Sci U S A, 108*(20), 8485-8490. doi:10.1073/pnas.1103029108

Revel, F. G., Moreau, J. L., Gainetdinov, R. R., Ferragud, A., Velazquez-Sanchez, C., Sotnikova, T. D., et al. (2012b). Trace amine-associated receptor 1 partial agonism reveals novel paradigm for neuropsychiatric therapeutics. *Biol Psychiatry, 72*(11), 934-942. doi:10.1016/j.biopsych.2012.05.014

Rich, T. C., Fagan, K. A., Tse, T. E., Schaack, J., Cooper, D. M. F., & Karpen, J. W. (2001). A uniform extracellular stimulus triggers distinct cAMP signals in different compartments of a simple cell. *Proc Natl Acad Sci U S A, 98*(23), 13049-13054. doi:10.1073/pnas.221381398

Roger, P. P., Baptist, M., & Dumont, J. E. (1992). A mechanism generating heterogeneity in thyroid epithelial cells: suppression of the thyrotropin/cAMP-dependent mitogenic pathway after cell division induced by cAMP-independent factors. *J Cell Biol, 117*(2), 383-393.

Scanlan, T. S., Suchland, K. L., Hart, M. E., Chiellini, G., Huang, Y., Kruzich, P. J., et al. (2004). 3-Iodothyronamine is an endogenous and rapid-acting derivative of thyroid hormone. *Nat Med, 10*(6), 638-642. doi:10.1038/nm1051

Schanze , N. (2017). Role of the thyroid hormone metabolite 3-iodothyronamine in the regulation of the thyroid hormone homeostasis. Freie Universität Berlin, Dissertation. http://www.diss.fu-berlin.de/diss/receive/FUDISS_thesis_000000105687

Schanze, N., Jacobi, S. F., Rijntjes, E., Mergler, S., Del Olmo, M., Hoefig, C. S., et al. (2017). 3-Iodothyronamine Decreases Expression of Genes Involved in Iodide Metabolism in Mouse Thyroids and Inhibits Iodide Uptake in PCCL3 Thyrocytes. *Thyroid, 27*(1), 11-22. doi:10.1089/thy.2016.0182

Suzuki, K., Kawashima, A., Yoshihara, A., Akama, T., Sue, M., Yoshida, A., et al. (2011). Role of thyroglobulin on negative feedback autoregulation of thyroid follicular function and growth. *J Endocrinol, 209*(2), 169-174. doi:10.1530/joe-10-0486

Szumska, J., Qatato, M., Rehders, M., Fuhrer, D., Biebermann, H., Grandy, D. K., et al. (2015). Trace Amine-Associated Receptor 1 Localization at the Apical Plasma Membrane Domain of Fisher Rat Thyroid Epithelial Cells Is Confined to Cilia. *Eur Thyroid J, 4*(Suppl 1), 30-41. doi:10.1159/000434717

Tepel, C., Bromme, D., Herzog, V., & Brix, K. (2000). Cathepsin K in thyroid epithelial cells: sequence, localization and possible function in extracellular proteolysis of thyroglobulin. *J Cell Sci, 113 Pt 24*, 4487-4498.

Weber, J., McInnes, J., Kizilirmak, C., Rehders, M., Qatato, M., Wirth, E. K., et al. (2017). Interdependence of thyroglobulin processing and thyroid hormone export in the mouse thyroid gland. *Eur J Cell Biol, 96*(5), 440-456. doi:10.1016/j.ejcb.2017.02.002

Weber, J., Rehders, M., Saftig, P., Verrey, F., Schweizer, U., Wirth, E. K., et al. (2015). Functional analysis of the angio-follicular unit of the mouse thyroid gland. *Exp Clin Endocrinol Diabetes, 123*(03), P12_13. doi:10.1055/s-0035-1547747

Werthmann, R. C., Volpe, S., Lohse, M. J., & Calebiro, D. (2012). Persistent cAMP signaling by internalized TSH receptors occurs in thyroid but not in HEK293 cells. *Faseb j, 26*(5), 2043-2048. doi:10.1096/fj.11-195248

Wirth, E. K., Rijntjes, E., Meyer, F., Kohrle, J., & Schweizer, U. (2015). High T3, Low T4 Serum Levels in Mct8 Deficiency Are Not Caused by Increased Hepatic Conversion through Type I Deiodinase. *Eur Thyroid J, 4*(Suppl 1), 87-91. doi:10.1159/000381021

Wolinsky, T. D., Swanson, C. J., Smith, K. E., Zhong, H., Borowsky, B., Seeman, P., et al. (2007). The Trace Amine 1 receptor knockout mouse: an animal model with relevance to schizophrenia. *Genes Brain Behav, 6*(7), 628-639. doi:10.1111/j.1601-183X.2006.00292.x

10   Figures

follicle area per mid-section

A

follicle count per mid-section

B
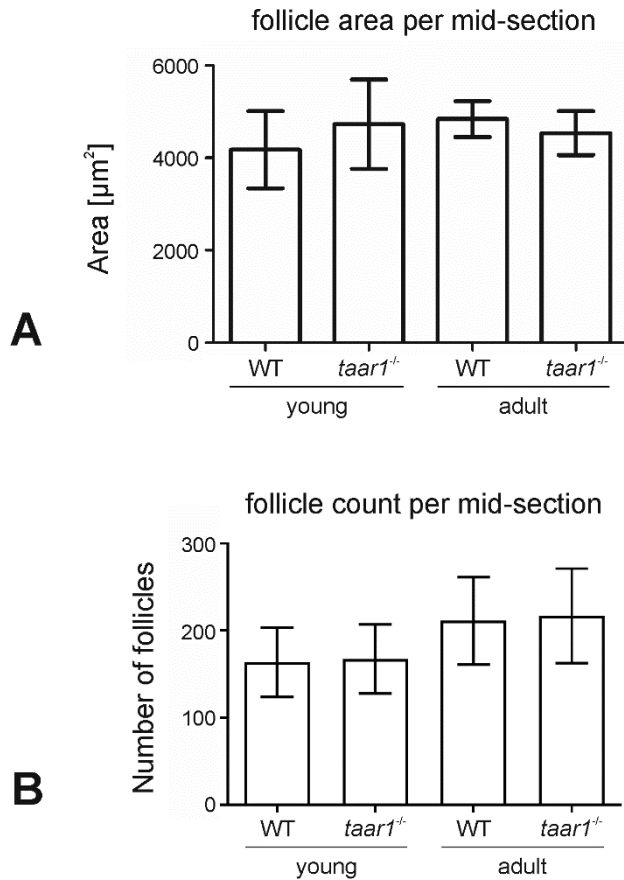
10.1   Figure 1: Morphometry of thyroid lobes revealing no gross alteration upon Taar1 deficiency

Cryosections through thyroid tissue obtained from young or adult C57BL/6 WT and *taar1*^{-/-} mice were analyzed by semi-automated morphometry through a Cell Profiler-based pipeline (Weber et al., 2015). Average follicle area per thyroid mid-section denotes the area covered by the thyroid follicles (A). Follicle area is defined as the external edge, *i.e.* the collagen IV-positive basal lamina, of the follicular epithelia encircling the thyroid follicle lumen. Follicle counts per thyroid mid-section are depicted in (B). Note that there were no differences in follicle areas, and no changes were observed in the number of follicles per thyroid mid-section when tissue from *taar1*^{-/-} and WT of both age groups, namely young and adult mice, were compared, respectively.

The number of biological replicates in (A) were n= 4, 4, 4 and 3 biological replicas for young WT, young *taar1*^{-/-}, adult WT, and adult *taar1*^{-/-}, respectively, with 208, 270, 275 and 200 total number of technical replicas per experimental group, respectively. In (B), the number of replicates was n=8 from 4 biological replicas for the young WT, n=10 from 5 biological replicas for the young *taar1*^{-/-}, and n=6 from 3 biological replicas for the adult WT and *taar1*^{-/-}, respectively.
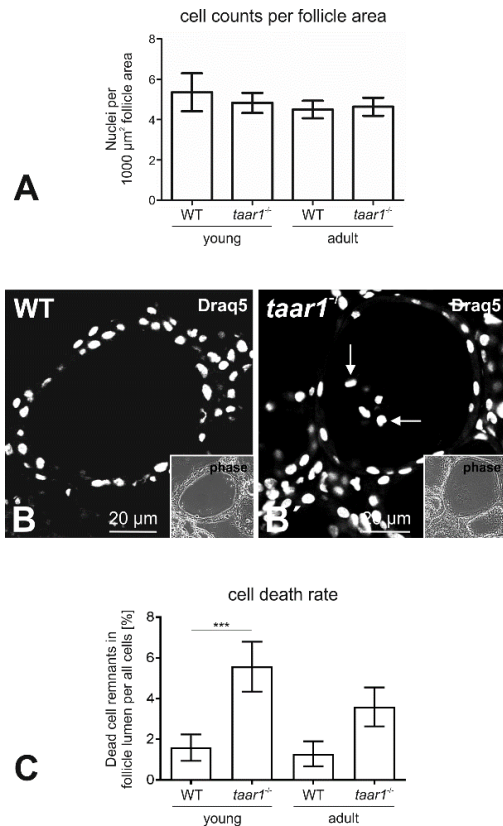
10.2 Figure 2: Number of cells per thyroid mid-section declines upon Taar1 deficiency, consistent with a higher cell death rate in Taar1-deficient follicles

Cryosections through thyroid tissue obtained from young or adult C57BL/6 WT and *taar1*^{-/-} mice were analyzed by semi-automated morphometry through a Cell Profiler-based pipeline (Weber et al., 2015). The number of cells is given per 1000 µm^2 area of thyroid mid-section (average counts ± SD) in (A). Note that young *taar1*^{-/-} mice were characterized by fewer numbers of cells per thyroid mid-section than corresponding WT controls, while there were no differences in the numbers of thyrocytes per 1000 µm^2 tissue area observed for adult *taar1*^{-/-} and WT mice.

Single channel fluorescence micrographs of Draq5™-stained nuclei and corresponding phase contrast micrographs of thyroid follicular epithelia from young WT and *taar1*^{-/-} mice are depicted in (B) and (B'), respectively. Note that remnants of dead cells were found to be present in follicle lumina of *taar1*^{-/-} but mostly absent from WT controls (B', arrows). Scale bars represent 20 µm.

The average percentage of dead cells (± SD) was found to be significantly higher in young and adult *taar1*^{-/-} thyroid epithelia than in WT controls (C). Levels of statistical significance are indicated as *** for *P*<0.0005.

Number of replicas analyzed in (A) is n= 4, 4, 4 and 3 biological replicas for young WT, young *taar1*^{-/-}, adult WT, and adult *taar1*^{-/-}, respectively, with 208, 270, 275 and 200 total number of technical replicas per experimental group, respectively. In (b), three to six different images were analyzed from each animal, while 6, 5, 3, and 3, biological replicas were included for young WT, young *taar1*^{-/-}, adult WT, and adult *taar1*^{-/-}, respectively.

height of epithelial cells

A

B   **WT**   ***taar1*** $^{-/-}$
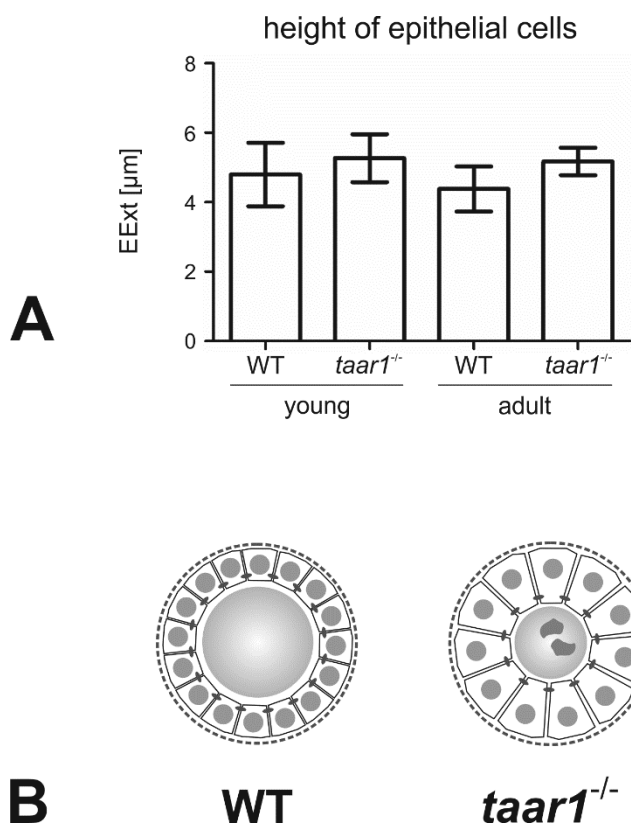
10.3 Figure 3: Thyroid follicular epithelia are more extended in mice with Taar1 deficiency

Cryosections through thyroid tissue obtained from young or adult C57BL/6 WT and *taar1*$^{-/-}$ mice were analyzed by semi-automated morphometry through a Cell Profiler-based pipeline (Weber et al., 2015). Epithelial extensions (EExt) were determined per thyroid mid-section (A). Note that EExts were higher in *taar1*$^{-/-}$ mice when compared to the WT controls, thus implying *taar1*$^{-/-}$ thyrocytes to be more prismatic, possibly indicating a higher activation state in the thyroid gland upon Taar1 deficiency. The scheme in (B) represents a comparison in sizes of thyrocytes relative to follicle lumen diameters in WT and *taar1*$^{-/-}$ mice, respectively, not drawn to scale.

Number of replicas analyzed in (A) is n= 4, 4, 4 and 3 biological replicas for young WT, young *taar1*$^{-/-}$, adult WT, and adult *taar1*$^{-/-}$, respectively, with 208, 270, 275 and 200 total number of technical replicas per experimental group, respectively.
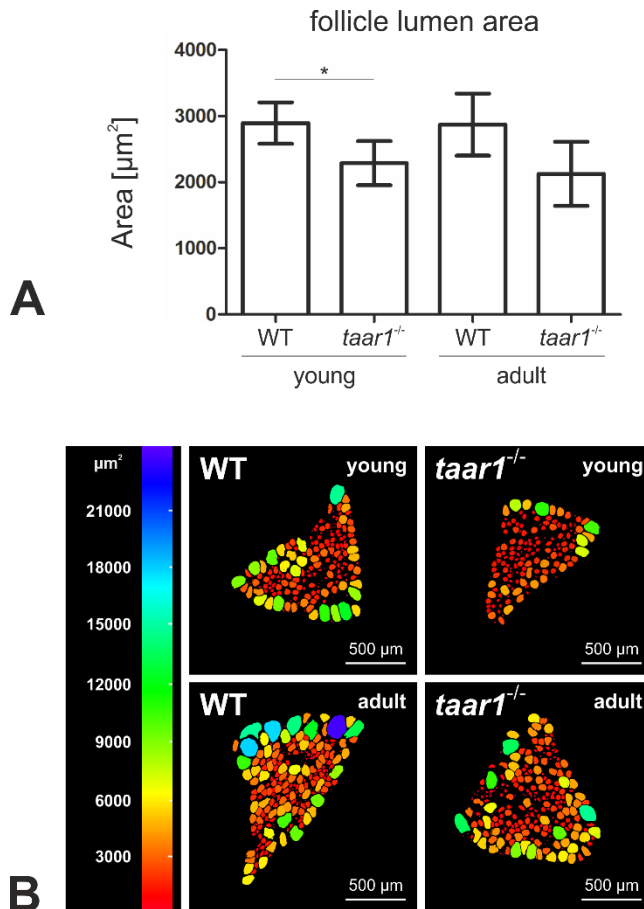
10.4 Figure 4: Follicle lumen areas decrease upon Taar1 deficiency

Cryosections through thyroid tissue obtained from young or adult C57BL/6 WT and *taar1*⁻/⁻ mice were analyzed by semi-automated morphometry through a Cell Profiler-based pipeline (Weber et al., 2015) to determine the follicle lumen areas per thyroid mid-section. Note that the average luminal area, depicted as means ± SD, was smaller in *taar1*⁻/⁻ mice when compared to the WT controls (A). A color-coded depiction of luminal area distribution per thyroid mid-section shows there to be considerable heterogeneity among the follicle population per thyroid section, with bigger follicles tending to localize on the thyroid lobe periphery, thus surrounding smaller, more centrally located follicles. This pattern of follicle distribution is maintained in both genotypes and similar for thyroid lobes from young and adult mice, respectively. Scale bars represent 500 µm.

Levels of statistical significance are indicated as * for P=0.0071. The number of replicas analyzed is 7, 6, 4, and 3 for young WT, young *taar1*⁻/⁻, adult WT, and adult *taar1*⁻/⁻, respectively.
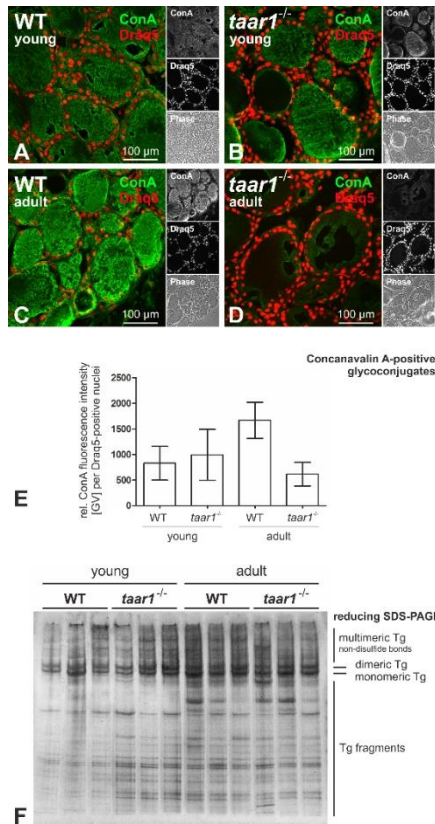
10.5 Figure 5: Protein glycosylation is reduced in adult Taar1-deficient mouse thyroid tissue, while gross Tg degradation states are not affected

Cryosections through thyroid tissue obtained from young and adult WT C57BL/6 and *taar1*^{-/-} mice were stained with the lectin ConA in order to determine the glycosylation status of luminal Tg (A-D, green). Nuclei were counter-stained with Draq5™ (red signals). Merged, single channel fluorescence and corresponding phase contrast micrographs are depicted as indicated. Scale bars represent 100 µm.

The fluorescence intensities of lectin staining of glycosylated tissue components of young and adult mice of both genotypes, respectively, as indicated were determined through a Cell Profiler-based pipeline and normalized to the numbers of cells (E); data are depicted in bar charts as means ± SD.

Protein lysates prepared from young or adult WT C57BL/6 and *taar1*^{-/-} mice, as indicated, were separated by SDS-PAGE under reducing conditions on a horizontal gel, which was silver-stained. The relative positions of bands representing multi-, di- and monomeric Tg, as well as Tg fragments of lower molecular masses, are indicated in the right margin. Note that changes in glycosylation states were prevalent in thyroid tissue from young *vs.* adult *taar1*^{-/-} mice and adult WT *vs. taar1*^{-/-} mice (cf. B with D, and C with D, respectively, and E), but did not affect the extent or pattern of Tg degradation, which was comparable between *taar1*^{-/-} and WT mice (F).

The number of images analyzed were n=3, 5, 3, and 3 for young WT, young *taar1*^{-/-}, adult WT, and adult *taar1*^{-/-}, respectively.
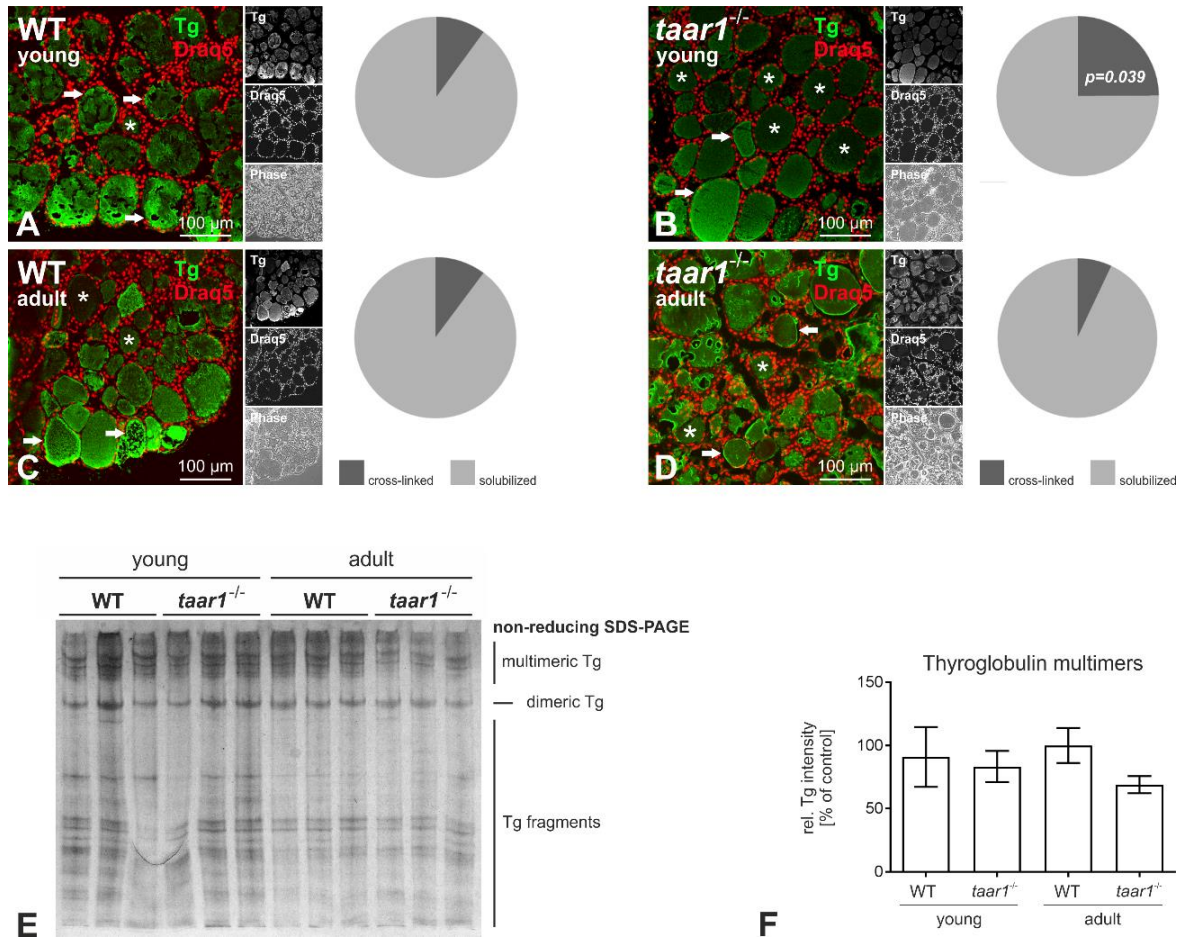
10.6 Figure 6: Thyroid follicles of *taar1*^{-/-} mice present a difference in Tg storage capacity

Morphological assessment of intra-luminal Tg was performed by immunolabeling thyroid cryosections from young and adult WT C57BL/6 and *taar1*^{-/-} mice with antibodies against Tg. The homogeneous, dimmer signal denotes cross-linked Tg (A-D, asterisks), as opposed to a higher-intensity labeling of Tg, owing to more accessible Tg epitopes for antibody binding, reflect the multilayered, partially solubilized Tg (A-D, arrows). At 24.9%, the prevalence of cross-linked Tg-containing follicle lumina was highest in the young *taar1*^{-/-} thyroid tissue, as compared to 10.0% in the young WT, and 10.2% and 7.0% in the adult WT and *taar1*^{-/-}, respectively (A-D).

Proteins isolated from young or adult WT C57BL/6 and *taar1*^{-/-} mice were separated under non-reducing conditions by SDS-PAGE followed by silver staining (E). Note that the less prominent signal of silver staining representing Tg multimers observed for adult *taar1*^{-/-} (E), also represented in the reduction of multimeric Tg band intensities (F).

Data are depicted as means ± SD. The number of follicles morphometrically analyzed is n=264 from 4 biological samples, n=434 from 6 biological samples, n=487 from 3 biological samples, and n=346 from 3 biological samples for young WT, young *taar1*^{-/-}, adult WT, and adult *taar1*^{-/-}, respectively.
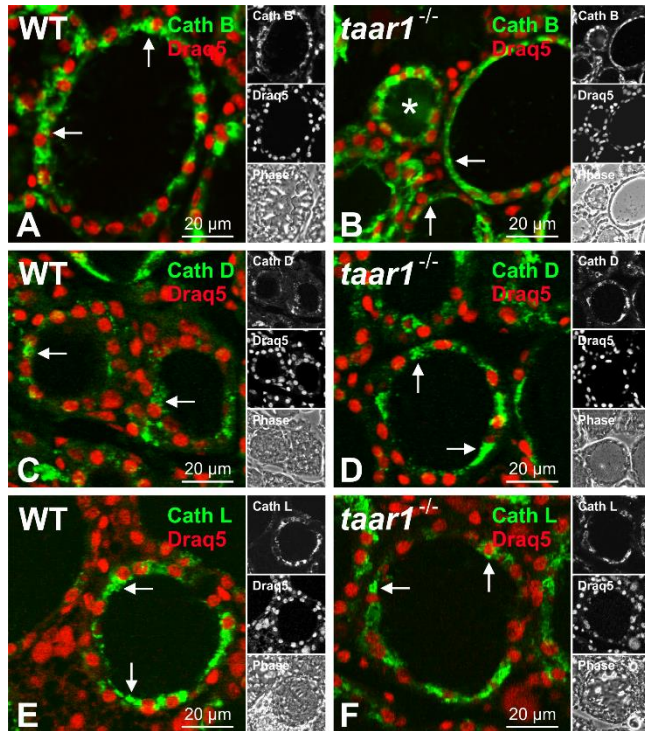
10.7 Figure 7: Subcellular localization of Tg-processing cathepsins remains unchanged in mouse thyroid gland epithelia upon Taar1 deficiency

Cryosections through thyroid tissue obtained from C57BL/6 WT and *taar1*^{-/-} mice were stained with antibodies against cathepsin B (A and B), cathepsin D (C and D), and cathepsin L (E and F), and analyzed by confocal laser scanning microscopy. Single channel fluorescence micrographs in right panels: top cathepsin B, D, or L, as indicated, middle Draq5, bottom phase contrast. Images represent data obtained from young mice, only. Note that subcellular localization of cathepsins was not altered upon Taar1 deficiency and was mainly confined to endo-lysosomal compartments (A-F, arrows). Scale bars represent 20 µm.
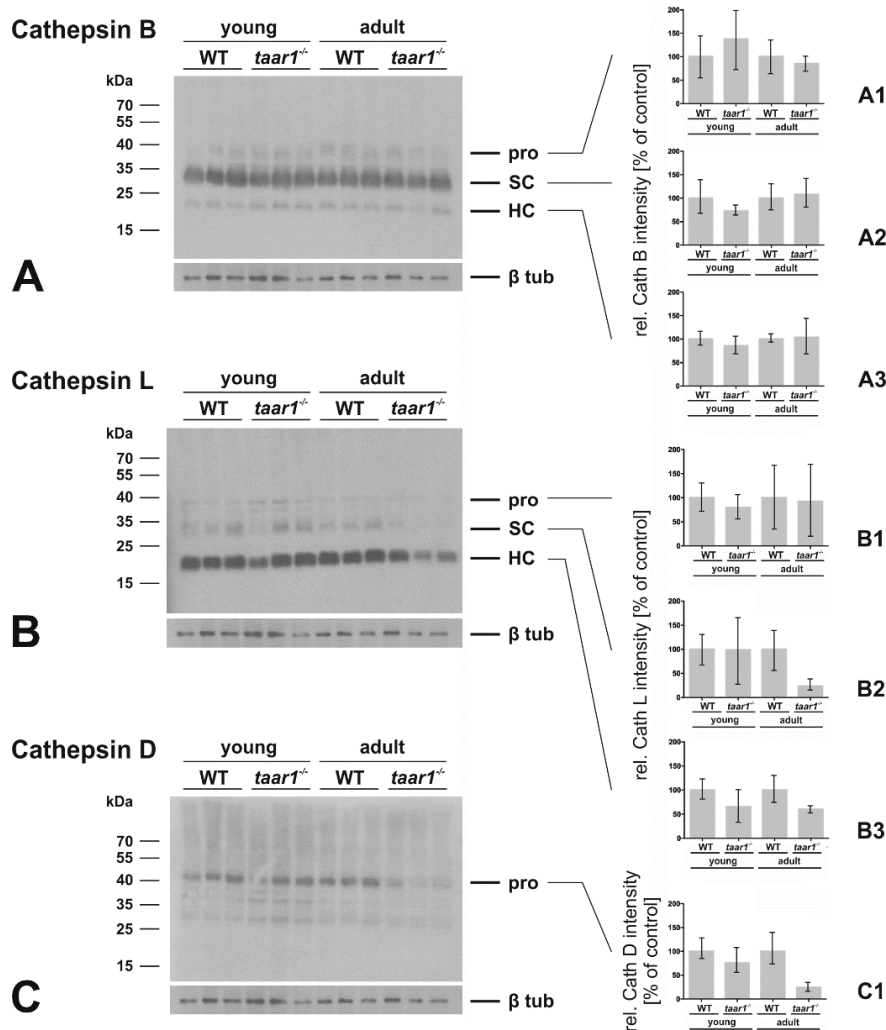
10.8 Figure 8: Variations in protein amounts of cathepsin B, L, and D in mouse thyroid gland upon Taar1 deficiency

Proteins were isolated from thyroid tissue obtained from young or adult C57BL/6 WT and *taar1*^{-/-} mice, and separated by SDS-PAGE, followed by immunoblotting with antibodies against cathepsins B, L, or D. Protein amounts of the proform (pro), single chain (SC) and heavy chain of two-chain mature forms (HC) of cathepsin B (A-A3) and cathepsin L (B-B3), and the proform of cathepsin D (C-C1) were analyzed by densitometry and normalized to β-tubulin to enable comparison between young or adult *taar1*^{-/-} thyroid protein content and their WT controls. Molecular mass markers are indicated in the left margins (A, B and C). Protein amounts of all forms of cathepsin B were not altered in *taar1*^{-/-} thyroids in comparison to WT controls (A1-A3). Single chain and two chain mature form protein amounts of cathepsin L were insignificantly decreased in adult *taar1*^{-/-} thyroids in comparison to WT controls (B2 and B3, respectively). Similarly, the proform of cathepsin D was reduced in adult *taar1*^{-/-} thyroids, as compared to WT controls (C1), although not reaching the threshold of statistical significance.

Data are depicted as means ± SD. Number of biological replicates was n=3.
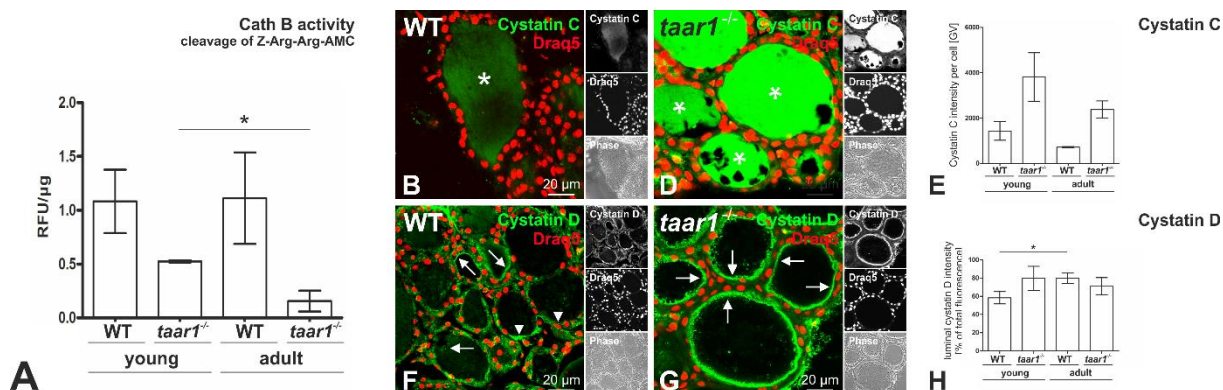
10.9 Figure 9: Proteolytic activity of cathepsin B is reduced in adult mouse thyroid glands upon Taar1 deficiency, consistent with an increase in cystatin levels

Proteins were isolated from thyroid tissue obtained from young or adult C57BL/6 WT and *taar1*-/- mice, and proteolytic activity of cathepsin B was determined. The graph represents cleavage of Z-Arg-Arg-AMC*HCl (A). Cathepsin B activity levels of each sample were obtained by calculating relative fluorescence units (RFU) per protein concentration. Note that cathepsin B activity is age-dependently decreased in *taar1*-/- mice in comparison to WT controls.

Cryosections through thyroid tissue obtained from young or adult C57BL/6 WT and *taar1*-/- mice, were labeled with antibodies against cystatin C or D, and analyzed by confocal laser scanning microscopy (B, C, F and G). Single channel fluorescence micrographs in right panels: top cystatin C or D as indicated, middle Draq5, and bottom phase contrast. Images represent data obtained from young mice. The graph in (E) represents quantification of the fluorescence intensity of cystatin C-positive signals per cell given in grey values (GV) for *taar1*-/- mice *vs* WT control. The graph in (H) represents quantification of fluorescence intensity of cystatin D-positive signals in the lumena, depicted as percentage of total fluorescence intensity of cystatin D per cell for *taar1*-/- mice *vs* WT control.

Cystatin C was mainly localized in the follicle lumen (B and C, asterisks) in both WT and *taar1*-/- mice. Note that protein amounts of cystatin C were increased in *taar1*-/- mice in comparison to WT controls.

Cystatin D was mainly localized to the pericellular space of the lumena (F and G) in both WT and *taar1*-/- mice, and featured an increase in thyroids of young *taar1*-/- mice. Scale bars represent 20 μm.

Data are depicted as means ± SD. Levels of statistical significance are indicated as * for P<0.025. For cathepsin B activity assays, n=3 biological replicas per experimental group were analyzed in triplicates.

total T$_4$ concentration in serum

A

total T$_3$ concentration in serum

B

total TSH concentration in serum

C
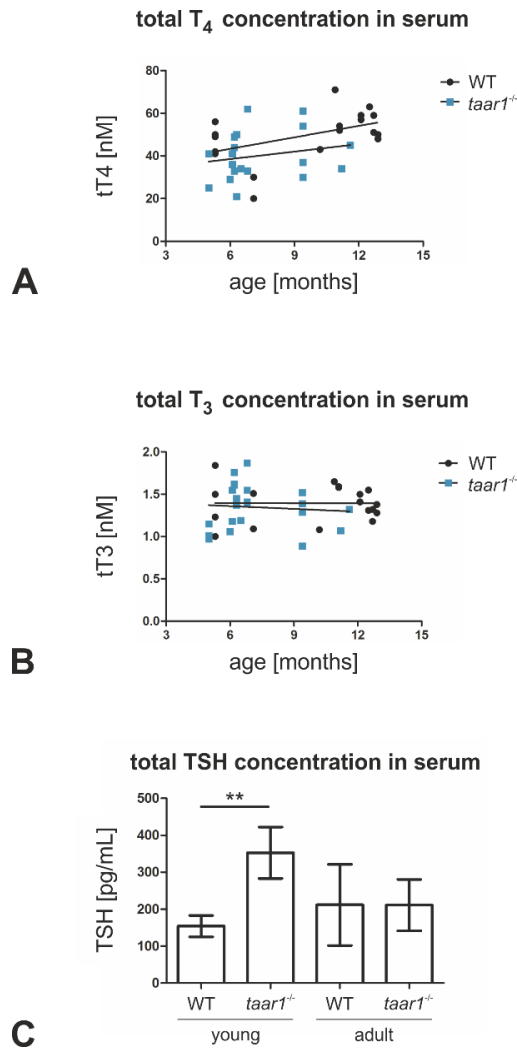
10.10 Figure 10: Elevated serum TSH concentrations in young *taar1$^{-/-}$* mice, while thyroid hormones concentrations remain comparable to the WT

Total T$_4$ (A) and total T$_3$ (B) serum concentrations of *taar1$^{-/-}$ vs* WT mice were quantified by radioimmunoassay. Data showed total T$_4$ and T$_3$ serum concentrations were not altered in *taar1$^{-/-}$* mice in comparison to WT controls (A and B). Serum TSH was determined by ELISA, revealing an elevation in TSH concentration in the serum of young *taar1$^{-/-}$* mice, as compared to the WT controls (C).

Data are depicted as means ± SD. Levels of statistical significance are indicated as ** for *P*<0.01 determined by the students' T-test.

The number of biological replicas are n= 18 and 20 for WT and *taar1$^{-/-}$*, respectively, for total T$_4$ determination, and n=19 and 24 for WT and *taar1$^{-/-}$*, respectively, for total T$_3$, taken as averaged duplicates. For the serum TSH, n= 5 and 4 for young WT and young *taar1$^{-/-}$*, respectively, and n= 3 and 5 for adult WT and adult *taar1$^{-/-}$*, respectively. Samples were run in triplicates or duplicates. Values for the young and adult experimental groups represent two independent experiments, therefore, no intra-age groups statistical comparison was performed.
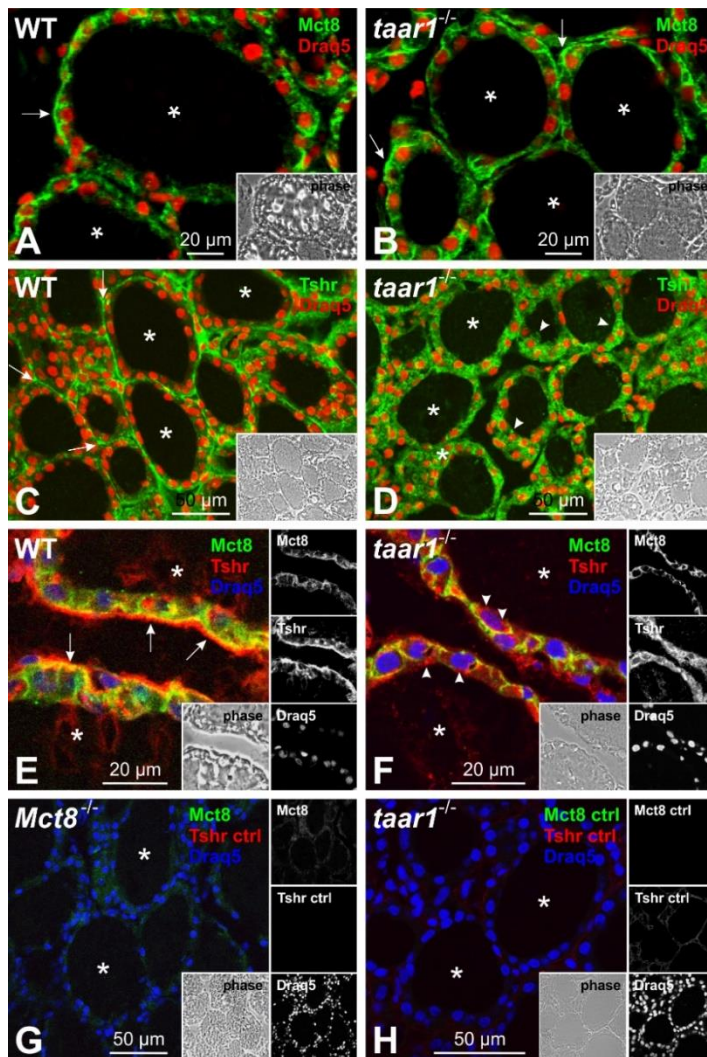
10.11 Figure 11: Taar1 deficiency alters Tshr localization in the mouse thyroid glands, but does not affect Mct8 localization

Cryosections through thyroid tissue obtained from young C57BL/6 WT and *taar1*^{-/-} mice were labeled with antibodies against TSHR and Mct8 and examined by confocal laser scanning microscopy. Mct8 maintains a basolateral localization in both WT and in *taar1*^{-/-} thyroid tissue (A and B, arrows), while Tshr is more prominently localized at intracellular plasma membranes of *taar1*^{-/-} thyrocytes in young mice (D and F, arrowheads), as opposed to predominantly basolateral distribution in the WT (C and E, arrows). (E and F) present a close-up on thyroid epithelia of WT and in *taar1*^{-/-} mice, respectively, as merged Tshr and Mct8 images. Secondary antibody controls are shown in (G and H) as indicated. Single channel fluorescence micrographs in right panels: top Mct8, middle Tshr, bottom Draq5™ as nuclear counter-stain. Insets represent corresponding phase contrast micrographs. Images represent data obtained from 5-7 months old mice. Scale bars represent 20 µm in (A, B, E and F) and 50 µm in (C, D, G and H).

WT   *taar1*⁻ᐟ⁻
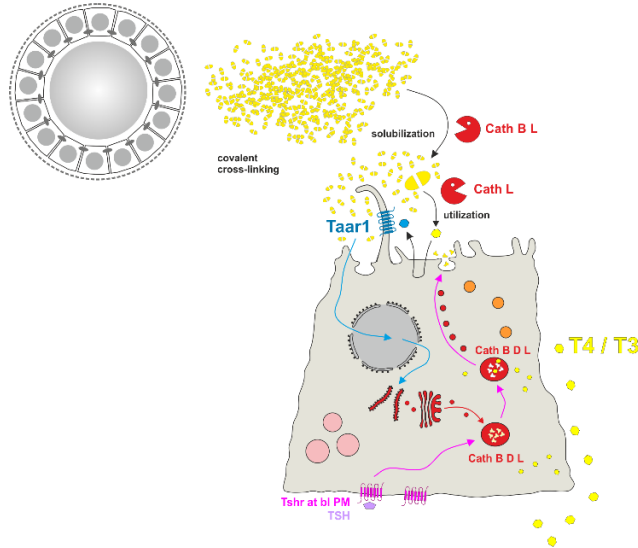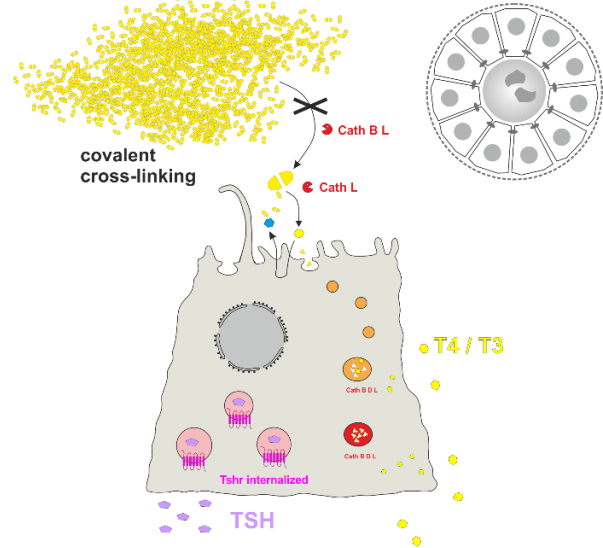
10.12 Figure 12: The influence of Taar1 deficiency on liberation of TH in thyroid follicles.

Tg (yellow) is synthesized and secreted at the apical plasma membrane of thyrocytes for storage in covalently cross-linked form in the thyroid follicle lumen of WT (left). TSH (violet) binding to basolateral Tshr (pink) triggers retrograde trafficking of endo-lysosomal enzymes (red) for secretion at the apical pole into the peri-cellular follicle luminal space. Subsequently, Tg is solubilized extracellularly by the action of cathepsins B and L before being internalized for endo-lysosomal degradation (orange to red). TH release (yellow) from thyroid follicles is through balanced proteolytic processing of Tg by extra- and intracellular means of proteolysis, and subsequent Mct8-mediated translocation across the basolateral plasma membrane. This study asks whether Tg solubilization and processing to yield TH is possibly co-regulated by Taar1 (cyan), which is localized to cilia at the apical plasma membrane of thyrocytes where it can, in principle, interact with intra-follicular generated TH derivatives triggering signaling of this GPCR.

Smaller thyroid follicle lumina in male *taar1*⁻ᐟ⁻ vs. WT mice reveal thyroglobulin storage in more compacted form (right). Enhanced luminal cystatins C and D (not depicted) render thyroglobulin-solubilizing cathepsin B (red) less active in thyroid tissue of male *taar1*⁻ᐟ⁻ mice. Cathepsin L amounts (red) are diminished in *taar1*⁻ᐟ⁻ vs. WT thyroid glands, featuring more dead cell remnants (dark grey irregular shaped symbols) in the follicle lumen. More extended epithelia do not affect gross thyroid hormone (yellow polygons) release from thyroid follicles of *taar1*⁻ᐟ⁻ mice.

TSH (violet) concentrations in the blood serum are enhanced upon Taar1 deficiency, while TSH receptors (pink) are non-canonically located in intracellular vesicles.

The results indicate Taar1 is necessary to maintain canonical HPT-axis regulation of thyroid function in male mice.

11   Table 1: Antibodies used in this study

Antigen	Specificity	Company / Provider	Catalog Number	Dilution in immuno-fluorescence	Dilution in immuno-blotting
β-Tubulin	Rabbit anti-human	Abcam	#ab6067	_	1:1000
Cathepsin B	Goat anti-mouse	Neuromics	#GT15047	1:100	1:1000
Cathepsin D	Rabbit anti-human	Calbiochem	#IM-16	1:10	1:250
Cathepsin L	Goat anti-mouse	Neuromics	#GT15049	1:100	1:1000
Collagen IV	Rabbit anti-mouse	Novotech	#CO20451	1:100	_
Cystatin C	Rabbit anti-mouse	Dr. Magnus Abrahamson, Lund, Sweden	_	1:25	_
Cystatin D	Rabbit anti-mouse	Dr. Magnus Abrahamson, Lund, Sweden	_	1:25	_
Monocarboxylate transporter 8 (Mct8, Slc16A2)	Rabbit anti-human	Atlas Antibodies	#HPA003353, lot A61491	1:200	_
Thyroglobulin	Rabbit anti-bovine	(Brix et al., 1998)		1:100	1:1000
TSHR	Mouse anti-human	Abcam	#ab6047	1:100	1:1000

5. Discussion

5.1 Thyroid hormone transporters Mct8 and Mct10 serve as sensors of intrathyroidal TH levels and contribute to regulating Tg-processing cathepsins by TSH-independent means

Thyroid regulation is a complex process that is achieved by an interaction between the classical, HPT axis dependent pathways, and non-classical, TSH-independent pathways. We hypothesised the THT, being molecules that selectively translocate TH across the membrane, to be part of the non-classical regulatory ensemble, and to act as sensors of intrathyroidal TH levels. Moreover, we hypothesised that a molecular association exists between THT and Tg-processing cathepsins that regulate Tg proteolysis and intrafollicular TH liberation. Our results support this hypothesis, indicating that a deficiency in Mct8 or/and Mct10 results in an intrafollicular shift in equilibrium between covalently cross-linked and soluble Tg, facilitated by an upregulation in Tg-processing cathepsins, and leading to an intrathyroidal thyrotoxic state. This also indicates a counterintuitive mode of regulation that is TSH-independent. The latter notion is further corroborated by the fact that while auto-thyrotoxicity is more grave in Mct8/Mct10 double deficient mice, these animals maintain elevated levels of TSH and T_3 in the serum, despite adequate T_4 concentrations (Müller and Heuer 2014).

In conclusion, Mct8 and Mct10 not only translocate TH across membranes of TH-producing and TH-target cells, but also feature in an intrathyroidal sensing mechanism that co-regulates the extent of Tg-processing by regulating the amount of Tg-processing proteases available for Tg degradation. In order to better explore this relationship, future experiments are planned to characterised the thyroid and Tg profiles from animals with THT deficiencies combined with a cathepsin deficiency. To this end, a colony of mice with a cathepsin K deficiency additional to an Mct8/Mct10 single or double deficiency has been established. This is of particular interest since Mct8 was shown to be significantly upregulated in thyroid tissue deficient in cathepsin K (this study). This can be explained as the thyroid's attempt to compensate for its reduced TH liberation capacity, by upregulating TH export to maintain adequate supply for peripheral tissue (Friedrichs et al. 2003). This can be seen as a counterintuitive mechanism too, since the thyroid might become hypothyroid itself, at least transiently.

5.2 Taar1 localisation on the apical plasma membrane domain and ciliary appendages of thyrocytes *in situ* and *in vitro*

The primary cilium is essentially a thin extension of the apical plasma membrane of a cell into an intercellular milieu (Nachury 2014). The constrictive area of a cilium is commonly viewed as providing an advantageous signalling environment in that it concentrates molecules, thereby increasing their chemical activities, or else, by serving as a scaffold to bring signalling intermediates to close proximity, therefore, the primary cilium provides a signalling platform to many molecules, including GPCRs (Mahjoub and Stearns 2012, Nachury 2014).

In light of the studies suggesting Taar1 to be the putative receptor for 3-T_1AM (Scanlan et al. 2004, Panas et al. 2010), demonstrating that Taar1 is essentially localised on ciliary appendages on the apical plasma membrane of thyroid epithelial cells, where it is in direct contact with intraluminal molecules, proves an interesting finding. Although the site of 3-T_1AM synthesis remains a valid question, it cannot be excluded that it may be, at least in part, liberated already in the follicle lumen. Likewise, it may well be that other non-classical thyroid hormones, such as downstream metabolites of 3-T_1AM, act as endogenous Taar1 ligands, at least in the local environment of the thyroid follicle. Accordingly, it would be necessary to understand the molecular make-up of the thyroid follicle lumen in wild type mice and, comparably, whether or not it is altered in the Taar1-deficient thyroid lumena. This could, in principle, be achieved by MALDI imaging mass spectrometry of preserved thyroid epithelial cryosections, however, the currently available coating matrix and limited spatial resolution appear to be sub-optimal for luminal thyronome profiling.

Thus, Taar1 localising at the primary cilia of thyrocytes speaks in favour of the cilia being the site of Taar1 signalling. On the other hand, various studies have emerged describing GPCR signalling from subcellular compartments, highlighting that it is not a strictly cell surface-dependent phenomenon (Sato et al. 2006, Calebiro et al. 2010). *In vitro* experiments involving rodent, rhesus monkey, or human Taar1/TAAR1 expressed in HEK 293 cells have shown the GPCR to respond to agonist stimulation (including thyronamines and biogenic amines) with the accumulation of intracellular cAMP (Borowsky et al. 2001, Bunzow et al. 2001, Scanlan et al. 2004, Lindemann et al. 2005, Miller et al. 2005, Reese et al. 2007), indicating that Taar1 signals mainly via the $G_{\alpha s}$-coupled pathway. To date, no additional pathways were reported for Taar1 signalling.

So a question to address would be if Taar1 signals exclusively from the ciliary membranes, or rather, in terms of an experimental setting, the question would be: how much of the total intracellularly accumulated cAMP is due to ciliary Taar1 signal transduction? To this end, the established mTaar1-EGFP cellular model systems can be used, particularly KTC-1 cells stably expressing mTaar1-EGFP (KTC-Z), as they maintain a degree of cell polarity, therefore, feature ciliary appendages on their apical plasma membrane domains. To test for mTaar1-EGFP functionality, activity assays featuring stimulation of stably mTaar1-EGFP-expressing cell lines with increasing doses of 3-T$_1$AM will be in order, where the rise in intracellular cAMP levels can be tested for using immunoassay screening, such as the cAMP AlphaScreen assay. Assuming mTaar1-EGFP passes the functionality test, and in order to attempt to distinguish between apical/ciliary Taar1-EGFP signalling versus intracellularly localised mTaar1-EGFP signalling contributing to intracellular cAMP accumulation, KTC-Z cells can be grown on filter membranes. Since these cells retain structural polarity, they will form a tight monolayer in which the apical and basolateral poles can be separately stimulated by Taar1-agonists such as 3-T$_1$AM. Such a system, however, is still challenged by the fact that the endogenous Taar1 ligand is unconfirmed, nor are the potential transporting molecules and that could facilitate TAM entry into the thyrocyte. Therefore, if cAMP accumulation resulting from apical and basolateral stimulation is comparable, it would not be possible to conclude definitively as to whether the ligand is indeed acting from within the thyroid follicle lumen, or triggers Taar1 signalling from elsewhere.

This study also showed that, following incubation for 17 hours at 18°C, mTaar1-EGFP continued to colocalise with acetylated α-tubulin on cilia, suggesting a slow turnover rate. This could mean that few Taar1 molecules are ever required on the cell surface due to their stability, which could explain why less mTaar1-EGFP is seen on the plasma membrane, compared to intracellular compartments, *in vitro*, bearing in mind that low expression levels of *Taar1* were ever reported in various tissues or cells *in situ (Liberles and Buck 2006)*. Therefore, it would be worthwhile to determine the half-life (t$_{1/2}$) of mTaar1-EGFP in the *in vitro* models. One way to approach this would be, once the functionality of mTaar1-EGFP has been established, to pulse cells with excess Taar1-agonist and chase the mTaar1-EGFP over a certain period of time. The shortcomings of such an approach, however, would primarily be the relatively low detection levels of surface mTaar1-EGFP, which would speak strongly in favour of relying on live cell imaging. The latter would not be very practical over prolonged durations, as it could lead to photobleaching of EGFP.

Alternatively, the reduction in the ratio of Taar1-positive surface signal to total Taar1-EGFP signal over a period of time following agonist stimulation of Taar1 can be achieved by fluorescence-activated cell sorting. This, however, is challenging in the absence of specific Taar1 antibodies that would recognise an epitope on an extracellular Taar1 domain. Hence, engineering an additional HA-tag to the N-terminus of mTaar1-EGFP would be an alternative.

Other approaches may involve using a complementation assay based on β-arrestin 2 to observe and quantify Taar1 association with β-arrestin 2 which occurs upon internalisation (Harmeier et al. 2015). Such an assay would involve β-arrestin 2 tagged with a *Renilla* luciferase (RLuc) and mTaar1-EGFP in a bioluminescence resonance energy transfer (BRET) setup (Zhang and Xie 2012). Thus, upon association with mTaar1-EGFP, the RLuc reaction emits blue light at 480 nm which excites the EGFP whose emission is detected at a higher wavelength, therefore, BRET is calculated as EGFP/RLuc emission (Zhang and Xie 2012).

5.3 Altered TSHR localisation *in situ* in Taar1-deficient mouse thyroid epithelial cells

The inevitable fate of an activated GPCR, including the TSHR, is to be internalised into endo-lysosomal compartments, generally a β-arrestin-chaperoned and clathrin-mediated pathway, from where the receptor is either recycled back to the cell surface, or proceeds to be degraded by endo-lysosomal enzymes (Luttrell and Lefkowitz 2002). Contrary to previous beliefs, receptor internalisation is not exclusively a GPCR down-regulation mechanism (Lohse 1993), but is also essential for efficient receptor desensitisation (Calebiro 2011). In the case of the TSHR, facilitated predominantly by β-arrestin 2 (Frenzel et al. 2006), it is co-internalised complexed to its ligand into subcellular compartments, from where it continues to persistently signal *via* the cAMP-related pathways (Calebiro et al. 2009, Calebiro et al. 2010, Werthmann et al. 2012), including even in the trans-Golgi network, following retrograde trafficking from the cell surface (Godbole et al. 2017). The latter transport pathways was described only very recently and proves thyroid epithelial cells and the molecules that govern their physiological functions interesting to study further as they seem to deliver peculiar solutions to cell biological problems that remained unanswered for long. It is noteworthy that downstream cellular targets of cAMP signalling appear to be dependent on the subcellular site of signal origin (Rich et al. 2001), i.e. endosomally signalling GPCRs do not necessarily activate the same downstream pathways as classically activated by cell surface-localised signalling GPCRs.

In mouse thyroid epithelia lacking a functional Taar1, a remarkable change in TSHR localisation is seen, whereby a TSHR-immunopositive signal was predominantly seen in intracellular compartments as opposed to the wild type, largely basolateral distribution. It remains to be checked whether the intracellular distribution of TSHR in the Taar1-deficient thyroid tissue is due to enhanced internalisation, which could be the result of β-arrestin 2 upregulation (Frenzel et al. 2006), or whether it is caused by poor targeting of the TSHR to the cell surface, which would lead to partial TSH resistance (Calebiro et al. 2005). The direct way to experimentally address these questions would be to first verify TSHR signalling and the level of cAMP production in Taar1-deficient thyroid epithelial tissue, versus WT thyroid tissue. It would also be interesting to find whether the downstream targets of this signalling in the Taar1-deficient thyroid are different from the wild type situation.

In order to perform signalling assays on mouse thyroid tissue, it would be advisable to prepare primary cells from fragments of Taar1-deficient and WT mouse thyroid follicles *in situ* that would form inside-out-follicles *in vitro* when kept on hydrophobic surface. These essentially are isolated follicle segments from thyroid tissue, forming closed follicular spheres, but which are inverted in terms of cell polarity, the notion that the apical plasma membrane domain of these cells is exposed to the medium, as opposed to facing the follicle lumen as *in situ* (Herzog and Miller 1981, Graebert et al. 1997). The advantage of such a system is that the cells can be prepared directly following tissue isolation from mice of the required age and genotypes, plus, suspension in TSH-supplemented medium ensures ligand delivery to the cells. This *in vitro* system is prepared by carefully isolating thyroid tissue fragments devoid of connective tissue, washing out its luminal content, then subjecting the tissue fragments to enzymatic and mechanical dissociation (Graebert et al. 1997).

Additionally, the relationship between Taar1 and TSHR can also be investigated *in vitro* to see whether Taar1 signalling directly affects TSHR localisation. To begin with, antibodies specific for TSHR can be used to determine the subcellular localisation of the GPCR in thyroid epithelial cell lines grown steadily at 37°C, and used to compare whether this localisation is altered upon inhibiting Taar1 by subjecting the cells to treatment with EPPTB, the selective Taar1 antagonist (Bradaia et al. 2009). Subsequently, the mTaar1-EGFP-expessing cellular systems can be used in the same way, while subjecting the cells to 3-T1AM stimulation, EPPTB inhibition, TSH stimulation or combinations. Additionally, inside-out-follicles can be used instead in a similar experimental setup as they closely mimic the *in situ* structural arrangement of thyrocytes, in

addition to maintaining functional differentiation, thereby providing an arguably more authentic model than immortalised cell lines.

Because the Taar1-deficient mouse model is characterised by altered TSHR localisation, coupled to a slight elevation in serum TSH concentration, another interesting aspect would be to put further strain on the HPT axis by inducing hyperthyroidism and aggravating hypothyroidism in the Taar1-deficient mouse and re-examine the same thyroidal parameters, especially with regard to TSHR localisation, Tg-processing cathepsin protein levels, cystatin C and D levels, in addition to the localisation and protein amounts of TH transporters, particularly Mct8 and Mct10. Hyper- and hypothyroidism can be induced by relying on well-established protocols (Engels et al. 2016, Rakov et al. 2016) specific for rodent models. Induced hypothyroidism was shown to cause lowering in endogenous TAM serum concentrations (Hackenmueller et al. 2012), therefore, it is important to first establish whether serum and intrathyroidal TAM concentrations are altered in the Taar1-deficient mouse in comparison to the WT, and then examine how imposing further stain on the HPT axis would alter TAM content relative to TH liberation capacity of the Taar1-deficient thyroid gland.

Interestingly, in a study where male C57BL/6 mice were repeatedly injected intraperitonially with 5 mg/kg 3-T_1AM, Schanze et al. reported a significant decrease in expression levels of the TSH-dependent genes *Nis* and *Tg,* and *pendrin*, in comparison to control mice (Schanze et al. 2017). On the other hand, *Tshr, Tpo* and type 1 deiodinase activity in the thyroid were not affected, nor did serum T_3 and T_4 concentrations change. Besides, pituitary transcription levels of genes encoding TSH, TRH receptor and TRH were not affected by 3-T_1AM treatment either (Schanze et al. 2017). This led the authors to conclude that the effects of circulating 3-T_1AM on the thyroid were HPT axis-independent, unless an unknown compensatory mechanism becomes involved (Schanze et al. 2017).

While the present study shows that Taar1-deficiency results in an intracellular distribution of TSHR in thyrocytes and mild hyperthyrotropinaemia, the results from Schanze *et al.* may suggest that the 3-T_1AM effect is not Taar1-mediated. However, it can be argued that Taar1, being apically and not basolaterally localised in thyrocytes, simply had no access to the 3-T_1AM in the circulation. On the other hand, it also cannot be ruled out that the alterations observed by Schanze et al. following 3-T_1AM administration *via* the blood circulation may have been mediated by the latter's metabolites, such as the mono-iodinated thyronamine (T_0AM), N-acetyl-T_1AM (Ac-T_1AM)

and 3-iodothyroacetic acid (TA$_1$) (Hackenmueller and Scanlan 2012, Hoefig et al. 2016). This speaks further in favour of determining the molecular content of follicle lumina in Taar1-deficient and WT thyroid glands, as suggested above, but also that it would be of interest to conduct a similar experiment involving 3-T1AM administration to Taar1-deficient mice under identical experimental conditions as chosen in the study by Schanze and colleagues (Schanze et al. 2017).

5.4 The absence of functional Taar1 leads to a subtle disbalance in the proteolytic to anti-proteolytic activities in male mouse thyroid tissue

Biochemical analyses of Taar1-deficient mouse thyroid tissue showed that, in comparison to WT tissue, cathepsin B activity was mildly decreased, in addition to slightly diminished cathepsin L protein levels. These changes were accompanied by a higher prevalence of cystatins C and D – endogenous cysteine peptidase inhibitors – in the Taar1-deficient thyroid tissue, as shown by immunohistochemical analysis of the tissue. This indicates a mild disturbance in the equilibrium of proteolytic to anti-proteolytic activity in the thyroid gland. Such disturbances would eventually translate as alterations in Tg degradation that could, on the long run, affect TH liberation and TAM generation.

In order to better understand the relationship between Taar1 function and proteostasis in thyroid epithelial cells, cathepsin B and L activity assays can be performed, plus cathepsin and cystatin protein levels can be checked by both immunoblotting and immunofluorescence in the mTaar1-EGFP-expressing cell systems. These could further be subjected to either Taar1 stimulation with 3-T$_1$AM, or to Taar1 inhibition with EPPTB, the latter to mimic the Taar1-deficient state, and compared to those of KTC-1 and Nthy-ori 3-1 cells, i.e. non mTaar1-EGFP-expressing. This should additionally be correlated to studying protein and/or transcript levels of THT, such as Mct8 and Mct10.

6. References

Ackermans, M. T., L. P. Klieverik, P. Ringeling, E. Endert, A. Kalsbeek and E. Fliers (2010). "An online solid-phase extraction-liquid chromatography-tandem mass spectrometry method to study the presence of thyronamines in plasma and tissue and their putative conversion from 13C6-thyroxine." J Endocrinol **206**(3): 327-334.

Agretti, P., G. De Marco, L. Russo, A. Saba, A. Raffaelli, M. Marchini, G. Chiellini, L. Grasso, A. Pinchera, P. Vitti, T. S. Scanlan, R. Zucchi and M. Tonacchera (2011). "3-Iodothyronamine metabolism and functional effects in FRTL5 thyroid cells." J Mol Endocrinol **47**(1): 23-32.

Alvarsson, A., X. Zhang, T. L. Stan, N. Schintu, B. Kadkhodaei, M. J. Millan, T. Perlmann and P. Svenningsson (2015). "Modulation by Trace Amine-Associated Receptor 1 of Experimental Parkinsonism, L-DOPA Responsivity, and Glutamatergic Neurotransmission." J Neurosci **35**(41): 14057-14069.

Babusyte, A., M. Kotthoff, J. Fiedler and D. Krautwurst (2013). "Biogenic amines activate blood leukocytes via trace amine-associated receptors TAAR1 and TAAR2." J Leukoc Biol **93**(3): 387-394.

Barak, L. S., A. Salahpour, X. Zhang, B. Masri, T. D. Sotnikova, A. J. Ramsey, J. D. Violin, R. J. Lefkowitz, M. G. Caron and R. R. Gainetdinov (2008). "Pharmacological characterization of membrane-expressed human trace amine-associated receptor 1 (TAAR1) by a bioluminescence resonance energy transfer cAMP biosensor." Mol Pharmacol **74**(3): 585-594.

Barrett, A. J. (1980). "Fluorimetric assays for cathepsin B and cathepsin H with methylcoumarylamide substrates." Biochem J **187**(3): 909-912.

Bassett, J. H., C. B. Harvey and G. R. Williams (2003). "Mechanisms of thyroid hormone receptor-specific nuclear and extra nuclear actions." Mol Cell Endocrinol **213**(1): 1-11.

Bergh, J. J., H. Y. Lin, L. Lansing, S. N. Mohamed, F. B. Davis, S. Mousa and P. J. Davis (2005). "Integrin alphaVbeta3 contains a cell surface receptor site for thyroid hormone that is linked to activation of mitogen-activated protein kinase and induction of angiogenesis." Endocrinology **146**(7): 2864-2871.

Bernstein, H. G., B. Bogerts and U. Lendeckel (2008). "Cathepsin K and metabolic abnormalities in schizophrenia." Arterioscler Thromb Vasc Biol **28**(12): e163.

Bernstein, H. G., A. Bukowska, H. Dobrowolny, B. Bogerts and U. Lendeckel (2007). "Cathepsin K and schizophrenia." Synapse **61**(4): 252-253.

Berry, M. D. (2004). "Mammalian central nervous system trace amines. Pharmacologic amphetamines, physiologic neuromodulators." J Neurochem **90**(2): 257-271.

Berry, M. D., E. Scarr, M. Y. Zhu, I. A. Paterson and A. V. Juorio (1994). "The effects of administration of monoamine oxidase-B inhibitors on rat striatal neurone responses to dopamine." Br J Pharmacol **113**(4): 1159-1166.

Borowsky, B., N. Adham, K. A. Jones, R. Raddatz, R. Artymyshyn, K. L. Ogozalek, M. M. Durkin, P. P. Lakhlani, J. A. Bonini, S. Pathirana, N. Boyle, X. Pu, E. Kouranova, H. Lichtblau, F. Y. Ochoa, T. A. Branchek and C. Gerald (2001). "Trace amines: identification of a family of mammalian G protein-coupled receptors." Proc Natl Acad Sci U S A **98**(16): 8966-8971.

Boulton, A. A. (1984). Trace Amines and the Neurosciences: An Overview. Neurobiology of the Trace Amines: Analytical, Physiological, Pharmacological, Behavioral, and Clinical Aspects. A. A. Boulton, G. B. Baker, W. G. Dewhurst and M. Sandler. Totowa, NJ, Humana Press**:** 13-24.

Bradaia, A., G. Trube, H. Stalder, R. D. Norcross, L. Ozmen, J. G. Wettstein, A. Pinard, D. Buchy, M. Gassmann, M. C. Hoener and B. Bettler (2009). "The selective antagonist EPPTB reveals TAAR1-mediated regulatory mechanisms in dopaminergic neurons of the mesolimbic system." Proc Natl Acad Sci U S A **106**(47): 20081-20086.

Branchek, T. A. and T. P. Blackburn (2003). "Trace amine receptors as targets for novel therapeutics: legend, myth and fact." Curr Opin Pharmacol **3**(1): 90-97.

Braulke, L. J., M. Klingenspor, A. DeBarber, S. C. Tobias, D. K. Grandy, T. S. Scanlan and G. Heldmaier (2008). "3-Iodothyronamine: a novel hormone controlling the balance between glucose and lipid utilisation." J Comp Physiol B **178**(2): 167-177.

Brix, K., D. Fuhrer and H. Biebermann (2011). "Molecules important for thyroid hormone synthesis and action - known facts and future perspectives." Thyroid Res **4 Suppl 1**: S9.

Brix, K., P. Lemansky and V. Herzog (1996). "Evidence for extracellularly acting cathepsins mediating thyroid hormone liberation in thyroid epithelial cells." Endocrinology **137**(5): 1963-1974.

Brix, K., M. Linke, C. Tepel and V. Herzog (2001). "Cysteine proteinases mediate extracellular prohormone processing in the thyroid." Biol Chem **382**(5): 717-725.

Brix, K., W. Summa, F. Lottspeich and V. Herzog (1998). "Extracellularly occurring histone H1 mediates the binding of thyroglobulin to the cell surface of mouse macrophages." J Clin Invest **102**(2): 283-293.

References

Bunzow, J. R., M. S. Sonders, S. Arttamangkul, L. M. Harrison, G. Zhang, D. I. Quigley, T. Darland, K. L. Suchland, S. Pasumamula, J. L. Kennedy, S. B. Olson, R. E. Magenis, S. G. Amara and D. K. Grandy (2001). "Amphetamine, 3,4-methylenedioxymethamphetamine, lysergic acid diethylamide, and metabolites of the catecholamine neurotransmitters are agonists of a rat trace amine receptor." Mol Pharmacol **60**(6): 1181-1188.

Burchett, S. A. and T. P. Hicks (2006). "The mysterious trace amines: protean neuromodulators of synaptic transmission in mammalian brain." Prog Neurobiol **79**(5-6): 223-246.

Calebiro, D. (2011). "Thyroid-stimulating hormone receptor activity after internalization." Ann Endocrinol (Paris) **72**(2): 64-67.

Calebiro, D., T. de Filippis, S. Lucchi, C. Covino, S. Panigone, P. Beck-Peccoz, D. Dunlap and L. Persani (2005). "Intracellular entrapment of wild-type TSH receptor by oligomerization with mutants linked to dominant TSH resistance." Hum Mol Genet **14**(20): 2991-3002.

Calebiro, D., V. O. Nikolaev, M. C. Gagliani, T. de Filippis, C. Dees, C. Tacchetti, L. Persani and M. J. Lohse (2009). "Persistent cAMP-signals triggered by internalized G-protein-coupled receptors." PLoS Biol **7**(8): e1000172.

Calebiro, D., V. O. Nikolaev and M. J. Lohse (2010). "Imaging of persistent cAMP signaling by internalized G protein-coupled receptors." J Mol Endocrinol **45**(1): 1-8.

Cao, Q., M. Martinez, J. Zhang, A. R. Sanders, J. A. Badner, A. Cravchik, C. J. Markey, E. Beshah, J. J. Guroff, M. E. Maxwell, D. M. Kazuba, R. Whiten, L. R. Goldin, E. S. Gershon and P. V. Gejman (1997). "Suggestive evidence for a schizophrenia susceptibility locus on chromosome 6q and a confirmation in an independent series of pedigrees." Genomics **43**(1): 1-8.

Chabaud, O., M. Chambard, N. Gaudry and J. Mauchamp (1988). "Thyrotrophin and cyclic AMP regulation of thyroglobulin gene expression in cultured porcine thyroid cells." J Endocrinol **116**(1): 25-33.

Chambard, M., D. Depetris, D. Gruffat, S. Gonzalvez, J. Mauchamp and O. Chabaud (1990). "Thyrotrophin regulation of apical and basal exocytosis of thyroglobulin by porcine thyroid monolayers." J Mol Endocrinol **4**(3): 193-199.

Chen, L., M. He, E. Sibille, A. Thompson, Z. Sarnyai, H. Baker, T. Shippenberg and M. Toth (1999). "Adaptive Changes in Postsynaptic Dopamine Receptors Despite Unaltered Dopamine Dynamics in Mice Lacking Monoamine Oxidase B." J Neurochem **73**(2): 647-655.

Cheng, S. Y., J. L. Leonard and P. J. Davis (2010). "Molecular aspects of thyroid hormone actions." Endocr Rev **31**(2): 139-170.

120

Chiellini, G., L. Bellusci, M. Sabatini and R. Zucchi (2017). "Thyronamines and Analogues - The Route from Rediscovery to Translational Research on Thyronergic Amines." Mol Cell Endocrinol.

Di Cosmo, C., X. H. Liao, A. M. Dumitrescu, N. J. Philp, R. E. Weiss and S. Refetoff (2010). "Mice deficient in MCT8 reveal a mechanism regulating thyroid hormone secretion." J Clin Invest **120**(9): 3377-3388.

Dietrich, J. W., G. Landgrafe and E. H. Fotiadou (2012). "TSH and Thyrotropic Agonists: Key Actors in Thyroid Homeostasis." J Thyroid Res **2012**: 351864.

Dong, C., C. M. Filipeanu, M. T. Duvernay and G. Wu (2007). "Regulation of G protein-coupled receptor export trafficking." Biochim Biophys Acta **1768**(4): 853-870.

Doyle, K. P., K. L. Suchland, T. M. P. Ciesielski, N. S. Lessov, D. K. Grandy, T. S. Scanlan and M. P. Stenzel-Poore (2007). "Novel Thyroxine Derivatives, Thyronamine and 3-iodothyronamine, Induce Transient Hypothermia and Marked Neuroprotection Against Stroke Injury." Stroke **38**(9): 2569-2576.

Duan, J., M. Martinez, A. R. Sanders, C. Hou, N. Saitou, T. Kitano, B. J. Mowry, R. R. Crowe, J. M. Silverman, D. F. Levinson and P. V. Gejman (2004). "Polymorphisms in the Trace Amine Receptor 4 (TRAR4) Gene on Chromosome 6q23.2 Are Associated with Susceptibility to Schizophrenia." Am J Hum Genet **75**(4): 624-638.

Dumitrescu, A. M., X. H. Liao, R. E. Weiss, K. Millen and S. Refetoff (2006). "Tissue-specific thyroid hormone deprivation and excess in monocarboxylate transporter (mct) 8-deficient mice." Endocrinology **147**(9): 4036-4043.

Dunn, A. D., H. E. Crutchfield and J. T. Dunn (1991). "Thyroglobulin processing by thyroidal proteases. Major sites of cleavage by cathepsins B, D, and L." J Biol Chem **266**(30): 20198-20204.

Durden, D. A. and S. R. Philips (1980). "Kinetic measurements of the turnover rates of phenylethylamine and tryptamine in vivo in the rat brain." J Neurochem **34**(6): 1725-1732.

Engels, K., H. Rakov, D. Zwanziger, G. S. Hones, M. Rehders, K. Brix, J. Kohrle, L. C. Moller and D. Fuhrer (2016). "Efficacy of protocols for induction of chronic hyperthyroidism in male and female mice." Endocrine **54**(1): 47-54.

Espinoza, S., V. Ghisi, M. Emanuele, D. Leo, I. Sukhanov, T. D. Sotnikova, E. Chieregatti and R. R. Gainetdinov (2015). "Postsynaptic D2 dopamine receptor supersensivity in the striatum of mice lacking TAAR1." Neuropharmacology **93**: 308-313.

References

Espinoza, S., A. Salahpour, B. Masri, T. D. Sotnikova, M. Messa, L. S. Barak, M. G. Caron and R. R. Gainetdinov (2011). "Functional interaction between trace amine-associated receptor 1 and dopamine D2 receptor." Mol Pharmacol **80**(3): 416-425.

Felbor, U., B. Kessler, W. Mothes, H. H. Goebel, H. L. Ploegh, R. T. Bronson and B. R. Olsen (2002). "Neuronal loss and brain atrophy in mice lacking cathepsins B and L." Proc Natl Acad Sci U S A **99**(12): 7883-7888.

Forman, B. M., J. Casanova, B. M. Raaka, J. Ghysdael and H. H. Samuels (1992). "Half-site spacing and orientation determines whether thyroid hormone and retinoic acid receptors and related factors bind to DNA response elements as monomers, homodimers, or heterodimers." Mol Endocrinol **6**(3): 429-442.

Frascarelli, S., S. Ghelardoni, G. Chiellini, R. Vargiu, S. Ronca-Testoni, T. S. Scanlan, D. K. Grandy and R. Zucchi (2008). "Cardiac effects of trace amines: pharmacological characterization of trace amine-associated receptors." European journal of pharmacology **587**(1-3): 231-236.

Frenzel, R., C. Voigt and R. Paschke (2006). "The Human Thyrotropin Receptor Is Predominantly Internalized by β-Arrestin 2." Endocrinology **147**(6): 3114-3122.

Friedrichs, B., C. Tepel, T. Reinheckel, J. Deussing, K. von Figura, V. Herzog, C. Peters, P. Saftig and K. Brix (2003). "Thyroid functions of mouse cathepsins B, K, and L." J Clin Invest **111**(11): 1733-1745.

Friesema, E. C., S. Ganguly, A. Abdalla, J. E. Manning Fox, A. P. Halestrap and T. J. Visser (2003). "Identification of monocarboxylate transporter 8 as a specific thyroid hormone transporter." J Biol Chem **278**(41): 40128-40135.

Friesema, E. C., J. Jansen, H. Heuer, M. Trajkovic, K. Bauer and T. J. Visser (2006). "Mechanisms of disease: psychomotor retardation and high T3 levels caused by mutations in monocarboxylate transporter 8." Nat Clin Pract Endocrinol Metab **2**(9): 512-523.

Friesema, E. C., J. Jansen, J. W. Jachtenberg, W. E. Visser, M. H. Kester and T. J. Visser (2008). "Effective cellular uptake and efflux of thyroid hormone by human monocarboxylate transporter 10." Mol Endocrinol **22**(6): 1357-1369.

Furuya, F., C. Lu, C. J. Guigon and S. Cheng (2009). "Nongenomic Activation of Phosphatidylinositol 3-kinase Signaling by Thyroid Hormone Receptors." Steroids **74**(7): 628-634.

Galli, E., M. Marchini, A. Saba, S. Berti, M. Tonacchera, P. Vitti, T. S. Scanlan, G. Iervasi and R. Zucchi (2012). "Detection of 3-iodothyronamine in human patients: a preliminary study." J Clin Endocrinol Metab **97**(1): E69-74.

Ghelardoni, S., G. Chiellini, S. Frascarelli, A. Saba and R. Zucchi (2014). "Uptake and metabolic effects of 3-iodothyronamine in hepatocytes." J Endocrinol **221**(1): 101-110.

Godbole, A., S. Lyga, M. J. Lohse and D. Calebiro (2017). "Internalized TSH receptors en route to the TGN induce local Gs-protein signaling and gene transcription." Nat Commun **8**(1): 443.

Goldstein, I. J., C. M. Reichert and A. Misaki (1974). "INTERACTION OF CONCANAVALIN A WITH MODEL SUBSTRATES*." Annals of the New York Academy of Sciences **234**(1): 283-296.

Graebert, K. S., H. Bauch, W. Neumüller, K. Brix and V. Herzog (1997). "Epithelial Foldingin Vitro:Studies on the Cellular Mechanism Underlying Evagination of Thyrocyte Monolayers." Experimental Cell Research **231**(1): 214-225.

Grandy, D. K. (2007). "Trace Amine-Associated Receptor 1 – Family Archetype or Iconoclast?" Pharmacol Ther **116**(3): 355-390.

Grimsby, J., M. Toth, K. Chen, T. Kumazawa, L. Klaidman, J. D. Adams, F. Karoum, J. Gal and J. C. Shih (1997). "Increased stress response and beta-phenylethylamine in MAOB-deficient mice." Nat Genet **17**(2): 206-210.

Hackenmueller, S. A., M. Marchini, A. Saba, R. Zucchi and T. S. Scanlan (2012). "Biosynthesis of 3-iodothyronamine (T1AM) is dependent on the sodium-iodide symporter and thyroperoxidase but does not involve extrathyroidal metabolism of T4." Endocrinology **153**(11): 5659-5667.

Hackenmueller, S. A. and T. S. Scanlan (2012). "Identification and quantification of 3-iodothyronamine metabolites in mouse serum using liquid chromatography-tandem mass spectrometry." Journal of chromatography. A **1256**: 89-97.

Hage, M. P. and S. T. Azar (2012). "The Link between Thyroid Function and Depression." J Thyroid Res **2012**: 590648.

Harmeier, A., S. Obermueller, C. A. Meyer, F. G. Revel, D. Buchy, S. Chaboz, G. Dernick, J. G. Wettstein, A. Iglesias, A. Rolink, B. Bettler and M. C. Hoener (2015). "Trace amine-associated receptor 1 activation silences GSK3β signaling of TAAR1 and D2R heteromers." European Neuropsychopharmacology **25**(11): 2049-2061.

References

Hashiguchi, Y. and M. Nishida (2007). "Evolution of Trace Amine–Associated Receptor (TAAR) Gene Family in Vertebrates: Lineage-Specific Expansions and Degradations of a Second Class of Vertebrate Chemosensory Receptors Expressed in the Olfactory Epithelium." Molecular Biology and Evolution **24**(9): 2099-2107.

Hennemann, G., R. Docter, E. C. Friesema, M. de Jong, E. P. Krenning and T. J. Visser (2001). "Plasma membrane transport of thyroid hormones and its role in thyroid hormone metabolism and bioavailability." Endocr Rev **22**(4): 451-476.

Herzog, V. and F. Miller (1981). "Structural and functional polarity of inside-out follicles prepared from pig thyroid gland." Eur J Cell Biol **24**(1): 74-84.

Heuer, H., M. K. Maier, S. Iden, J. Mittag, E. C. Friesema, T. J. Visser and K. Bauer (2005). "The monocarboxylate transporter 8 linked to human psychomotor retardation is highly expressed in thyroid hormone-sensitive neuron populations." Endocrinology **146**(4): 1701-1706.

Heuer, H. and T. J. Visser (2009). "Minireview: Pathophysiological importance of thyroid hormone transporters." Endocrinology **150**(3): 1078-1083.

Hillier, A. P. (1970). "The binding of thyroid hormones to phospholipid membranes." J Physiol **211**(3): 585-597.

Hoefig, C. S., J. Kohrle, G. Brabant, K. Dixit, B. Yap, C. J. Strasburger and Z. Wu (2011). "Evidence for extrathyroidal formation of 3-iodothyronamine in humans as provided by a novel monoclonal antibody-based chemiluminescent serum immunoassay." J Clin Endocrinol Metab **96**(6): 1864-1872.

Hoefig, C. S., J. Köhrle, G. Brabant, K. Dixit, B. Yap, C. J. Strasburger and Z. Wu (2011). "Evidence for Extrathyroidal Formation of 3-Iodothyronamine in Humans as Provided by a Novel Monoclonal Antibody-Based Chemiluminescent Serum Immunoassay." The Journal of Clinical Endocrinology & Metabolism **96**(6): 1864-1872.

Hoefig, C. S., T. Wuensch, E. Rijntjes, I. Lehmphul, H. Daniel, U. Schweizer, J. Mittag and J. Kohrle (2015). "Biosynthesis of 3-Iodothyronamine From T4 in Murine Intestinal Tissue." Endocrinology **156**(11): 4356-4364.

Hoefig, C. S., R. Zucchi and J. Kohrle (2016). "Thyronamines and Derivatives: Physiological Relevance, Pharmacological Actions, and Future Research Directions." Thyroid **26**(12): 1656-1673.

Holschneider, D. P., K. Chen, I. Seif and J. C. Shih (2001). "Biochemical, behavioral, physiologic, and neurodevelopmental changes in mice deficient in monoamine oxidase A or B." Brain Res Bull **56**(5): 453-462.

124

Ianculescu, A. G., E. C. Friesema, T. J. Visser, K. M. Giacomini and T. S. Scanlan (2010). "Transport of thyroid hormones is selectively inhibited by 3-iodothyronamine." <u>Mol Biosyst</u> **6**(8): 1403-1410.

Ianculescu, A. G., E. C. H. Friesema, T. J. Visser, K. M. Giacomini and T. S. Scanlan (2010). "Transport of thyroid hormones is selectively inhibited by 3-iodothyronamine." <u>Mol Biosyst</u> **6**(8): 1403-1410.

Ianculescu, A. G., K. M. Giacomini and T. S. Scanlan (2009). "Identification and characterization of 3-iodothyronamine intracellular transport." <u>Endocrinology</u> **150**(4): 1991-1999.

Kleinau, G., J. Pratzka, D. Nurnberg, A. Gruters, D. Fuhrer-Sakel, H. Krude, J. Kohrle, T. Schoneberg and H. Biebermann (2011). "Differential modulation of Beta-adrenergic receptor signaling by trace amine-associated receptor 1 agonists." <u>PLoS One</u> **6**(10): e27073.

Klieverik, L. P., E. Foppen, M. T. Ackermans, M. J. Serlie, H. P. Sauerwein, T. S. Scanlan, D. K. Grandy, E. Fliers and A. Kalsbeek (2009). "Central effects of thyronamines on glucose metabolism in rats." <u>J Endocrinol</u> **201**(3): 377-386.

Kohrle, J. (2000). "The deiodinase family: selenoenzymes regulating thyroid hormone availability and action." <u>Cell Mol Life Sci</u> **57**(13-14): 1853-1863.

Kuehnen, P., A. Grueters and H. Krude (2009). "Two puzzling cases of thyroid dysgenesis." <u>Horm Res</u> **71 Suppl 1**: 93-97.

Lamprecht, M. R., D. M. Sabatini and A. E. Carpenter (2007). "CellProfiler: free, versatile software for automated biological image analysis." <u>Biotechniques</u> **42**(1): 71-75.

Lanni, A., M. Moreno and F. Goglia (2011). Mitochondrial Actions of Thyroid Hormone. <u>Comprehensive Physiology</u>, John Wiley & Sons, Inc.

Liberles, S. D. (2015). "Trace amine-associated receptors: ligands, neural circuits, and behaviors." <u>Curr Opin Neurobiol</u> **34**: 1-7.

Liberles, S. D. and L. B. Buck (2006). "A second class of chemosensory receptors in the olfactory epithelium." <u>Nature</u> **442**(7103): 645-650.

Lin, H. Y., F. B. Davis, J. K. Gordinier, L. J. Martino and P. J. Davis (1999). "Thyroid hormone induces activation of mitogen-activated protein kinase in cultured cells." <u>Am J Physiol</u> **276**(5 Pt 1): C1014-1024.

References

Lindemann, L., M. Ebeling, N. A. Kratochwil, J. R. Bunzow, D. K. Grandy and M. C. Hoener (2005). "Trace amine-associated receptors form structurally and functionally distinct subfamilies of novel G protein-coupled receptors." <u>Genomics</u> **85**(3): 372-385.

Lindemann, L. and M. C. Hoener (2005). "A renaissance in trace amines inspired by a novel GPCR family." <u>Trends Pharmacol Sci</u> **26**(5): 274-281.

Lindemann, L., C. A. Meyer, K. Jeanneau, A. Bradaia, L. Ozmen, H. Bluethmann, B. Bettler, J. G. Wettstein, E. Borroni, J. L. Moreau and M. C. Hoener (2008). "Trace amine-associated receptor 1 modulates dopaminergic activity." <u>J Pharmacol Exp Ther</u> **324**(3): 948-956.

Linke, M., V. Herzog and K. Brix (2002). "Trafficking of lysosomal cathepsin B-green fluorescent protein to the surface of thyroid epithelial cells involves the endosomal/lysosomal compartment." <u>J Cell Sci</u> **115**(Pt 24): 4877-4889.

Linke, M., S. Jordans, L. Mach, V. Herzog and K. Brix (2002). "Thyroid stimulating hormone upregulates secretion of cathepsin B from thyroid epithelial cells." <u>Biol Chem</u> **383**(5): 773-784.

Lohse, M. J. (1993). "Molecular mechanisms of membrane receptor desensitization." <u>Biochim Biophys Acta</u> **1179**(2): 171-188.

Luttrell, L. M. and R. J. Lefkowitz (2002). "The role of beta-arrestins in the termination and transduction of G-protein-coupled receptor signals." <u>J Cell Sci</u> **115**(Pt 3): 455-465.

Lynch, M. A., J. F. Andrews and R. E. Moore (1985). "Low doses of T3 induce a rapid metabolic response in young lambs." <u>Horm Metab Res</u> **17**(2): 63-66.

Mahjoub, M. R. and T. Stearns (2012). "Supernumerary centrosomes nucleate extra cilia and compromise primary cilium signaling." <u>Current biology : CB</u> **22**(17): 1628-1634.

Mayer, K., A. Vreemann, H. Qu and K. Brix (2009). "Release of endo-lysosomal cathepsins B, D, and L from IEC6 cells in a cell culture model mimicking intestinal manipulation." <u>Biol Chem</u> **390**(5-6): 471-480.

Miller, G. M. (2011). "The emerging role of trace amine-associated receptor 1 in the functional regulation of monoamine transporters and dopaminergic activity." <u>J Neurochem</u> **116**(2): 164-176.

Miller, G. M., C. D. Verrico, A. Jassen, M. Konar, H. Yang, H. Panas, M. Bahn, R. Johnson and B. K. Madras (2005). "Primate trace amine receptor 1 modulation by the dopamine transporter." <u>J Pharmacol Exp Ther</u> **313**(3): 983-994.

Morgan, S. J., S. Neumann, B. Marcus-Samuels and M. C. Gershengorn (2016). "Thyrotropin Stimulates Differentiation Not Proliferation of Normal Human Thyrocytes in Culture." Front Endocrinol (Lausanne) **7**.

Müller, J. and H. Heuer (2014). "Expression Pattern of Thyroid Hormone Transporters in the Postnatal Mouse Brain." Front Endocrinol (Lausanne) **5**.

Muller, J., S. Mayerl, T. J. Visser, V. M. Darras, A. Boelen, L. Frappart, L. Mariotta, F. Verrey and H. Heuer (2014). "Tissue-specific alterations in thyroid hormone homeostasis in combined Mct10 and Mct8 deficiency." Endocrinology **155**(1): 315-325.

Mullur, R., Y. Y. Liu and G. A. Brent (2014). "Thyroid Hormone Regulation of Metabolism." Physiol Rev **94**(2): 355-382.

Nachury, M. V. (2014). "How do cilia organize signalling cascades?" Philos Trans R Soc Lond B Biol Sci **369**(1650).

Nachury, M. V. (2014). "How do cilia organize signalling cascades?" Philos Trans R Soc Lond B Biol Sci **369**(1650): 20130465.

Neuhoff, V., K. Philipp, H. G. Zimmer and S. Mesecke (1979). "A simple, versatile, sensitive and volume-independent method for quantitative protein determination which is independent of other external influences." Hoppe Seylers Z Physiol Chem **360**(11): 1657-1670.

Nilsson, M. and H. Fagman (2017). "Development of the thyroid gland." Development **144**(12): 2123-2140.

Nussey, S. and S. Whitehead (2001). Endocrinology: An Integrated Approach. Oxford, BIOS Scientific Publishers

BIOS Scientific Publishers Limited.

Othman, S. S., K. Abdul Kadir, J. Hassan, G. K. Hong, B. B. Singh and N. Raman (1994). "High prevalence of thyroid function test abnormalities in chronic schizophrenia." Aust N Z J Psychiatry **28**(4): 620-624.

Panas, H. N., L. J. Lynch, E. J. Vallender, Z. Xie, G. L. Chen, S. K. Lynn, T. S. Scanlan and G. M. Miller (2010). "Normal thermoregulatory responses to 3-iodothyronamine, trace amines and amphetamine-like psychostimulants in trace amine associated receptor 1 knockout mice." J Neurosci Res **88**(9): 1962-1969.

References

Pei, Y., A. Asif-Malik and J. J. Canales (2016). "Trace Amines and the Trace Amine-Associated Receptor 1: Pharmacology, Neurochemistry, and Clinical Implications." Front Neurosci 10: 148.

Piehl, S., C. S. Hoefig, T. S. Scanlan and J. Kohrle (2011). "Thyronamines--past, present, and future." Endocr Rev 32(1): 64-80.

Rakov, H., K. Engels, G. S. Hones, K. H. Strucksberg, L. C. Moeller, J. Kohrle, D. Zwanziger and D. Fuhrer (2016). "Sex-specific phenotypes of hyperthyroidism and hypothyroidism in mice." Biol Sex Differ 7(1): 36.

Reese, E. A., J. R. Bunzow, S. Arttamangkul, M. S. Sonders and D. K. Grandy (2007). "Trace Amine-Associated Receptor 1 Displays Species-Dependent Stereoselectivity for Isomers of Methamphetamine, Amphetamine, and Para-Hydroxyamphetamine." Journal of Pharmacology and Experimental Therapeutics 321(1): 178-186.

Revel, F. G., J. L. Moreau, R. R. Gainetdinov, A. Bradaia, T. D. Sotnikova, R. Mory, S. Durkin, K. G. Zbinden, R. Norcross, C. A. Meyer, V. Metzler, S. Chaboz, L. Ozmen, G. Trube, B. Pouzet, B. Bettler, M. G. Caron, J. G. Wettstein and M. C. Hoener (2011). "TAAR1 activation modulates monoaminergic neurotransmission, preventing hyperdopaminergic and hypoglutamatergic activity." Proc Natl Acad Sci U S A 108(20): 8485-8490.

Revel, F. G., J. L. Moreau, R. R. Gainetdinov, A. Ferragud, C. Velazquez-Sanchez, T. D. Sotnikova, S. R. Morairty, A. Harmeier, K. Groebke Zbinden, R. D. Norcross, A. Bradaia, T. S. Kilduff, B. Biemans, B. Pouzet, M. G. Caron, J. J. Canales, T. L. Wallace, J. G. Wettstein and M. C. Hoener (2012). "Trace amine-associated receptor 1 partial agonism reveals novel paradigm for neuropsychiatric therapeutics." Biol Psychiatry 72(11): 934-942.

Revel, F. G., J. L. Moreau, B. Pouzet, R. Mory, A. Bradaia, D. Buchy, V. Metzler, S. Chaboz, K. Groebke Zbinden, G. Galley, R. D. Norcross, D. Tuerck, A. Bruns, S. R. Morairty, T. S. Kilduff, T. L. Wallace, C. Risterucci, J. G. Wettstein and M. C. Hoener (2013). "A new perspective for schizophrenia: TAAR1 agonists reveal antipsychotic- and antidepressant-like activity, improve cognition and control body weight." Mol Psychiatry 18(5): 543-556.

Rich, T. C., K. A. Fagan, T. E. Tse, J. Schaack, D. M. F. Cooper and J. W. Karpen (2001). "A uniform extracellular stimulus triggers distinct cAMP signals in different compartments of a simple cell." Proc Natl Acad Sci U S A 98(23): 13049-13054.

Roy, G., E. Placzek and T. S. Scanlan (2012). "ApoB-100-containing lipoproteins are major carriers of 3-iodothyronamine in circulation." J Biol Chem 287(3): 1790-1800.

Ruf, J. and P. Carayon (2006). "Structural and functional aspects of thyroid peroxidase." Arch Biochem Biophys 445(2): 269-277.

Saba, A., G. Chiellini, S. Frascarelli, M. Marchini, S. Ghelardoni, A. Raffaelli, M. Tonacchera, P. Vitti, T. S. Scanlan and R. Zucchi (2010). "Tissue distribution and cardiac metabolism of 3-iodothyronamine." Endocrinology **151**(10): 5063-5073.

Santos, N. C., P. Costa, D. Ruano, A. Macedo, M. J. Soares, J. Valente, A. T. Pereira, M. H. Azevedo and J. A. Palha (2012). "Revisiting thyroid hormones in schizophrenia." J Thyroid Res **2012**: 569147.

Sato, M., J. B. Blumer, V. Simon and S. M. Lanier (2006). "Accessory proteins for G proteins: partners in signaling." Annu Rev Pharmacol Toxicol **46**: 151-187.

Scanlan, T. S., K. L. Suchland, M. E. Hart, G. Chiellini, Y. Huang, P. J. Kruzich, S. Frascarelli, D. A. Crossley, J. R. Bunzow, S. Ronca-Testoni, E. T. Lin, D. Hatton, R. Zucchi and D. K. Grandy (2004). "3-Iodothyronamine is an endogenous and rapid-acting derivative of thyroid hormone." Nat Med **10**(6): 638-642.

Scarlett, A., M. P. Parsons, P. L. Hanson, K. K. Sidhu, T. P. Milligan and J. M. Burrin (2008). "Thyroid hormone stimulation of extracellular signal-regulated kinase and cell proliferation in human osteoblast-like cells is initiated at integrin alphaVbeta3." J Endocrinol **196**(3): 509-517.

Schanze, N., S. F. Jacobi, E. Rijntjes, S. Mergler, M. Del Olmo, C. S. Hoefig, N. Khajavi, I. Lehmphul, H. Biebermann, J. Mittag and J. Kohrle (2017). "3-Iodothyronamine Decreases Expression of Genes Involved in Iodide Metabolism in Mouse Thyroids and Inhibits Iodide Uptake in PCCL3 Thyrocytes." Thyroid **27**(1): 11-22.

Schmidt, B. M., N. Martin, A. C. Georgens, H. C. Tillmann, M. Feuring, M. Christ and M. Wehling (2002). "Nongenomic cardiovascular effects of triiodothyronine in euthyroid male volunteers." J Clin Endocrinol Metab **87**(4): 1681-1686.

Schwartz, C. E., M. M. May, N. J. Carpenter, R. C. Rogers, J. Martin, M. G. Bialer, J. Ward, J. Sanabria, S. Marsa, J. A. Lewis, R. Echeverri, H. A. Lubs, K. Voeller, R. J. Simensen and R. E. Stevenson (2005). "Allan-Herndon-Dudley syndrome and the monocarboxylate transporter 8 (MCT8) gene." Am J Hum Genet **77**(1): 41-53.

Schwartz, C. E. and R. E. Stevenson (2007). "The MCT8 thyroid hormone transporter and Allan--Herndon--Dudley syndrome." Best Pract Res Clin Endocrinol Metab **21**(2): 307-321.

Senese, R., F. Cioffi, P. de Lange, F. Goglia and A. Lanni (2014). "Thyroid: biological actions of 'nonclassical' thyroid hormones." J Endocrinol **221**(2): R1-12.

Snead, A. N., M. S. Santos, R. P. Seal, M. Miyakawa, R. H. Edwards and T. S. Scanlan (2007). "Thyronamines Inhibit Plasma Membrane and Vesicular Monoamine Transport." ACS Chemical Biology **2**(6): 390-398.

References

Spitzweg, C. and J. C. Morris (2002). "The sodium iodide symporter: its pathophysiological and therapeutic implications." Clin Endocrinol (Oxf) **57**(5): 559-574.

St Germain, D. L., V. A. Galton and A. Hernandez (2009). "Minireview: Defining the roles of the iodothyronine deiodinases: current concepts and challenges." Endocrinology **150**(3): 1097-1107.

Sukhanov, I., L. Caffino, E. V. Efimova, S. Espinoza, T. D. Sotnikova, L. Cervo, F. Fumagalli and R. R. Gainetdinov (2016). "Increased context-dependent conditioning to amphetamine in mice lacking TAAR1." Pharmacological Research **103**(Supplement C): 206-214.

Szumska, J., M. Qatato, M. Rehders, D. Fuhrer, H. Biebermann, D. K. Grandy, J. Kohrle and K. Brix (2015). "Trace Amine-Associated Receptor 1 Localization at the Apical Plasma Membrane Domain of Fisher Rat Thyroid Epithelial Cells Is Confined to Cilia." Eur Thyroid J **4**(Suppl 1): 30-41.

Tallman, K. R. and D. K. Grandy (2012). "A Decade of Pharma Discovery Delivers New Tools Targeting Trace Amine-Associated Receptor 1." Neuropsychopharmacology **37**(12): 2553-2554.

Tata, J. R. (2013). "The road to nuclear receptors of thyroid hormone." Biochimica et biophysica acta **1830**(7): 3860-3866.

Tepel, C., D. Bromme, V. Herzog and K. Brix (2000). "Cathepsin K in thyroid epithelial cells: sequence, localization and possible function in extracellular proteolysis of thyroglobulin." J Cell Sci **113 Pt 24**: 4487-4498.

Venditti, P., G. Napolitano, L. Di Stefano, G. Chiellini, R. Zucchi, T. S. Scanlan and S. Di Meo (2011). "Effects of the thyroid hormone derivatives 3-iodothyronamine and thyronamine on rat liver oxidative capacity." Molecular and cellular endocrinology **341**(1-2): 55-62.

Visser, W. E., E. C. H. Friesema and T. J. Visser (2011). "Minireview: Thyroid Hormone Transporters: The Knowns and the Unknowns." Molecular Endocrinology **25**(1): 1-14.

Visser, W. E. and T. J. Visser (2012). "Finding the way into the brain without MCT8." J Clin Endocrinol Metab **97**(12): 4362-4365.

Wainscott, D. B., S. P. Little, T. Yin, Y. Tu, V. P. Rocco, J. X. He and D. L. Nelson (2007). "Pharmacologic characterization of the cloned human trace amine-associated receptor1 (TAAR1) and evidence for species differences with the rat TAAR1." J Pharmacol Exp Ther **320**(1): 475-485.

Wang, Y. G., E. N. Dedkova, J. P. Fiening, K. Ojamaa, L. A. Blatter and S. L. Lipsius (2003). "Acute exposure to thyroid hormone increases Na(+) current and intracellular Ca(2+) in cat atrial myocytes." J Physiol **546**(Pt 2): 491-499.

Weber, J., J. McInnes, C. Kizilirmak, M. Rehders, M. Qatato, E. K. Wirth, U. Schweizer, F. Verrey, H. Heuer and K. Brix (2017). "Interdependence of thyroglobulin processing and thyroid hormone export in the mouse thyroid gland." Eur J Cell Biol **96**(5): 440-456.

Weber, J., M. Rehders, P. Saftig, F. Verrey, U. Schweizer, E. K. Wirth, H. Heuer and K. Brix (2015). "Functional analysis of the angio-follicular unit of the mouse thyroid gland." Exp Clin Endocrinol Diabetes **123**(03): P12_13.

Werthmann, R. C., S. Volpe, M. J. Lohse and D. Calebiro (2012). "Persistent cAMP signaling by internalized TSH receptors occurs in thyroid but not in HEK293 cells." Faseb j **26**(5): 2043-2048.

Wirth, E. K., E. Rijntjes, F. Meyer, J. Kohrle and U. Schweizer (2015). "High T3, Low T4 Serum Levels in Mct8 Deficiency Are Not Caused by Increased Hepatic Conversion through Type I Deiodinase." Eur Thyroid J **4**(Suppl 1): 87-91.

Wolinsky, T. D., C. J. Swanson, K. E. Smith, H. Zhong, B. Borowsky, P. Seeman, T. Branchek and C. P. Gerald (2007). "The Trace Amine 1 receptor knockout mouse: an animal model with relevance to schizophrenia." Genes Brain Behav **6**(7): 628-639.

Wrutniak-Cabello, C., F. Casas and G. Cabello (2001). "Thyroid hormone action in mitochondria." J Mol Endocrinol **26**(1): 67-77.

Xie, Z. and G. M. Miller (2007). "Trace amine-associated receptor 1 is a modulator of the dopamine transporter." J Pharmacol Exp Ther **321**(1): 128-136.

Xie, Z. and G. M. Miller (2009). "Trace amine-associated receptor 1 as a monoaminergic modulator in brain." Biochem Pharmacol **78**(9): 1095-1104.

Xie, Z., S. V. Westmoreland, M. E. Bahn, G. L. Chen, H. Yang, E. J. Vallender, W. D. Yao, B. K. Madras and G. M. Miller (2007). "Rhesus monkey trace amine-associated receptor 1 signaling: enhancement by monoamine transporters and attenuation by the D2 autoreceptor in vitro." J Pharmacol Exp Ther **321**(1): 116-127.

Yen, P. M. (2001). "Physiological and molecular basis of thyroid hormone action." Physiol Rev **81**(3): 1097-1142.

Zhang, R. and X. Xie (2012). "Tools for GPCR drug discovery." Acta Pharmacologica Sinica **33**(3): 372-384.

References

Zucchi, R., G. Chiellini, T. S. Scanlan and D. K. Grandy (2006). "Trace amine-associated receptors and their ligands." Br J Pharmacol **149**(8): 967-978.